Development of robust control based on sliding mode for nonlinear uncertain systems

Xinming Yan

UNIVERSITE BRETAGNE LOIRE

Centrale Nantes

Thèse de Doctorat

Xinming YAN

Mémoire présenté en vue de l'obtention du
grade de Docteur de l'École Centrale de Nantes
sous le sceau de l'Université Bretagne Loire

École doctorale : Sciences et Technologies de l'Information, et Mathématiques

Discipline : Automatique
Spécialité : Commande
Unité de recherche : Institut de Recherche en Communications et Cybernétique de Nantes

Soutenue le 27 Octobre 2016
Thèse n° :

Development of robust control based on sliding mode for nonlinear uncertain systems

JURY

Président :	**M. Jean-Pierre BARBOT**, Professeur des Universités, ENSEA, Cergy-Pontoise
Rapporteurs :	**M. Xavier BRUN**, Professeur des Universités, INSA, Lyon
	M. Salah LAGHROUCHE, Maître de Conférences-HDR, Université Technologique de Belfort-Montbéliard, Belfort
Invité :	**M. Elio USAI**, Professeur, Université de Cagliari, Italie
Directeur de thèse :	**M. Franck PLESTAN**, Professeur des Universités, École Centrale de Nantes, Nantes
Co-encadrante de thèse :	**M^{me} Muriel PRIMOT**, Maître de Conférences, Université de Nantes, Nantes

Contents

Abbreviations and notations

List of abbreviations

SM	Sliding mode	2SM	Second order sliding mode
TWC	Twisting control	TWLC	Twisting-like control
2SMOFC	Second order sliding mode output feedback control	STWC	Super-twisting control
3SMC	Third order sliding mode control	HOSMC	High order sliding mode control
TWLD	Twisting-like differentiator		

List of notations

$\mathbb{N}$	the natural numbers
$\mathbb{R}$	the field of real numbers
$\|a\|$	the absolute value of the real number a
$\text{sign}(\cdot)$	the signum function
A^T	the transpose of the matrix A
$x^{(n)}$	nth derivative of the variable x with respect to time
$\equiv$	equivalent to
$\max(a, b)$	the maximum of a and b
$\min(a, b)$	the minimum of a and b
$\text{floor}(a)$	gives the largest integer less than or equal to a
$\text{ceil}(a)$	gives the smallest integer greater than or equal to a

Contexte et organisation de la thèse

Motivations

Le travail de cette thèse a initialement été motivé par une application, à savoir la commande d'un système électropneumatique. En effet, l'IRCCyN est doté, depuis 2008, d'un tel système Plestan and Girin [2009] (voir Figure 1), l'objectif de cette plateforme étant d'évaluer des lois de commande dans le contexte des systèmes non linéaires incertains et perturbés. En effet, ce

Figure 1 – Photo du système électropneumatique de l'IRCCyN

système est typiquement non linéaire avec des incertitudes et est perturbé par des forces externes. Pour ce type de système, la commande par modes glissants présente des avantages grâce à sa robustesse et à la propriété de convergence en temps fini. Parmi les résultats obtenus sur des actionneurs électropneumatiques, on peut citer ceux issus d'une commande par modes glissants du premier ordre Bouri and Thomasset [2001]; Smaoui et al. [2005, 2001], d'ordre deux Smaoui et al. [2005], et d'ordre supérieur Laghrouche et al. [2004]; Girin et al. [2009].
La commande par modes glissants d'ordre supérieur force la variable de glissement (qui est liée à l'objectif de commande) et ses dérivées à converger vers zéro, tout en limitant le problème du *chattering*. Cependant, la variable de glissement et ses dérivées d'ordre supérieur se doivent d'être connues afin de calculer la commande. L'utilisation de ces dérivées d'ordre supérieur introduit du bruit, ainsi que du retard, en raison du processus de dérivations successives. Ainsi, dans le cas de la commande en position d'un actionneur électropneumatique, il est indispensable de calculer sa vitesse et son accélération, ce qui introduit du bruit sur la commande. Aussi, il y a un grand intérêt à proposer des solutions de commande par modes glissants ayant un recours

limité aux dérivées d'ordre supérieur de la variable de glissement. Par exemple, l'algorithme du *super-twisting* Levant [1998] est une loi de commande par retour de sortie; cependant, il ne peut être appliqué qu'à des systèmes avec un degré relatif égal à un par rapport à la variable de glissement.
A noter que, dans les cas pratiques, les dérivées de la variable de glissement sont déduites de la mesure, en utilisant des différentiateurs numériques. Cependant, en raison du bruit de mesure, la mauvaise précision de l'estimation peut introduire des perturbations supplémentaires dans la loi de commande Levant [1998]; Yan et al. [2014b] et donc réduire de manière significative l'efficacité de la loi de commande.
Cette thèse est consacrée au développement de stratégies de commande par modes glissants d'ordre supérieur avec une réduction du nombre de dérivées de la variable de glissement. **Dans le cadre de la commande par modes glissants d'ordre deux, un des objectifs de cette thèse est de proposer une nouvelle loi de commande qui assure l'établissement d'un régime glissant réel d'ordre deux, en temps fini, en utilisant uniquement l'information de la variable de glissement. De plus, contrairement au *super-twisting*, cet algorithme devra être applicable aux systèmes de degré relatif égal à 1 ou 2.**
En outre, dans cette thèse, la recherche d'une solution pour la commande par modes glissants d'ordre trois est également faite. D'un point de vue applicatif, cela est intéressant car le système électropneumatique présente une degré relatif égal à 3, dans le cas de la commande de sa position. **Dans le cas de la commande par modes glissants d'ordre trois, l'objectif de ce travail a été de supprimer l'utilisation de la dérivée d'ordre deux de la variable de glissement dans la loi de commande.**
Enfin, d'après les résultats de Plestan et al. [2010b]; Taleb et al. [2013], le mécanisme d'adaptation du gain est un outil très intéressant pour simplifier le processus de réglage de la lois de commande et améliorer ses performances (l'adaptation du gain limitant son amplitude, et donc le *chattering*). **Ainsi, une autre partie de cette thèse est axée sur le développement de processus d'adaptation du gain.**

Organisation et contributions de la thèse

A l'issue d'une introduction générale présentant le concept de mode glissant, le mémoire est divisé en trois parties, détaillant les contributions de cette thèse.

- La **Partie** I est dédiée à la présentation de trois différents types de commande par modes glissants d'ordre deux. Le point commun de ces trois stratégies est l'utilisation de gains commutants. Leurs performances sont comparées à la fin de cette partie à travers des exemples académiques.

  - Dans le **Chapitre** 3, la formalisation de commandes par modes glissants avec commutation du gain est présentée. Pour les lois de commande présentées sous cette forme, le gain commute entre deux niveaux: un niveau avec une faible amplitude, et un autre niveau avec un gain large. Ce formalisme a été présenté dans Yan et al. [2016e]. L'intérêt principal de ce formalisme est de réécrire plusieurs stratégies de commande par modes glissants d'ordre deux de manière uniforme. Afin d'assurer l'établissement d'un régime glissant réel d'ordre deux, certaines conditions basées sur une analyse géométrique des trajectoires du système sont données pour la durée de l'application du grand gain. Ensuite, l'algorithme du *twisting* Levantovsky [1985] (notée TWC) et une commande par modes glissants d'ordre deux par retour de sortie Plestan et al. [2010a] (notée 2SMOFC) sont reformulés à partir de la commutation du gain.

- Le **Chapitre** 4 présente une nouvelle approche appelée *Twisting-like* Yan et al. [2016d] (notée TWLC). Cette méthode peut être appliquée aux systèmes avec un degré relatif égal à deux par rapport à la variable de glissement. La caractéristique principale de cette méthode est que seule la variable de glissement est utilisée. De plus contrairement à la méthode 2SMOFC, le grand gain est appliqué pendant plusieurs périodes d'échantillonnage. Grâce à cette dernière caractéristique, le temps de convergence du système est nettement amélioré par rapport à la méthode 2SMOFC et s'approche de celui obtenu par le *twisting*, d'où le nom de *twisting-like*. L'utilisation du TWLC comme algorithme de différentiation est également présenté dans ce chapitre.
- Des comparaisons entre les méthodes TWC, 2SMOFC et TWLC sont faites dans le **Chapitre** 5 sur un exemple académique et sur un système pendulaire.

- La **Partie** II se concentre sur la commande par modes glissants avec gain adaptatif. La première contribution de cette partie est le développement des versions adaptatives pour les nouveaux algorithmes 2SMOFC et TWLC. Une autre contribution de cette partie est la proposition d'une stratégie de commande par modes glissants d'ordre trois (notée 3SMC). Par rapport à la méthode par modes glissants d'ordre supérieur quasi-continu Levant [2005b], cette technique utilise un ordre de différentiation réduit de la variable de glissement. En outre le résultat d'adaptation du gain des méthodes 2SMOFC et TWLC est étendu pour cette commande par modes glissants d'ordre supérieur.
  - Dans le **Chapitre** 7, les versions adaptatives des algorithmes 2SMOFC et TWLC sont présentées. L'adaptation du gain est basée sur la durée entre deux commutations successives du signe de la variable de glissement. Ensuite, le gain est ajusté en utilisant seulement l'information du signe de la variable de glissement.
  - Dans le **Chapitre** 8, une loi de commande par modes glissants d'ordre trois (3SMC) est proposée Yan et al. [2016c]. Dans le cas standard de la commande par modes glissants d'ordre trois, les dérivées premières et secondes de la variable de glissement doivent être connues. Dans ce nouvel algorithme, l'utilisation de la dérivée seconde est supprimée. Cela permet d'éviter l'introduction, par le dérivateur, de bruit supplémentaire. De plus, l'adaptation du gain est également abordée afin de simplifier son réglage.

- La **Partie** III présente l'application des nouvelles stratégies de commande à deux systèmes expérimentaux.
  - Le **Chapitre** 9 traite du problème de commande de la position d'un système électropneumatique. Il s'agit typiquement d'un système non linéaire avec incertitudes et perturbation. Des lois de commande basées sur la théorie des modes glissants ont déjà montré leur intérêt sur ce type d'applications, par rapport à d'autres Chillari et al. [2001]; Brun et al. [1999]. En premier lieu, les commandes par modes glissants d'ordre deux TWC, 2SMOFC et TWLC sont appliquées au système électropneumatique, et leurs performances comparées. Ensuite, les versions adaptatives des méthodes 2SMOFC et TWLC sont mises en oeuvre. L'effet de l'utilisation d'un gain adaptatif est mis en évidence à partir des résultats expérimentaux. Enfin, la commande par modes glissants d'ordre trois (3SMC), présentée dans le chapitre 8, est appliquée. Ses performances sont comparées à celles obtenues avec la commande par modes glissants d'ordre supérieur (HOSMC) Levant [2005b].
  - Dans le **Chapitre** 10, la commande de l'attitude d'un système volant (hélicoptère à 3 degrés de liberté Quanser Quanser [2006]) est abordée. Puisque les hélices sont

sensibles aux vibrations, ce système nécessite une entrée continue. Ainsi, une version “intégrale” de la méthode TWLC est développée Yan et al. [2016b]. Cette loi de commande permet d’obtenir une entrée continue. Grâce aux essais expérimentaux, la performance de cette nouvelle méthode de commande est comparée à l’algorithme du *super-twisting* Levant [1998].

Publications

Ci-dessous sont indiquées les publications et communications liées au travail de thèse.

Revues internationales à comité de lecture

- Xinming Yan, Antonio Estrada, and Franck Plestan, “Adaptive pulse output feedback controller based on second order sliding mode: methodology and application”, *IEEE Transactions on Control Systems Technology*, available online, 2016, DOI: 10.1109/TCST.2016.2532801.
  Yan et al. [2016a]
- Xinming Yan, Franck Plestan, and Muriel Primot, “A new third order sliding mode controller – application to an electropneumatic actuator”, *IEEE Transactions on Control Systems Technology*, available online, 2016, DOI: 10.1109/TCST.2016.2571664.
  Yan et al. [2016c]
- Xinming Yan, Muriel Primot, and Franck Plestan, “Electropneumatic actuator position control using second order sliding mode”, *e& i Elektrotechnik und Informationstechnik Special Issue on Automation and Control - Sliding Mode Applications in Hydraulics and Pneumatics*, available online, 2016, DOI: 10.1007/s00502-016-0423-9.
  Yan et al. [2016f]
- Xinming Yan, Muriel Primot, and Franck Plestan, “Output feedback relay control in the second order sliding mode context with application to electropneumatic system” submitted (third lecture) to *International journal of robust and nonlinear control* , 2016.
  Yan et al. [2016d]

Chapitre d’ouvrage collectif à diffusion internationale et comité de lecture.

- Franck Plestan, Xinming Yan, Mohammed Taleb, and Antonio Estrada, “Adaptive solutions for robust control of electro-pneumatic actuators”, in *Recent Trends in Sliding Mode Control*, eds. L. Fridman, J. P. Barbot, F. Plestan, IET, PP 387-404, 2016.

Conférences internationales avec comité de lecture

- Xinming Yan, Franck Plestan, and Muriel Primot, “Perturbation observer for a pneumatic system: high gain versus higher order sliding mode solutions”, *European Control Conference ECC*, Strasbourg, France, 2014.
  Yan et al. [2014a]
- Xinming Yan, Muriel Primot, and Franck Plestan, “Comparison of differentiation schemes for the velocity and acceleration estimations of a pneumatic system”, *IFAC World Congress*, Cape Town, South-Africa, 2014.
  Yan et al. [2014b]
- Mohammed Taleb, Xinming Yan, and Franck Plestan, “Third order sliding mode controller based on adaptive integral sliding mode concept: experimental application to an

electropneumatic actuator", *IEEE Conference on Decision and Control CDC*, Los Angeles, California, USA, 2014.
Taleb et al. [2014]

- Xinming Yan, Franck Plestan, and Muriel Primot, "Higher order sliding mode control with a reduced use of sliding variable time derivatives", *American Control Conference ACC*, Chicago, USA, 2015.
Yan et al. [2015]
- Xinming Yan, Muriel Primot, and Franck Plestan, "An unified formalism based on gain switching for second order sliding mode control", *International Workshop on Variable Structure Systems VSS*, Nanjing, China, 2016.
Yan et al. [2016e]
- Xinming Yan, Franck Plestan, and Muriel Primot, "Integral twisting-like control with application to UAVs attitude control", *IEEE Multi-Conference on Systems and Control, International Conference on Control Applications CCA*, Buenos Aires, Argentina, 2016.
Yan et al. [2016b]

1

General introduction to sliding mode control

Contents

This chapter provides an overview of the sliding mode concept. Section 1.1 is devoted to the introduction of the basic concepts of the first order sliding mode control. Then, the chattering phenomenon is presented and solutions developed to reduce the chattering are presented. Section 1.3 is devoted to the high order sliding mode control, whereas sliding mode control with gain adaptation is described in Section 1.4. Finally, the motivations for research works in this thesis are exposed in Section 1.6, as well as the organization and contribution of the thesis in Section 1.7.

1.1 Principle of sliding mode control

The sliding mode control approach is an efficient tool to the complex control problem of nonlinear uncertain systems. The main advantages of sliding mode control consist in its low

sensitivity to parameter uncertainties and disturbances, the finite time convergence and its relative simplicity for application. The principle of the sliding mode control is to force the system trajectories to reach a domain (named sliding surface) in a finite time. This domain is attractive: once the system trajectory has reached it, it is insensitive to the perturbations and uncertainties, and the dynamics of the closed-loop system is linked to the sliding surface definition. The design of the sliding mode control is made in two steps. The first one consists in defining the sliding surface from the control objective (it is generally described as a differential equation involving the system output). The second step consists in designing a discontinuous control law, in order to force the system trajectories to reach and to remain on the sliding surface after a finite time, in spite of the uncertainties and perturbations.

In the sequel, one considers the uncertain nonlinear system

$$\begin{array}{rcl} \dot{x} & = & f(x,t) + g(x,t) \cdot u \\ y & = & h(x) \end{array} \tag{1.1}$$

with $x \in \mathcal{X} \subset \mathbb{R}^n$ the system state ($\mathcal{X}$ being a bounded subset of $\mathbb{R}^n$), and $u \in \mathbb{R}$ the control input. The control output is $y \in \mathbb{R}$ [1]. Functions $f(x,t)$ and $g(x,t)$ are differentiable uncertain vector-fields.

1.1.1 Sliding variable and sliding surface

Define the function $\sigma(x,t) : \mathcal{X} \times \mathbb{R}^+ \to \mathbb{R}$ as a sufficiently differentiable function which can be viewed as a fictive output for system (1.1) (in the sequel, details concerning the relation between σ and y will be given). The function σ is named *sliding variable*. The sliding surface S is defined by

$$S = \{x \in \mathcal{X}, t \geq 0 | \sigma(x,t) = 0\} \tag{1.2}$$

Definition 1.1.1 (Utkin [1992]). *There exists an ideal sliding mode (or called sliding motion) on S if, after a finite time t_F, the solution of system (1.1) satisfies $\sigma(x,t) = 0$ for all $t \geq t_F$.*

The sliding surface can be considered as a hypersurface in the state space. Once the system trajectories are evolving on the sliding surface, the dynamics of the system is determined by its definition. Furthermore, the choice of S (and then of σ) must lead to the convergence of the system output towards the control objective.
The standard sliding mode control firstly proposed by Utkin [1977] is the first order sliding mode control. It can be applied to systems with relative degree equal to one with respect to the sliding variable.

Definition 1.1.2 (Isidori [2013]). *Consider system (1.1), with the sliding variable σ. It is said to have the relative degree r, if the Lie derivatives locally satisfy the conditions*

$$L_g\sigma = L_f L_g\sigma = \ldots = L_f^{r-2} L_g\sigma = 0, \; L_f^{r-1} L_g\sigma \neq 0 \; .$$

The relative degree of the sliding variable is interpreted as the minimum number of times that one has to differentiate σ, with respect to time in order to make appearing explicitly of u .
Supposing that the control objective is to make the output $y(t)$ of system (1.1) track a reference signal $y_{ref}(t)$, then the control task is to force the tracking error

$$e \;\; = \;\; y(t) - y_{ref}(t) \tag{1.3}$$

towards zero. Consider the following assumption

1. For a sake of clarity, the sliding mode concepts are presented in single input-single output (SISO) case.

Assumption 1.1.1. *The relative degree of system (1.1) with respect to the tracking error e equals r, i.e.*

$$\begin{aligned} e^{(r)} &= y^{(r)}(t) - y_{ref}^{(r)}(t) \\ &= \psi(x,t) + b(x,t)u \end{aligned} \tag{1.4}$$

with $b(x,t) \neq 0$.

Then, consider the following definition of the sliding variable

$$\sigma(x,t) = e^{(r-1)} + \ldots + c_2\ddot{e} + c_1\dot{e} + c_0 e \,, \tag{1.5}$$

the coefficients c_i $(0 \leq i \leq r-2)$ being chosen such that the polynomial

$$P(\lambda) = \lambda^{r-1} + \sum_{i=0}^{r-1} c_i \lambda^i \tag{1.6}$$

is a Hurwitz polynomial. Therefore, the convergence of σ to zero leads to the asymptotic convergence of the tracking error e to zero. Moreover, the sliding variable has a relative degree equal to one, given that

$$\begin{aligned} \dot{\sigma}(x,t) &= e^r + \sum_{i=0}^{r-2} c_i e^{i+1} \\ &= \psi(x,t) + \sum_{i=0}^{r-2} c_i e^{i+1} + b(x,t)u \\ &= a(x,t) + b(x,t)u \end{aligned} \tag{1.7}$$

with

$$a(x,t) = \psi(x,t) + \sum_{i=0}^{r-2} c_i e^{i+1} \tag{1.8}$$

Consider now the following assumption

Assumption 1.1.2. *Function $a(x,t)$ is a bounded uncertain function, whereas $b(x,t)$ is a positive and bounded function. Thus, there exist positive constants a_M, b_m, b_M such that*

$$\begin{aligned} &|a(x,t)| \leq a_M \\ &0 < b_m \leq b(x,t) \leq b_M \end{aligned} \tag{1.9}$$

for $x \in \mathcal{X}$ and $t \geq 0$.

Once the sliding variable is defined, the second step consists in designing the control input u in order to stabilize system (1.7) in a finite time, and in spite of uncertainties on both functions a and b.

1.1.2 First order sliding mode control input design

The control input u must be designed in order to force the system trajectories to reach and evolve on the sliding surface (1.2) in spite of the uncertainties and perturbations. This task can be achieved by applying Lyapunov function technique.

Definition 1.1.3. *A function $V : \mathbb{R}^n \to \mathbb{R}$ is a candidate Lyapunov function if*

- $V(0) = 0$;

- $\forall x \in \mathcal{X} \setminus \{0\}$, *one has* $V(x) > 0$.

Then, the sign of the derivative of the candidate Lyapunov function gives the information about the system stability. For the sliding variable σ (1.5), a candidate Lyapunov function takes the form

$$V(\sigma) = \tfrac{1}{2}\sigma^2 \tag{1.10}$$

which is positive definite; so Definition 1.1.3 is satisfied. In order to ensure the asymptotic convergence of the sliding variable σ, the time derivative of V has to be negative definite *i.e.*

$$\dot{V}(\sigma) = \sigma\dot{\sigma} < 0 \; . \tag{1.11}$$

The inequality (1.11) is called the attractive condition. Remark that in order to achieve the **finite time** convergence of σ towards zero, a more strict condition called η-attractive condition Utkin [1992] reading as

$$\sigma\dot{\sigma} \leq -\eta|\sigma|, \qquad \eta > 0 \tag{1.12}$$

must be fulfilled. It means that

$$\dot{V} \leq -\eta\sqrt{2V} \; . \tag{1.13}$$

This latter yields that

$$\frac{d\sqrt{2V(t)}}{dt} \leq -\eta \tag{1.14}$$

then

$$\sqrt{2V(t)} - \sqrt{2V(0)} \leq -\eta t \; . \tag{1.15}$$

One has

$$\eta t \leq |\sigma(0)| - |\sigma(t)| \; . \tag{1.16}$$

Consequently, σ reaches zero in a finite time t_F with

$$t_F \leq \frac{|\sigma(0)|}{\eta} \; . \tag{1.17}$$

Therefore, a control u computed to satisfy condition (1.12) will drive the sliding variable σ to zero in a finite time. A such control u takes the form

$$u = -K\text{sign}(\sigma) \; . \tag{1.18}$$

The control gain K must be chosen large enough to ensure the η-attractive condition. Then, from (1.12), the gain K must verify

$$K \geq \frac{|a(x,t)| + \eta}{b(x,t)} \; . \tag{1.19}$$

From Assumption 1.1.2, a sufficient condition reads as

$$K \geq \frac{a_M + \eta}{b_m} \tag{1.20}$$

Then, with the control input (1.18) where the gain verifies (1.20), the convergence of σ to zero is ensured in a finite time t_F given by (1.17). Once the system trajectory is evolving on the sliding surface, the dynamics of the system is determined by the parameters in the definition of the sliding variable (1.5). Then, given the feature (1.6), the tracking error will asymptotically converge to zero.

1.1.3 Example

In order to clarify the first order sliding mode control design, an academic example in Laghrouche [2004] is introduced. Consider the following system which is under the form (1.1)

$$\begin{array}{rcl} \dot{x}_1 & = & x_2 \\ \dot{x}_2 & = & u + \alpha \sin(y) \\ y & = & x_1 \end{array} \tag{1.21}$$

with $\alpha \in \mathbb{R}$, $\alpha sin(y)$ being a matched perturbation. Define the sliding variable as

$$\sigma = x_2 + c_1 x_1 \quad \text{with } c_1 > 0 \; . \tag{1.22}$$

Then, the sliding surface is given by

$$S \;=\; \{x \in \mathcal{X} | x_2 + c_1 x_1 = 0\} \; . \tag{1.23}$$

Once the system trajectories are evolving on the sliding surface, one has $x_2 = \dot{x_1} = -c_1 x_1$. It yields that $x_1(t) = x_1(0) e^{-c_1 t}$. Then, the system output $y = x_1$ will exponentially converge to zero, with a convergence rate defined by c_1. Then, design the control input as

$$u \;=\; -K \text{sign}(\sigma) \; . \tag{1.24}$$

According to (1.19), the gain K must be large enough such that

$$K \;\geq\; \eta + |c_1 \dot{y}| + \alpha |\sin(y)| \; . \tag{1.25}$$

If it is the case, the controller forces the system trajectories to the sliding surface in a finite time.
Figure 1.1 displays the system trajectories on the phase plane, where the sliding surface is represented by the red dotted line crossing the origin point. The initial condition is chosen on the x_1-axis ($x_2 = 0$). In a finite time, the system trajectory reaches the sliding surface. Then, the system dynamics is determined by the definition of the sliding surface (*i.e.* by the choice of c_1). Figure 1.2 shows the states variables (top), the control input (middle) and the sliding variable σ (bottom). Thanks to the discontinuous control input, the system states x_1 and x_2 converge to zero in spite of the perturbation.

1.2 Chattering phenomenon

The "ideal" sliding motion $\sigma = 0$ requires the switching of the control input at an infinite frequency. Obviously, in practice, only the switching at a finite frequency can be achieved. Then, in practical cases, the discontinuous control input causes an oscillation phenomenon, called *chattering* phenomenon Utkin and Lee [2006]. The chattering may be a harmful phenomenon because it leads to low control accuracy, high wear of moving mechanical parts, and high heat losses in power circuits. There are two main reasons which can cause the chattering: firstly, it can be caused by fast dynamics which have been neglected Utkin and Shi [1996]; the second reason is the use of digital controllers with finite sampling period Guldner and Utkin [2000]. Since the control is constant within a sampling period, the limited sampling frequency leads to the chattering as well. In the previous example, the simulation has been made with a limited sampling period. So, if one makes a zoom around the sliding surface ($\sigma = 0$) (see Figure 1.3), under the discontinue control input, the chattering phenomenon clearly appears.

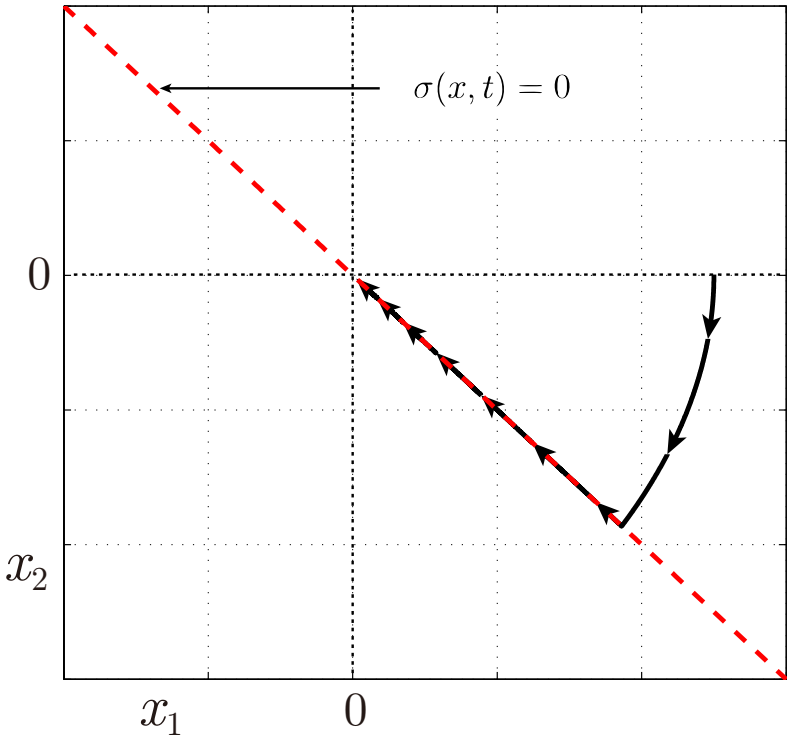

Figure 1.1 – Trajectory of system (1.21) in the phase plane (x_1, x_2).

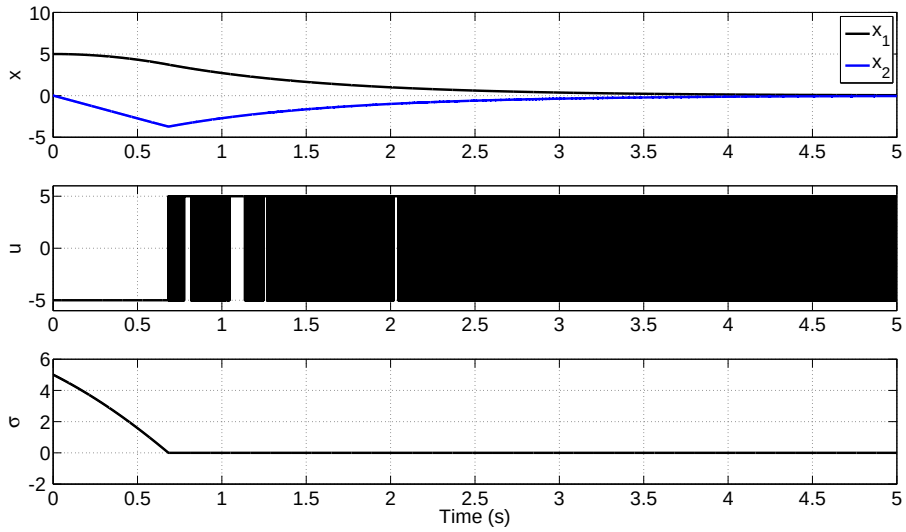

Figure 1.2 – **Top.** State variables x_1 and x_2 versus time (sec); **Middle.** control input u versus time (sec); **Bottom.** sliding variable σ versus time (sec).

In order to reduce the chattering phenomenon, several solutions have been proposed. For example, a method consists in replacing the "sign" function by an approximate continuous one, in a vicinity of the sliding surface S Burton and Zinober [1986]. In this case, the system is said to have a "pseudo" sliding motion Yu and Potts [1992]. In the sequel, some approximate functions are introduced.

The saturation function. The function $\text{sign}(\sigma)$ (Figure 1.4 (a)) is replaced by a linear function when the system trajectory is evolving around a vicinity of the sliding surface with a width of

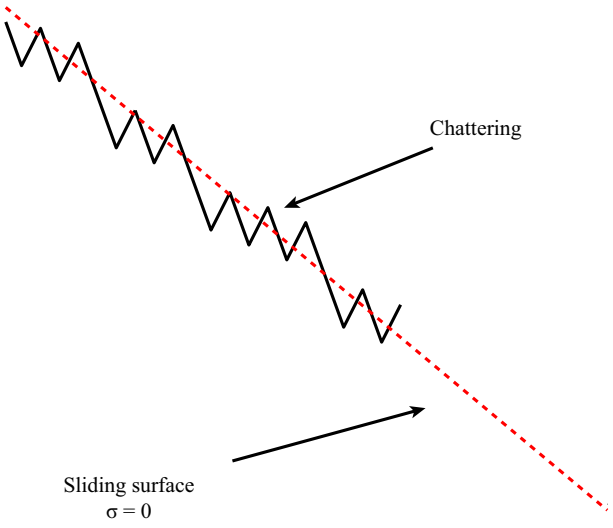

Figure 1.3 – The chattering phenomenon.

2δ (see Figure 1.4 (b)). Its expression is given by

$$\text{sat}(\sigma, \delta) = \begin{cases} \text{sign}(\sigma) & \text{if } |\sigma| > \delta \\ \dfrac{\sigma}{\delta} & \text{if } |\sigma| \leq \delta \end{cases} \tag{1.26}$$

The *atan* function. For a small enough parameter δ, the function

$$v(\sigma, \delta) = \frac{2}{\pi}\text{atan}(\frac{\sigma}{\delta}) \tag{1.27}$$

is an accurate approximation of the sign function. The graph of this function with $\delta = 0.02$ is shown in Figure 1.4 (c).
The *htan* function. Another solution is to use the hyperbolic tangent function

$$v(\sigma, \delta) = \text{htan}(\frac{\sigma}{\delta}) \tag{1.28}$$

with $0 < \delta < 1$. Its graph with $\delta = 0.1$ is given by Figure 1.4 (d).

Note that replacing the sign function by its continuous approximation allows to reduce the chattering, but also reduce the robustness of the controller.
Another solution to reduce the chattering phenomenon, that is displayed in the sequel, consists in designing high order sliding mode controller.

1.3 High order sliding mode control

The standard sliding mode control can be applied to systems with relative degree equal to one with respect to the sliding variable. As viewed previously, the high frequency switching of the control input induces chattering phenomenon. Since the two last decades, the development of high order sliding mode control attracts a lot of attention such as the works Bartolini et al. [1998]; Levant [2003, 2005a]; Laghrouche et al. [2007]. This class of controllers consists in driving the sliding variable and a finite number of its consecutive time derivatives to zero in a finite time. By this way, the discontinuous control acts on high order time derivative of the sliding variable which leads to the chattering attenuation.

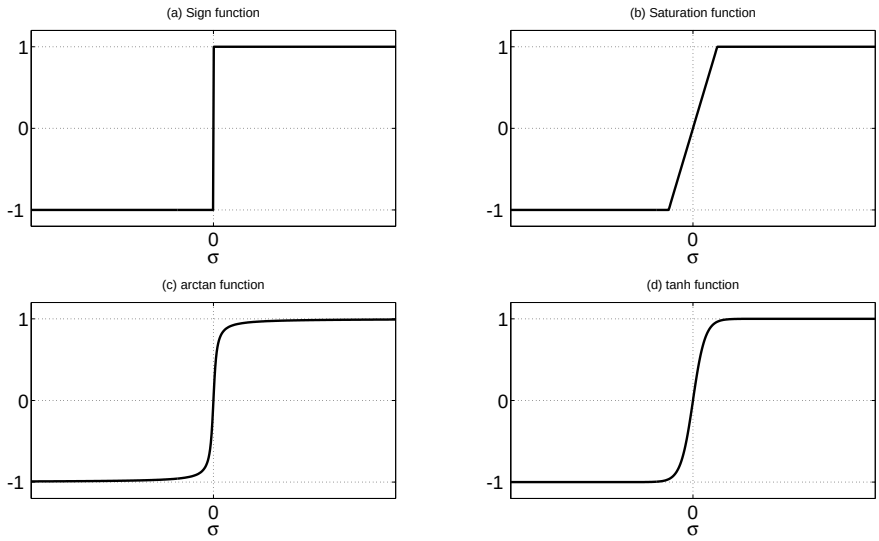

Figure 1.4 – Sign function and some approximate functions.

Definition 1.3.1. *Shtessel et al. [2014] Consider system (1.1) with the sliding variable $\sigma(x)$, let $r \geq 1$ be an integer. Then, if*

1. *the successive time derivatives $\sigma, \dot{\sigma}, \ldots \sigma^{(r-1)}$ are continuous functions of x;*
2. *the set*
$$\{x \in \mathcal{X} | \sigma = \dot{\sigma} = \ldots = \sigma^{(r-1)} = 0\} \tag{1.29}$$
is a nonempty integral set;
3. *the Filippov set of admissible velocities at the r-sliding points (1.29) contains more than one vector;*

the motion on the set (1.29) is said to exist in an r^{th}-order sliding mode. The set (1.29) is called the r^{th}- order sliding mode set.

If the controller switches with an infinite frequency, the system trajectories will theoretically reach in a finite time the r^{th}-order sliding set. However, in reality, it is impossible to satisfy this condition, such sliding mode cannot be attained. The sliding motion can only take place in a vicinity of the r^{th}-order sliding mode set. This behavior is called *real r^{th}-order sliding mode*.

Definition 1.3.2. *Levant [2003] Consider the nonlinear system (1.1) and the sliding variable σ, let $r \geq 1$ be an integer; consider also an integer $r \geq 1$. Assume that the successive time derivatives $\sigma, \dot{\sigma}, \ldots, \sigma^{(r-1)}$ are continuous functions. The manifold defined as (T_e being the sampling period of the control law)*
$$\left\{x \mid |\sigma| \leq \mu_0 T_e^r, \cdots, |\sigma^{(r-1)}| \leq \mu_{r-1} T_e\right\} \tag{1.30}$$
with $\mu_i \geq 0$ (with $0 \leq i \leq r-1$), is called "real r^{th}-order sliding mode set", which is non-empty and is locally an integral set in the Fillipov sense. The motion on this manifold is called "real r^{th}-order sliding mode" with respect to the sliding variable σ.

In the sequel, only some algorithms which are involved in the thesis work, are presented. However, readers can found other high order sliding mode controllers in

- the works Bartolini et al. [1996, 1998, 1999, 2001]; Plestan et al. [2010a] concerning second order sliding mode control;
- the papers Levant [2005a]; Laghrouche et al. [2007]; Plestan et al. [2008a] about higher order sliding mode control.

1.3.1 Twisting and super-twisting algorithms

Consider the system (1.1) and the sliding variable $\sigma(x,t)$, the objective of the second order sliding mode control being to drive σ and its first time derivative to zero in a finite time *i.e.*

$$\sigma = \dot{\sigma} = 0 \ . \tag{1.31}$$

Twisting control [Levantovsky [1985]]

This method can be applied to a class of systems with a relative degree equal to one or two with respect to the sliding variable. Consider the system (1.1), and without loss of generality, define from the control objective the sliding variable $\sigma(x,t)$ with a relative degree equal to two. One gets

$$\ddot{\sigma} \ = \ a(x,t) + b(x,t) \cdot u \tag{1.32}$$

with functions $a(x,t)$ and $b(x,t)$ supposed to be bounded. Suppose that there exist positive constants a_M, b_m, b_M such that

$$\begin{array}{l} |a(x,t)| \leq a_M \\ 0 < b_m \leq b(x,t) \leq b_M \end{array} \tag{1.33}$$

for $x \in \mathcal{X}$ and $t > 0$. The twisting algorithm Levantovsky [1985]; Shtessel et al. [2014] reads as

$$u(t) = -K_1 \text{sign}\,(\sigma) - K_2 \text{sign}\,(\dot{\sigma}) \ . \tag{1.34}$$

If K_1 and K_2 satisfy the conditions

$$\begin{array}{l} K_1 > K_2 > 0 \ , \ (K_1 - K_2) b_m > a_M \\ (K_1 + K_2) b_m - a_M > (K_1 - K_2) b_M + a_M \ , \end{array} \tag{1.35}$$

the controller guarantees the establishment of a second order sliding mode with respect to σ in a finite time. Remark that in the twisting algorithm, both the sliding variable and its time derivative are required.

Super-twisting control [Levant [1998]]

The super-twisting algorithm Levant [1998] can be only applied to systems with a relative degree equal to one with respect to the sliding variable. Then, the discontinuity acts on the first time derivative of the control input. Due to the structure of the algorithm, a continuous input is obtained, which means that the chattering is reduced. Consider the system (1.1), the dynamics of the sliding variable reading as

$$\dot{\sigma} \ = \ a(x,t) + b(x,t) \cdot u \tag{1.36}$$

with functions $a(x,t)$ and $b(x,t)$ supposed to be bounded. There exist positive constants C, b_m, b_M, U_M, q such that

$$\begin{array}{l} |\dot{a}| + U_M |\dot{b}| \leq C \\ 0 < b_m \leq b \leq b_M \\ |a/b| < q U_M \\ 0 < q < 1 \end{array} \tag{1.37}$$

Then, the super-twisting algorithm is given by Levant [1998]

$$\begin{array}{rcl} u & = & -\lambda |\sigma|^{1/2} \text{sign}(\sigma) + u_1 \\ \dot{u}_1 & = & \left\{ \begin{array}{lll} -u & \text{if} & |u| > U_M \\ -\alpha \text{sign}(\sigma) & \text{if} & |u| \leq U_M \end{array} \right. \ . \end{array} \tag{1.38}$$

With $\alpha > C/b_m$ and large enough λ, the controller (1.38) ensures the establishment of a second order sliding mode with respect to σ *i.e.* $\sigma = \dot{\sigma} = 0$.

1.3.2 High order sliding mode controllers

Among various algorithms Laghrouche et al. [2007]; Plestan et al. [2008a]; Levant [2005b] only the quasi-continuous sliding mode controller Levant [2005b] is detailed in the following: this algorithm will be used for the electropneumatic system for performances comparisons. Consider the system (1.1), and suppose that the sliding variable σ is defined such that the relative degree of (1.1) with respect to σ equals r, which is constant and known. It means that

$$\sigma^{(r)} = a(x,t) + b(x,t)u \tag{1.39}$$

with functions $a(x,t)$ and $b(x,t)$ supposed to be bounded. There exist positive constants a_M, b_m, b_M such that

$$\begin{array}{l} |a(x,t)| \leq a_M \\ 0 < b_m \leq b(x,t) \leq b_M \end{array} \tag{1.40}$$

for $x \in \mathcal{X}$ and $t > 0$. The quasi-continuous controller is defined by the following algorithm Levant [2005b]

$$\begin{array}{l} \varphi_{0,r} = \sigma,\ N_{0,r} = |\sigma|,\ \psi_{0,r} = \text{sign}(\sigma) \\ \varphi_{i,r} = \sigma^{(i)} + \beta_i N_{i-1,r}^{(r-i)/(r-i+1)} \psi_{i-1,r} \\ N_{i,r} = |\sigma^{(i)}| + \beta_i N_{i-1,r}^{(r-i)/(r-i+1)} \\ \psi_{i,r} = \frac{\varphi_{i,r}}{N_{i,r}},\ i = 1, \ldots . r-1 \end{array} \tag{1.41}$$

with $\beta_1, \ldots, \beta_{r-1}$ being positive constants, and

$$u = -\alpha \psi_{r-1,r}(\sigma, \dot{\sigma}, \ldots, \sigma^{(r-1)}) \,. \tag{1.42}$$

If the control gain α is chosen large enough depending on a_M, b_m, b_M, the control law (1.42) guarantees the establishment of a r^{th}-order sliding mode with respect to σ (1.39) in a finite time Levant [2005b]. For specific $r \leq 3$, the control form is given as follows.

- For $r = 2$, the control input is given by

$$u = -\alpha \frac{\dot{\sigma} + \beta_1 |\sigma|^{1/2} \text{sign}(\sigma)}{|\dot{\sigma}| + \beta_1 |\sigma|^{1/2}} \,. \tag{1.43}$$

- For $r = 3$, one gets

$$u = -\alpha \frac{\ddot{\sigma} + \beta_2 (|\dot{\sigma}| + \beta_1 |\sigma|^{2/3})^{-1/2} (\dot{\sigma} + \beta_1 |\sigma|^{2/3} \text{sign}(\sigma))}{|\ddot{\sigma}| + \beta_2 (|\dot{\sigma}| + \beta_1 |\sigma|^{2/3})^{1/2}} \tag{1.44}$$

For the tuning of the control gain α, the redundantly large estimation of a_M, b_m, b_M may lead to an oversized gain, then enhances the chattering phenomenon. So, there is a real interest to develop an adaptation algorithm for the gain. In the next section, the gain adaptation concept is presented.

1.4 Sliding mode control with gain adaptation

As viewed previously, in many cases, tuning of controller gains is not a trivial task, because the gain is depending on the bounds of uncertainties. The determination of these bounds can require tedious process of identification, and usually induces overestimation of the gain. Then, the gain adaptation offers a solution to the control problem for which the bounds of uncertainties and perturbations are unknown or not well-known. The gain adaptation allows a gain adjustment with respect to a predefined criterion and then strongly simplifies the tuning process. As used in Shtessel et al. [2012], the gain adaptation is based on the following principle:

- if the system trajectories are not evolving on the sliding surface, it could be caused by a not sufficiently large gain or a too long convergence time. In this case, the control gain must be increased in order to reduce the convergence time and ensure the establishment of the sliding mode;
- on the other hand, if the system trajectories are evolving on the sliding surface, it means that the control gain is large enough to reject the perturbations and to guarantee the sliding mode, then it has to be reduced.

Consider the system (1.1), and the sliding variable dynamics is defined as

$$\dot{\sigma} = a(x,t) + b(x,t)u \tag{1.45}$$

where function $a(x,t)$ is a bounded uncertain function and $b(x,t)$ is positive and bounded. Thus, there exist positive constants a_M, b_m, b_M such that

$$\begin{array}{l} |a(x,t)| \leq a_M \\ 0 < b_m \leq b(x,t) \leq b_M \end{array} \tag{1.46}$$

for $x \in \mathcal{X}$ and $t > 0$.
There exist several gain adaptation laws for second order sliding mode controllers Taleb et al. [2013]; Taleb and Plestan [2012]; Estrada et al. [2013]. However, for a sake of clarity, only the gain adaptation law for standard sliding mode control is presented in this section.
In Plestan et al. [2010b], an adaptive gain algorithm is designed for a first order sliding mode control

$$u = -K(t)\text{sign}(\sigma) \tag{1.47}$$

with $K(t)$ the time varying gain. The design of the adaptation gain law is usually composed by two parts: the design of a sliding mode detector and the design of a gain adaptation law.

Sliding mode detector. Through the parameter ϵ, define the real first order sliding surface as

$$S = \{x \in \mathcal{X} || \sigma | < \epsilon\} \tag{1.48}$$

It means that, when the sliding variable reaches the vicinity of zero with accuracy ϵ, one declares that a real first order sliding mode is established. Note that it is totally related to Definition 1.3.2.

Gain adaptation law. The time varying gain $K(t)$ is defined through the following dynamics

$$\dot{K} = \left\{ \begin{array}{ll} \Gamma |\sigma| \text{sign}(|\sigma| - \epsilon) & \text{if} \quad K > \mu \\ \mu & \text{if} \quad K \leq \mu \end{array} \right. \tag{1.49}$$

with $K(0) > 0$, $\Gamma > 0$, $\epsilon > 0$ and $\mu > 0$ very small. The parameter μ is introduced only to ensure a positive gain K. Given (1.49), one has

- $\dot{K} > 0$ if $|\sigma| > \epsilon$: real sliding mode is not established, then the gain increases;
- $\dot{K} < 0$ if $|\sigma| < \epsilon$: real sliding mode is established, then the gain decreases.

By this way, the sliding mode is ensured in a finite time by a bounded gain K Plestan et al. [2010b].

1.5 High order differentiation problem

As viewed previously, for the second order sliding mode control, the twisting method requires both the sliding variable and its time derivative. It is not the case of super-twisting

algorithm, but it can be applied only to systems with relative degree equal to one with respect to the sliding variable, which means that the sliding variable will contain the time derivatives of the output in many cases. For r^{th}-order sliding mode controller (1.42), the $r-1^{th}$-order time derivatives of the sliding variable are required.
In practice, the numerical differentiators are used to estimate the derivatives. As presented in Yan et al. [2014b], there exist many numerical differentiation approaches, including the most common Euler method and the high order sliding mode differentiator that is detailed below.

High order sliding mode differentiator.

Let the input signal $f(t)$ be a function defined on $[0,+\infty]$ and consisting of a bounded Lebesgue-measurable noise with unknown features and an unknown basic signal $f_0(t)$, whose k-th time derivative has a known Lipschitz constant $L>0$. Its time derivatives $f_0^{(i)}(t)$, $i=0,1,\ldots,k$, can be estimated by the differentiator Levant [2003]

$$\begin{array}{rcl}
\dot{z_0} & = & v_0 \\
v_0 & = & -\hat{\lambda}_k L^{1/k+1}|z_0-f|^{k/k+1}\times \text{sign}(z_0-f)+z_1 \\
\dot{z_i} & = & v_i \\
v_i & = & -\hat{\lambda}_{k-i} L^{1/k-i+1}|z_i-v_{i-1}|^{k-i/k-i+1} \\
 & & \times \text{sign}(z_i-v_{i-1})+z_{i+1} \\
\dot{z_k} & = & -\hat{\lambda}_0 L\,\text{sign}(z_k-v_{k-1}) \\
i & = & 0,\ldots,k-1
\end{array} \tag{1.50}$$

with z_i the estimation of $f_0^{(i)}$ and $\hat{\lambda}_0,\ldots,\hat{\lambda}_k$ the differentiator parameters.

Remark 1.5.1. *According to Levant [2003], a possible choice for the parameters* $\hat{\lambda}_0,\ldots,\hat{\lambda}_k$, $(k\leq 5)$ *is*

$$\{\hat{\lambda}_i\}_{i=o}^{k-1} = 1.1, 1.5, 2, 3, 5$$

By substituting expressions v_i in (1.50), one gets the non-recursive form

$$\begin{array}{rcl}
\dot{z_i} & = & -\lambda_{k-i} L^{(i+1)/(k+1)}|z_0-f|^{(k-i)/(k+1)}\times \text{sign}(z_0-f)+z_{i+1} \\
\dot{z_k} & = & -\lambda_0 L\text{sign}(z_0-f)
\end{array} \tag{1.51}$$

with $\lambda_0,\lambda_1,\ldots,\lambda_k>0$ the new coefficients calculated from (1.50). The expressions of the high order sliding mode differentiator for $k=2$ reads as

$$\begin{array}{rcl}
\dot{z}_0 & = & z_1-\lambda_2 L^{1/3}|z_0-f|^{2/3}\text{sign}(z_0-f) \\
\dot{z}_1 & = & z_2-\lambda_1 L^{2/3}|z_0-f|^{1/3}\text{sign}(z_0-f) \\
\dot{z}_2 & = & -\lambda_0 L\text{sign}(z_0-f)\ .
\end{array} \tag{1.52}$$

It allows to estimate the first and second time derivatives of $f_0(t)$.

Example.

Consider the signal $f(t)$, which is composed by a basic signal $f_0(t)$ and a bounded Lebesgue-measurable noise $n(t)$, *i.e.*

$$f(t) = f_0(t)+n(t) \tag{1.53}$$

with $f_0(t)=5\text{sin}(t)$ and $n(t)$ chosen as a white noise with amplitude 10^{-2}. The signal is measured with a sampling period $T_e=0.01$s. The objective is to estimate the first and second order time derivatives of the basic signal $f_0(t)$ by using Euler method and high order sliding

mode differentiator (1.52). The parameter for the high order sliding mode differentiator is tuned as $L = 5$. The estimation results are presented in Figure 1.5-1.6.
For the first order differentiation (see Figure 1.5), the Euler differentiator is sensitive to the noise and the estimation result is less accurate than the one obtained with high order sliding mode differentiator. Calculating the standard deviation of the estimation error for $t \in [5,\ 10]$s, the performance of high order sliding mode differentiator (with $\mathrm{std} = 0.003$) is better than the one of Euler method with (with $\mathrm{std} = 0.015$).
For the estimation of second order derivative (see Figure 1.6), the Euler differentiator can not offer a reasonable estimation. And the high order sliding mode differentiator gives a much better result. However, it appears a time delay which is more or less unavoidable.

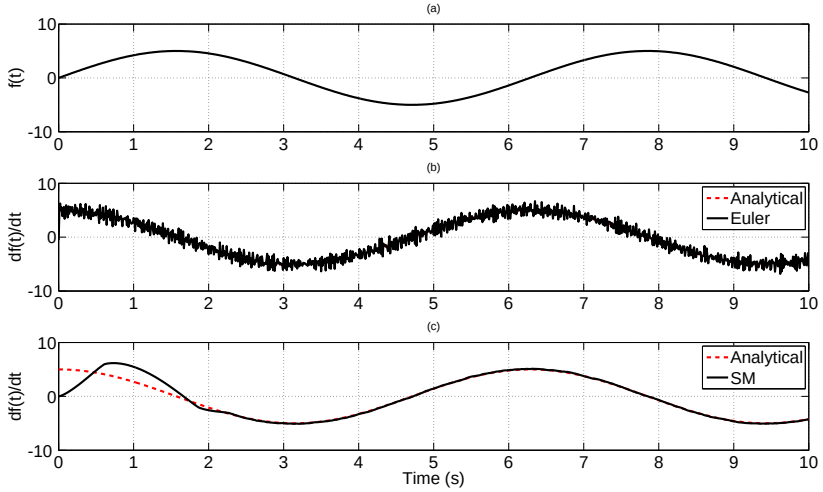

Figure 1.5 – **Top.** Signal $f(t)$ versus time (sec); **Middle.** Analytical first order time derivative $\dot{f}_0(t)$ (red dotted line) and estimated first order derivative using Euler method (black line) versus time (sec); **Bottom.** Analytical first order time derivative $\dot{f}_0(t)$ (red dotted line) and estimated first order derivative using high order sliding mode differentiator (black line) versus time (sec).

1.6 Motivations

The work of this thesis is firstly motivated by the control problem of an electropneumatic system. Since 2008, such system Plestan and Girin [2009] (see Figure 1.7) is equipped at laboratory IRCCyN. The objective of this platform is to evaluate the performances of control laws in the context of nonlinear systems with uncertainties and perturbations. This system is a typical nonlinear system with uncertainties and is perturbed by external forces. In the last decades, many robust control laws have been proposed to deal with the pneumatic system control. In Girin and Plestan [2009], the experimental electropneumatic actuator systems are designed, and state feedback control laws have been developed for the nonlinear model of the electropneumatic system. In Bouri and Thomasset [2001], sliding mode control laws have been applied to the electropneumatic system. In Chillari et al. [2001], an experimental comparison is made between several pneumatic position control methods. The sliding mode control shows its advantages due to its robustness features and the guarantee of finite time convergence.
One can cite results with first order sliding mode controllers Bouri and Thomasset [2001]; Smaoui et al. [2001], second order sliding mode ones Smaoui et al. [2005], and high order sliding mode ones Laghrouche et al. [2004]; Girin et al. [2009]. Note that high order sliding mode

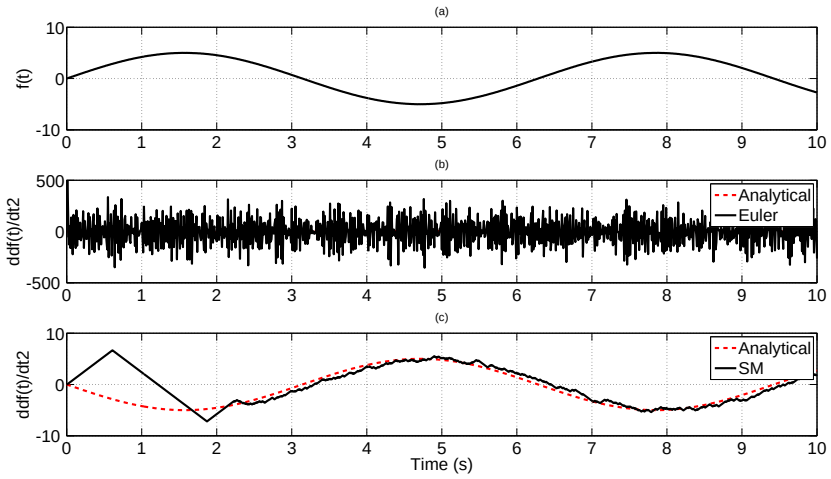

Figure 1.6 – **Top.** Signal $f(t)$ versus time (sec); **Middle.** Analytical second order time derivative $\ddot{f}_0(t)$ (red dotted line) and estimated second order derivative using Euler method (black line) versus time (sec); **Bottom.** Analytical second order time derivative $\ddot{f}_0(t)$ (red dotted line) and estimated second order derivative using high order sliding mode differentiator (black line) versus time (sec).

Figure 1.7 – Photo of electropneumatic system

controllers Levant [1993, 1998, 2003]; Shtessel et al. [2014] keep main features of sliding mode (robustness, finite convergence) but with strong reduction of the chattering phenomenon.
However, as claimed previously, for the high order sliding mode control, including the twisting control Levantovsky [1985] and the quasi-continuous control Levant [2005b], the sliding variable and its derivatives should be available. The use of these high order time derivatives introduce more disturbance, due to numerical differentiation process. Then, for the control of electropneumatic system, the velocity and acceleration should be estimated from the measurement of the position, which introduces disturbance into the controller. So, there is a really interest to develop new sliding mode control laws with a reduced use of time derivatives of the sliding variable. Such controllers already exist for example the *super-twisting* algorithm (1.38)

is an output feedback control law; however, it can only be applied to systems with a relative degree equal to one with respect to the sliding variable.
In practice, the numerical differentiators such as the Euler differentiator and the high order sliding mode differentiator Levant [2003], are used to estimate the derivatives. However, as presented in the previous section, for a noisy measurement, a bad estimation accuracy may lead to a possible degradation of the controller performance Levant [1998]; Yan et al. [2014b].
In order to over come such problem a solution is the sub-optimal controller proposed by Bartolini et al. [1997]. This method can be applied to the system with relative degree equal to two with respect to the sliding variable, and the use of time derivative of the sliding variable is removed. Nevertheless, this control law uses extremal detection of the sliding variable or the sign change of its time derivative, which can be highly sensible to the noise.
This thesis is dedicated to the development of high order sliding mode control with reduced use of time derivatives of the sliding variable. **In the context of second order sliding mode control, one of the objective of this thesis is to design a new control law which ensures the establishment of a real second order sliding mode, in a finite time, using only the information of the sliding variable.** Moreover, in opposition to the super-twisting algorithm, this method should be applicable to systems with relative degree equal to one or two with respect to the sliding variable.
Furthermore, in the position control of the electropneumatic system, the output has a relative degree equal to three. So, in this thesis, the research on third order sliding mode control is also made. **In the case of third order sliding mode control, the objective is to remove the use of the second order time derivative of the sliding variable in the controller.**
As introduced in Section 1.4, the gain adaptation mechanism is a very useful tool to simplify the gain tuning process and to improve the performance of the controller. **So, an other part of this thesis is focused on the development of adaptive gain algorithm for the proposed controllers**.

1.7 Organization and contribution of the thesis

This thesis is divided into three parts:

- **Part** I is dedicated to the presentation of three second order sliding mode control methods. A common point shared by these methods is the use of gain commutation technique. Their performances are compared.
    - In **Chapter** 3, the gain commutation formalism is presented. In this formalism, the control input is switching between two levels: a level with small magnitude and another one with large magnitude Yan et al. [2016e]. The main interest of this control formalism is to uniformly rewrite various second order sliding mode control laws. In order to ensure the establishment of second order sliding mode, some constraints based on a geometric analysis of the system trajectories are given on the duration of the large magnitude input application. Then, the twisting algorithm Levantovsky [1985] (denoted TWC) and a second order sliding mode output feedback control Plestan et al. [2010a] (denoted 2SMOFC) are reformulated in the gain commutation form.
    - **Chapter** 4 presents a new control approach named *Twisting-like* control (denoted TWLC) Yan et al. [2016d]. This method can be applied to systems with relative degree equal to two with respect to the sliding variable. The main feature of this method is that only the information of the sliding variable is used. Compared to the 2SMOFC, the large gain input is applied during several sampling periods. Thanks

to this latter feature, the convergence time for this proposed method is strongly improved with respect to 2SMOFC and close to the one obtained with twisting control, where the name twisting-like comes. The use of TWLC as a differentiator is presented as well.

- The comparisons between TWC, 2SMOFC and TWLC are made in **Chapter** 5 through an academic example and a pendulum system.

- **Part** II is focused on the sliding mode control with gain adaptation. The first contribution is the development of adaptive gain law for 2SMOFC and TWLC presented in Part I. Moreover, the result is extended to higher order sliding mode control. Indeed, an other contribution is the design of adaptive third order sliding mode control method (denoted 3SMC) Yan et al. [2016c]. Compared to the quasi-continuous high order sliding mode control, this method uses a reduced differentiation order of the sliding variable.

  - In **Chapter** 7 the adaptive versions of 2SMOFC and TWLC are presented. The gain adaptation law is based on the time gap between two successive sign commutations of the sliding variable. Then, the gain is adjusted using only the information of the sign of the sliding variable.
  - In **Chapter** 8, an adaptive third order sliding mode is proposed Yan et al. [2016c]. Only the first and second order time derivatives of the sliding variable should be known. For this new algorithm, the use of second order time derivative is removed. This feature helps to avoid the additional disturbance introduced by the high order differentiator. Moreover, the gain adaptation is also used to simplify the gain tuning process.

- **Part** III presents the applications of these new control laws on experimental systems.
  - **Chapter** 9 deals with the position control problem of the electropneumatic system. This is a typical nonlinear system with uncertainties and perturbations. The sliding mode methods show their advantages for the control of such systems. Firstly, second order sliding mode control laws TWC, 2SMOFC and TWLC are applied to the electropneumatic system, and their performances compared. Secondly, the adaptive versions of 2SMOFC and TWLC are applied. The effect for the use of gain adaptation mechanism is highlighted from the experimental results. Finally, the third order sliding mode controller (3SMC) presented in Chapter 8 is applied. Its performance is compared with higher order sliding mode controller (HOSMC) Levant [2005b].
  - In **Chapter** 10, the attitude control of an Unmanned Aerial Vehicles system with three degrees of freedom Quanser [2006] is considered. Due to the high sensitivity of the actuators to the vibration, continuous control input is required for this system. Then, in this chapter the integral version of twisting-like control (integral TWLC) is developed Yan et al. [2016b]. This control law can be applied to the system with relative degree equal to one, and gives a continuous input. Through the experimental tests, the performance of this new control law is compared to the super-twisting algorithm.

Some of the results presented in this thesis have been published or are under revision process for publication in journals and conferences.

Journal papers

- Xinming Yan, Antonio Estrada, and Franck Plestan, “Adaptive pulse output feedback controller based on second order sliding mode: methodology and application”, *IEEE*

Transactions on Control Systems Technology, available online, 2016, DOI: 10.1109/TCST.2016.2532801.
Yan et al. [2016a]

- Xinming Yan, Franck Plestan, and Muriel Primot, "A new third order sliding mode controller – application to an electropneumatic actuator", *IEEE Transactions on Control Systems Technology*, available online, 2016, DOI: 10.1109/TCST.2016.2571664.
Yan et al. [2016c]
- Xinming Yan, Muriel Primot, and Franck Plestan, "Electropneumatic actuator position control using second order sliding mode", *e& i Elektrotechnik und Informationstechnik Special Issue on Automation and Control - Sliding Mode Applications in Hydraulics and Pneumatics*, available online, 2016, DOI: 10.1007/s00502-016-0423-9.
Yan et al. [2016f]
- Xinming Yan, Muriel Primot, and Franck Plestan, "Adaptive output feedback twisting-like control with application to electropneumatic system" submitted (third lecture) to *International journal of robust and nonlinear control* , 2016.
Yan et al. [2016d]

Book chapter

- Franck Plestan, Xinming Yan, Mohammed Taleb, and Antonio Estrada, "Output feedback relay control in the second order sliding mode context with application to electropneumatic system", in *Recent Trends in Sliding Mode Control*, eds. L. Fridman, J. P. Barbot, F. Plestan, IET, PP 387-404, 2016.

Conference papers

- Xinming Yan, Franck Plestan, and Muriel Primot, "Perturbation observer for a pneumatic system: high gain versus higher order sliding mode solutions", *European Control Conference ECC*, Strasbourg, France, 2014.
Yan et al. [2014a]
- Xinming Yan, Muriel Primot, and Franck Plestan, "Comparison of differentiation schemes for the velocity and acceleration estimations of a pneumatic system", *IFAC World Congress*, Cape Town, South-Africa, 2014.
Yan et al. [2014b]
- Mohammed Taleb, Xinming Yan, and Franck Plestan, "Third order sliding mode controller based on adaptive integral sliding mode concept: experimental application to an electropneumatic actuator", *IEEE Conference on Decision and Control CDC*, Los Angeles, California, USA, 2014.
Taleb et al. [2014]
- Xinming Yan, Franck Plestan, and Muriel Primot, "Higher order sliding mode control with a reduced use of sliding variable time derivatives", *American Control Conference ACC*, Chicago, USA, 2015.
Yan et al. [2015]
- Xinming Yan, Muriel Primot, and Franck Plestan, "An unified formalism based on gain switching for second order sliding mode control", *International Workshop on Variable Structure Systems VSS*, Nanjing, China, 2016.
Yan et al. [2016e]

- Xinming Yan, Franck Plestan, and Muriel Primot, "Integral twisting-like control with application to UAVs attitude control", *IEEE Multi-Conference on Systems and Control, International Conference on Control Applications CCA*, Buenos Aires, Argentina, 2016. Yan et al. [2016b]

Second order sliding mode control under switching gain form

2

Introduction

As an important class of high order sliding mode control, the second order sliding mode control (2SMC) is well-known. The main property of 2SMC is the finite time convergence to zero (or to a vicinity of 0) of the sliding variable and its time derivative.
The twisting control (TWC) Levantovsky [1985], Shtessel et al. [2014] is a well-known 2SMC method. This method is applicable to systems with relative degree equal to 1 or 2, and guarantees the establishment of a second order sliding mode in finite time. However, a drawback of this controller is that both the sliding variable and its time derivative must be known. In practice, the sliding variable is usually measured with noise, and the use of numerical differentiators in this case may lead to a degradation of the controller performances Levant [1998], Yan et al. [2014b]. The super-twisting algorithm Levant [1998] may be the most popular solution of *output feedback* second order sliding mode controller (2SMC). However, it can only be applied to a system with relative degree equal to one ($r = 1$).
In order to overcome these drawbacks, an output feedback 2SMC algorithm (denoted 2SMOFC) using *only the sign* of the sliding variable and a switching gain strategy have been proposed in Plestan et al. [2010a], and then completed by Estrada and Plestan [2012], Estrada et al. [2013], Estrada and Plestan [2014]. This method deals with a class of nonlinear systems with sampled control input such that the relative degree with respect to the sliding variable is equal to 1 or 2. The main feature of this method is that a large gain input is applied during a single sampling step, when a switching of the sliding variable sign is detected. By this way, the control law ensures the establishment of a real second order sliding mode in a finite time. However, a disadvantage of this controller is that the convergence time strongly depends on the sampling step. When the sampling step tends to zero, the effect of the gain switching strategy is reduced, and the convergence time is increasing.
It appears that TWC and 2SMOFC use a similar strategy that can be called "switching gain" method. It means that the control input can switch between two levels: a low level with small magnitude and a high level with large gain. The first contribution of this part consists in proposing an unified control form based on a switching gain strategy. Thanks to this unified formalism, TWC and 2SMOFC are both reformulated; so that the advantages and disadvantages of each control law can be shown clearly.
The second objective of this part is to propose a new second order sliding mode control method based on the switching gain strategy. Similar to the 2SMOFC, the main idea is also to apply a large gain input when the sign switching of the sliding variable is detected. However, instead of

applying the high level control input during only one sampling period, it can be applied with a time varying duration. By this way, the use of derivative of the sliding variable is removed and the convergence time can be also improved.
Then, this second contribution consists in the presentation of a new output feedback control law named "twisting-like" control Yan et al. [2016d] (denoted TWLC). This name is given due to its performances close to those of twisting algorithm. Inherited from 2SMOFC, this control law only requires the sign of the sliding variable. Compared to TWC, this feature allows to avoid the additional noise introduced by the differentiator. Moreover, by improving the switching gain strategy of 2SMOFC, the system convergence time under this new controller is no longer sensitive to the sampling period and may reach dynamic performances close to those obtained by TWC.

2.1 Organization

This part is organized as follows: in Chapter 3, the unified switching gain form is presented and the convergence analysis tools are given. Then, the TWC and 2SMOFC are reformulated in the switching gain form, and their convergences are proved. The Twisting-like controller, presented in Chapter 4, is the main contribution of this part. The use of TWLC as a differentiator is presented as well. The comparisons between TWC, 2SMOFC and TWLC are made in Chapter 5 through an illustrative example and an application to a pendulum system.

2.2 System presentation

For the study of 2SMC, some general considerations have to be stated. Consider the uncertain nonlinear system

$$\dot{x} = f(x,t) + g(x,t) \cdot u \tag{2.1}$$

with $x \in \mathcal{X} \subset \mathbb{R}^n$ the state vector ($\mathcal{X}$ being a bounded subset of $\mathbb{R}^n$) and $u \in \mathbb{R}$ the control input. Functions $f(x,t)$ and $g(x,t)$ are differentiable uncertain vector-fields. Define from the control objective the sliding variable $\sigma(x,t)$, with relative degree equal to 2. It means that the control objectives are fulfilled when $\sigma = 0$ and

$$\ddot{\sigma} = a(x,t) + b(x,t) \cdot u \tag{2.2}$$

with functions $a(x,t)$ and $b(x,t)$ supposed to be uncertain. Then, the second order sliding mode control problem of system (2.1) with respect to σ is equivalent to the finite time stabilization around the origin of

$$\begin{aligned} \dot{z}_1 &= z_2 \\ \dot{z}_2 &= a(x,t) + b(x,t) \cdot u \end{aligned} \tag{2.3}$$

with $z_1 = \sigma$, $z_2 = \dot{\sigma}$. Suppose that the following assumptions are fulfilled.

Assumption 2.2.1. *The system trajectories are supposed to be infinitely extendible in time for any bounded Lebesgue measurable inputs.*

Assumption 2.2.2. *The controller is updated in discrete-time with the sampling period T_e which is a strictly positive constant. The control input u is constant between two successive sampling steps, i.e*

$$\forall t \in [kT_e,\ (k+1)T_e[\ \ u(t) = u(kT_e)\,. \tag{2.4}$$

Assumption 2.2.3. *The function $a(x,t)$ is a bounded uncertain function and $b(x,t)$ is positive and bounded. Thus, there exist positive constants a_M, b_m, b_M such that*

$$\begin{array}{l} |a(x,t)| \leq a_M \\ 0 < b_m \leq b(x,t) \leq b_M \end{array} \tag{2.5}$$

for $x \in \mathcal{X}$ and $t > 0$.

For the continuous system (2.3), the objective is to force z_1 and z_2 to zero in a finite time. However, if a sampled controller with positive sampling period T_e is considered, only a *real* second order sliding mode can be established after a finite time.

Definition 2.2.1 (Levant [1993])**.** *A real second order sliding mode is established for z_1 if, after a finite time,*

$$|z_1| < \mu_0 T_e^2, \;\; |\dot{z}_1| < \mu_1 T_e$$

hold for some positive constants μ_0, μ_1.

3

TWC and 2SMOFC under an unified form

Contents

As presented previously, two different types of 2SMC, the twisting control Levantovsky [1985] (TWC) and the second order sliding mode output feedback control Plestan et al. [2010a] (2SMOFC) use a similar strategy: the so-called "switching gain" concept. It means that the control input can switch between two levels: a low level with small magnitude and a high level with large magnitude. The motivation of the work developed in this chapter is to find an unified formalism for these two control laws. Moreover, in order to verify the convergence of system (2.3) under these control laws, new convergence analysis tools are proposed.

3.1 Presentation of an unified formalism

Consider system (2.3); the so-called "switching gain" strategy means that the control input u can switch between two levels: a low level $u = u_L$, and a high level $u = u_H$, with $|u_L| < |u_H|$. More precisely, the switching gain control strategy can be described as follows

$$u(kT_e) = \begin{cases} u_L(kT_e) = U(kT_e) & \text{if} \quad kT_e \notin \mathcal{T}_{\mathcal{H}} \\ u_H(kT_e) = \gamma U(kT_e) & \text{if} \quad kT_e \in \mathcal{T}_{\mathcal{H}} \end{cases} \tag{3.1}$$

with $\gamma > 1$, $k \in \mathbb{N}$, and $\mathcal{T}_{\mathcal{H}}$ allowing to define the time interval during which u_H is applied. In order to reformulate the second order sliding mode control laws (TWC and 2SMOFC) under this formalism, one defines U as

$$U(kT_e) = -K_m \text{sign}(z_1(kT_e)) \tag{3.2}$$

with $K_m > 0$, and T_e being the sampling period. This class of controllers is composed of three parts:

- the general control form (3.1)-(3.2);
- two gain parameters: K_m and γ;
- a switching gain condition $\mathcal{T}_{\mathcal{H}}$.

The main features of this formalism can be summarized as follows.

Remark 3.1.1. *Consider the control form* (3.1)-(3.2).

- *The control input can switch between four values* $\pm K_m$ *and* $\pm\gamma K_m$*, except when* $z_1(kT_e) = 0$*;*
- *the sign of the input* u *depends only on the sign of sliding variable* z_1*.*
- *the amplitude of* u *is time-varying and is related to the definition of* $\mathcal{T}_{\mathcal{H}}$*.*

In order to analyze the convergence condition for system (2.3) under such controller, a new tool presented in the next section gives rules for the tuning of parameters K_m, γ and for the design of $\mathcal{T}_{\mathcal{H}}$.

3.2 Convergence analysis of closed-loop system

In this section, convergence conditions are given for the class of control laws which can be written as (3.1)-(3.2). Consider system (2.3) under Assumptions 2.2.1-2.2.3, and introduce the following notations

- Denote $u^*(t)$ as

$$u^*(t) = \begin{cases} -K_m^*(t)\cdot \text{sign}(z_1(kT_e)) & \text{if} \quad kT_e \notin \mathcal{T}_{\mathcal{H}} \\ -K_M^*(t)\cdot \text{sign}(z_1(kT_e)) & \text{if} \quad kT_e \in \mathcal{T}_{\mathcal{H}} \end{cases} \tag{3.3}$$

  with K_m^* and K_M^* defined by

$$\begin{array}{rcl} K_m^*(t) & = & b(x,t)K_m - a(x,t)\text{sign}(z_1(kT_e)) \\ K_M^*(t) & = & b(x,t)\gamma K_m - a(x,t)\text{sign}(z_1(kT_e)) \end{array} \tag{3.4}$$

Then, system (2.3) can be rewritten as

$$\begin{array}{rcl} \dot{z}_1 & = & z_2 \\ \dot{z}_2 & = & u^* \end{array} \tag{3.5}$$

Before presenting the convergence analysis tool, the following notations are stated.

- Denote

$$\begin{array}{l} K_m^{max} = \max(K_m^*) = b_M K_m + a_M \\ K_m^{min} = \min(K_m^*) = b_m K_m - a_M \\ K_M^{max} = \max(K_M^*) = \gamma b_M K_m + a_M \\ K_M^{min} = \min(K_M^*) = \gamma b_m K_m - a_M. \end{array} \tag{3.6}$$

- Denote $t = t_i$ the instant when the system trajectory crosses z_2-axis for the i^{th} time, with $z_1(t_i) = 0$.
- Denote T_s^i the time at which the i^{th} z_1-sign switching is detected [1], *i.e.*

$$\text{sign}(z_1(T_s^i)) \neq \text{sign}(z_1(T_s^i - T_e)) \tag{3.7}$$

1. In this thesis, the time value with capital letter $t = T_*^*$ represents a sampling time whereas the time value with letter $t = t_*^*$ presents an instant on continuous time.

- Define also τ_i as the duration of large scale control between T_s^i and T_s^{i+1}, *i.e.*

$$[T_s^i,\ T_s^i + \tau_i] \quad = \quad \left\{kT_e | T_s^i \leq kT_e \leq T_s^{i+1} \text{ and } u(kT_e) = u_H\right\} \tag{3.8}$$

Consider the control laws under the form (3.1)-(3.2), for which the i^{th} large input is applied when the z_1-sign switching is detected (*i.e.* starts from T_s^i) and with the duration of τ_i. Then, the following theorem is given to analyze the convergence of system (2.3).

Theorem 3.1 (Yan et al. [2016d]). *Consider system (2.3) controlled by the switching gain form controller (3.1)-(3.2) and fulfilling Assumptions 2.2.1-2.2.3. Then, the system trajectory tends to be closer from the origin if the following conditions hold*

- $K_m > \dfrac{a_M}{b_m}$
- $\gamma > 2 + \dfrac{b_M}{b_m}$
- *The duration of the large magnitude control τ_i satisfies*

$$\begin{aligned} \int_{T_s^i}^{T_s^i+\tau_i} K_M^*(t)dt &\geq |z_2(t_i)| + K_m^{max} T_e - \Delta \\ \int_{T_s^i}^{T_s^i+\tau_i} K_M^*(t)dt &\leq |z_2(t_i)| + K_m^{max} T_e + \Delta' \end{aligned} \tag{3.9}$$

with Δ the positive root of

$$(\frac{1}{K_m^{min}} - \frac{1}{K_M^{min}})\Delta^2 \quad = \quad (\frac{z_2^2(t_i)}{K_m^{max}} - \frac{z_{20}^2}{K_M^{min}}), \tag{3.10}$$

Δ' the positive root of

$$(\frac{1}{K_m^{max}} - \frac{1}{K_M^{max}})\Delta'^2 \quad = \quad (\frac{z_2^2(t_i)}{K_m^{max}} - \frac{z_{20}^2}{K_M^{min}}) \tag{3.11}$$

and

$$z_{20}^2 \quad = \quad (|z_2(t_i)| + K_m^{max} T_e)^2 + 2K_M^{min}(|z_2(t_i)|T_e + \tfrac{1}{2}K_m^{max} T_e^2)\ . \tag{3.12}$$

Remark 3.2.1. *In order to ensure that the gain K_m^* defined by (3.4) is always positive ($K_m^{min} > 0$), the gain K_m must be chosen such that*

$$K_m \quad > \quad a_M/b_m\ . \tag{3.13}$$

Moreover, in order to make sure that the magnitude of high level control input is always larger than the low one, (i.e. $K_M^{min} > K_m^{max}$) the following condition must be satisfied

$$\gamma \quad > \quad 2 + \frac{b_M}{b_m}\ . \tag{3.14}$$

For the duration of the large gain input τ_i, if it is too short, the effect of switching gain will be reduced, then it leads to a too long convergence time. On the other hand, if this duration is too long, the duration for the small gain input will be reduced, which also weaken the switching gain effect. So, the constraints for the duration τ_i is given by (3.9).

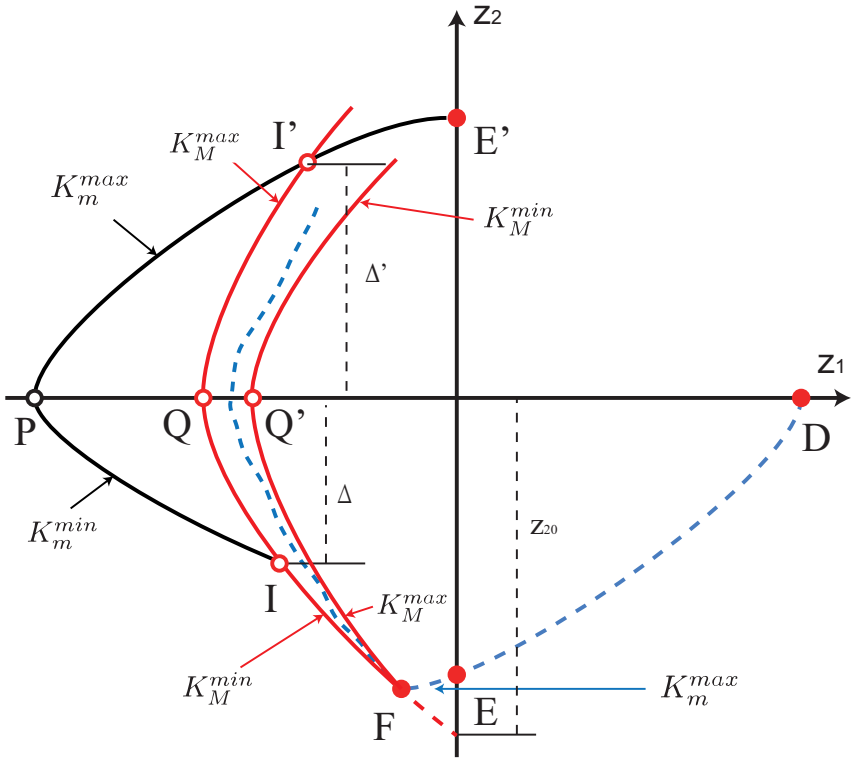

Figure 3.1 – Gain switching zone in the phase plane (z_1, z_2).

Proof. The proof of Theorem 3.1 is made in two steps

- the domain in which the system trajectories are going to evolve, just after the i^{th}-detection of z_1-sign switching, is defined; given that the duration τ_i is not *a priori* known, one has to consider the "worst" case: one evaluates the largest domain in which the system is evolving with $u = u_H$;
- the second step consists in evaluating the minimal and maximal values of τ_i-duration ensuring that, at the $i + 1^{th}$-detection of z_1-sign switching, the system trajectory is closer from the origin.

Step 1. Suppose that $t_i = t_E$ which is the time at which $\text{sign}(z_1)$ is switching, but it is not detected (see point E in Figure 3.1): system trajectory crosses z_2-axis such that $z_1(t_E) = 0$ and $z_2(t_E) < 0$. Consider the worst case, which corresponds to a delay for the detection of z_1-sign switching converging towards T_e, *i.e.* $t_F - t_E = T_e$. Early from the point F, $u = u_H$: in this case, the trajectory is evolving in the domain delimited by the two red curves of Figure 3.1 during a duration τ_i. The two curves delimiting the domain are obtained by the following way,

- from F to Q, one has $\dot{z}_2 = K_M^{min}$ whereas from Q, $\dot{z}_2 = K_M^{max}$. Given the perturbations bounds and the magnitude of the control input, it is the more external possible trajectory obtained from F;
- for the right-hand side red curve, from F to Q', $\dot{z}_2 = K_M^{max}$ whereas, from Q', $\dot{z}_2 = K_M^{min}$; it is the more internal possible trajectory.

Step 2. Denote now the point E' as the symmetric point of E with respect to the origin. Suppose that, all along the black trajectory between I and E', $u = u_L$, and evaluate the more external possible trajectory, which means that it is the trajectory for which the point P is the lefter

possible one. This trajectory is obtained by supposing that, from E' to P, $\dot{z}_2 = K_m^{max}$ whereas from P to I, $\dot{z}_2 = K_m^{min}$. Furthermore, this (black) trajectory obtained by supposing that $u = u_L$, intersects the (red) trajectories obtained with $u = u_H$ in two points, I and I'. It means that, considering the worst case, the point E' is reached from E if

- $u = u_H$ between F and I, and $u = u_L$ between I and E'
- or $u = u_H$ between F and I', and $u = u_L$ between I' and E'.

Therefore, a sufficient condition to ensure the convergence is that, denoting T_{SW} the time at which the control input u is switching between u_H to u_L, one has

$$z_2(I) \leq z_2(T_{SW}) \leq z_2(I'). \tag{3.15}$$

By considering (3.3)-(3.4)-(3.5), what follows is aim to prove that under the condition (3.15) the system trajectory will not pass beyond the point E' on z_2-axis. By this way the system trajectory will reach closer to the origin and the convergence of system (2.3) is then guaranteed. The following discussion is made to present what happens when the gain switching occurs at different points.

- Suppose that the gain of the control input u^* switches from K_M^* to K_m^* at point I. Then, consider the worst case with $K_m^* = K_m^{min}$ until the trajectory reaches the more left hand side point P. Finally, suppose $K_m^* = K_m^{max}$ so that the trajectory can reach the highest point E' when it crosses z_2-axis. It means that for a general case the system trajectory will pass beyond point E' on z_2-axis.
- Suppose that the switching of the control gain occurs at point I'. Consider also the worst case with $K_m^* = K_m^{max}$. The trajectory will track the curve I'-E', such that it reaches the highest point E' when it crosses z_2-axis. It means that for a general case the system trajectory will pass beyond point E' on z_2-axis neither.
- If the switching gain occurs between points I and I', the system trajectory will be on the right side of the curve I-P-I'. By this way the trajectory will reach a point "lower" than point E' on z_2-axis.

In conclusion under the condition (3.15), the system trajectory will reach closer to the origin, and the convergence is guaranteed.
Now determine the constraints on τ_i such that (3.15) is fulfilled. In order to calculate the vertical coordinate of point I and I', the expressions of curves E'-P-I and F-Q-I' are given by

$$\begin{aligned} z_1 &= \frac{z_2^2}{2K_m^{max}} + z_1(P) \text{ if } z_2 \geq 0 \\ z_1 &= \frac{z_2^2}{2K_m^{min}} + z_1(P) \text{ if } z_2 \leq 0 \end{aligned} \tag{3.16}$$

with $z_1(P) = -\dfrac{z_2^2(t_E)}{2K_m^{max}}$. Parabolas F-Q and Q-I' are respectively defined as

$$\begin{aligned} z_1 &= \frac{z_2^2 - z_{20}^2}{2K_M^{min}} \text{ between F and Q} \\ z_1 &= \frac{z_2^2}{2K_M^{max}} - \frac{z_{20}^2}{2K_M^{min}} \text{ between Q and I}' \end{aligned} \tag{3.17}$$

with

$$\begin{aligned} z_{20}^2 &= z_2^2(t_F) + 2|z_1(t_F)|K_M^{min}, \\ z_2^2(t_F) &= z_2^2(t_E) + (K_m^{max})^2 T_e^2 + 2|z_2(t_E)K_m^{max}T_e|, \\ |z_1(t_F)| &= |z_2(t_E)|T_e + \frac{1}{2}K_m^{max}T_e^2. \end{aligned} \tag{3.18}$$

Remarking that

$$|z_2(t_F)| = |z_2(t_E)| + K_m^{max}T_e \tag{3.19}$$

and

$$z_2(T_{SW}) = z_2(t_F) + \int_{T_s^i}^{T_s^i+\tau_i} K_M^*(t)dt \ , \tag{3.20}$$

The term $\int_{T_s^i}^{T_s^i+\tau_i} K_M^*(t)dt$ in (3.20) represents the length of system trajectory projected on z_2 axis under the large gain control input. In order to ensure that the gain switching point locates "between" (in the sense of z_2 coordinate) point I and I', this length should satisfy

$$\begin{aligned} \int_{T_s^i}^{T_s^i+\tau_i} K_M^*(t)dt &\geq |z_2(t_F)| - |z_2(I)| \\ \int_{T_s^i}^{T_s^i+\tau_i} K_M^*(t)dt &\leq |z_2(t_F)| + |z_2(I')| \end{aligned} \tag{3.21}$$

where $|z_2(t_F)|$ is given by (3.19). Then, consider the more general notation denoting, $t_E = t_i$ and $t_F = T_s^i$, from (3.21) the convergence condition reads as

$$\begin{aligned} &\int_{T_s^i}^{T_s^i+\tau_i} K_M^*(t)dt \geq |z_2(t_i)| + K_m^{max}T_e - \Delta \\ &\int_{T_s^i}^{T_s^i+\tau_i} K_M^*(t)dt \leq |z_2(t_i)| + K_m^{max}T_e + \Delta' \ . \end{aligned} \tag{3.22}$$

with $\Delta = -z_2(I)$ and $\Delta' = z_2(I')$. By calculating the intersections I and I' of curves E'-P-I and F-Q-I', the two positive numbers Δ and Δ' can be obtained from

$$\left(\frac{1}{K_m^{min}} - \frac{1}{K_M^{min}}\right)\Delta^2 = \left(\frac{z_2^2(t_i)}{K_m^{max}} - \frac{z_{20}^2}{K_M^{min}}\right) \tag{3.23}$$

and

$$\left(\frac{1}{K_m^{max}} - \frac{1}{K_M^{max}}\right)\Delta'^2 = \left(\frac{z_2^2(t_i)}{K_m^{max}} - \frac{z_{20}^2}{K_M^{min}}\right) \tag{3.24}$$

with

$$z_{20}^2 = (|z_2(t_i)| + K_m^{max}T_e)^2 + 2K_M^{min}(|z_2(t_i)|T_e + \tfrac{1}{2}K_m^{max}T_e^2) \ . \tag{3.25}$$

■

Remark 3.2.2. *A too small $|z_2(t_i)|$ may cause no real number root for (3.10)-(3.11). It means that the point $(0, z_2(t_i))$ has been already in a vicinity of zero. In this case, the condition (3.15) fails, the system trajectory can no longer converge closer to the origin. However, it will not cause divergence problem, because the system trajectories have already reached the vicinity of zero.*

In Theorem 3.1, the constraints of large gain input duration τ_i are given (3.9). In order to obtain more explicit constraints on τ_i, the following corollary is presented which gives a sufficient but not necessary condition for the convergence.

Corollary 3.2.1 (Yan et al. [2016e]). *Consider system (2.3) controlled by the switching gain form controller (3.1)-(3.2) and fulfilling Assumptions 2.2.1-2.2.3. Suppose that, at instant $t = t_i$, the system trajectory crosses z_2-axis for the i^{th} time, i.e. $z_1(t_i) = 0$. Then, the system trajectory tends to be closer from the origin at $t = t_{i+1}$, if $K_m > a_M/b_m$ and $\gamma > 2 + b_M/b_m$ and the duration of the large scale control τ_i satisfies*

$$\frac{|z_2(t_i)| + K_m^{max} T_e - \Delta}{K_M^{min}} \leq \tau_i \leq \frac{|z_2(t_i)| + K_m^{max} T_e + \Delta'}{K_M^{max}} \tag{3.26}$$

with Δ and Δ' defined by (3.10)-(3.11).

Proof. Knowing that $K_M^*(t) \geq K_M^{min}$ and $K_M^*(t) \leq K_M^{max}$ for $\forall t \in [T_s^i, T_s^i + \tau_i]$, one has

$$\begin{aligned} \int_{T_s^i}^{T_s^i+\tau_i} K_M^*(t)dt &\geq \tau_i K_M^{min} \\ \int_{T_s^i}^{T_s^i+\tau_i} K_M^*(t)dt &\leq \tau_i K_M^{max} \ . \end{aligned} \tag{3.27}$$

Then, if the following inequalities hold the condition (3.9) is also satisfied:

$$\begin{aligned} \tau_i K_M^{min} &\geq |z_2(t_i)| + K_m^{max} T_e - \Delta \\ \tau_i K_M^{max} &\leq |z_2(t_i)| + K_m^{max} T_e + \Delta' \end{aligned} \tag{3.28}$$

The condition (3.26) ensures. ■

As presented previously, the twisting-control (TWC) Levantovsky [1985]; Levant [1993]; Shtessel et al. [2014] and the second order sliding mode output feedback control law (2SMOFC) Plestan et al. [2010a], can be viewed by this switching gain strategy. So, in the following sections, these two control laws are reformulated in this form. Furthermore, the convergence of system (2.3) under these control laws is also analyzed by using Theorem 3.1 and Corollary 3.2.1.

3.3 Twisting control under switching gain form

The twisting control (TWC) is applicable to systems with relative degree equal to two [2] and ensures the establishment of a second order sliding mode with respect to the sliding variable in a finite time. In this section, system (2.3) is considered, the standard form of TWC is recalled. Then, TWC is revisited through the switching gain form, and the convergence of system trajectory under this controller is analyzed.

3.3.1 Control algorithm

Consider system (2.3); the twisting algorithm Levantovsky [1985]; Shtessel et al. [2014] reads as

$$u(t) = -K_1 \text{sign}\left(z_1(t) - K_2 \text{sign}\left(z_2(t)\right)\right) \ . \tag{3.29}$$

2. If one attempts to apply the TWC to a system with relative degree equal to one, the discontinuity should act on the derivative of the control input.

This controller guarantees the establishment of a second order sliding mode with respect to σ in a finite time *i.e.* $\sigma = \dot{\sigma} = 0$. If the system is sampled with a positive sampling period T_e, a *real* second order sliding mode is established Levant [1993].

Theorem 3.2 (Levantovsky [1985]). *Consider system (2.3) under Assumptions 2.2.1-2.2.3, with the control law reading as*

$$u(kT_e) = -K_1 \text{sign}\left(z_1(kT_e) - K_2 \text{sign}\left(z_2(kT_e)\right)\right) \tag{3.30}$$

with $k \in \mathbb{N}$. If K_1 and K_2 fulfill the conditions

$$\begin{array}{l} K_1 > K_2 > 0\ , \quad (K_1 - K_2)b_m > a_M \\ (K_1 + K_2)b_m - a_M > (K_1 - K_2)b_M + a_M\ , \end{array} \tag{3.31}$$

then a real second order sliding mode with respect to z_1 is ensured after a finite time.

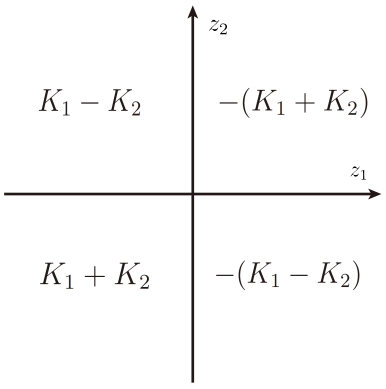

Under this control law, the amplitude of the input switches between four values $\pm(K_1 + K_2)$ and $\pm(K_1 - K2)$ [3]. As shown in the figure on the left, for the first and third quadrants on the $(z_1,\ z_2)$ phase plane, the large magnitude control input is applied. For the other two quadrants, the small gain is applied. This property offers the possibility to revisit TWC with the switching gain form proposed in Section 3.1. If one defines K_m and γ as

$$\begin{array}{rcl} K_m & = & K_1 - K_2 \\ \gamma & = & (K_1 + K_2)/(K_1 - K_2), \end{array} \tag{3.32}$$

the TWC can be written as

$$u \ = \ \left\{ \begin{array}{lll} -K_m \text{sign}(z_1) & \text{if} & z_1 z_2 \leq 0 \\ -\gamma K_m \text{sign}(z_1) & \text{if} & z_1 z_2 > 0 \end{array} \right. . \tag{3.33}$$

Then the twisting algorithm (3.30) can be written in the switching gain control form (3.1)-(3.2), with $\mathcal{T}_\mathcal{H}$ defined as

$$\mathcal{T}_\mathcal{H} \ = \ \{kT_e \mid \text{sign}(z_1(kT_e)) \cdot \text{sign}(z_2(kT_e)) = 1\}\ . \tag{3.34}$$

Theorem 3.3 (Yan et al. [2016e]). *Consider system (2.3) under Assumptions 2.2.1-2.2.3 and controlled by (3.1)-(3.2) with $\mathcal{T}_\mathcal{H}$ defined as (3.34). Then, if $K_m > a_M/b_m$ and $\gamma > 2 + b_M/b_m$, a real second order sliding mode with respect to z_1 is established after a finite time.*

The definition of $\mathcal{T}_\mathcal{H}$ is a key-point in the switching gain form, and strongly impacts the strategy of the large gain input application.

Duration of the large gain input. From (3.34), it is obvious that the duration of application of the large gain is time varying. The large input u_H is applied when z_1 and z_2 have the

3. There exist exceptional singularities when $z_1 = 0$ or $z_2 = 0$, but for a sampled measurement, it is not practically possible that these both variables are exactly equal to zero. Then, these singularities can be neglected.

same sign. Recalling that T_s^i (*resp.* T_s^{i+1})is the time at which the i^{th} (*resp.* $(i+1)^{th}$) z_1-sign switching is detected, and τ_i the duration of u_H for $T_s^i \leq kT_e \leq T_s^{i+1}$, it yields that this duration is a multiple of the sampling period, *i.e.* for $i > 0$,

$$\tau_i \;=\; k_i T_e < T_s^{i+1} - T_s^i \tag{3.35}$$

k_i being defined such that

$$\text{sign}(z_2(T_s^i + k_i T_e)) \neq \text{sign}(z_2(T_s^i + (k_i - 1)T_e)) \; . \tag{3.36}$$

Then, in the next section, the convergence of system (2.3) under the control law (3.1)-(3.2)-(3.34) is proved.

3.3.2 Convergence analysis

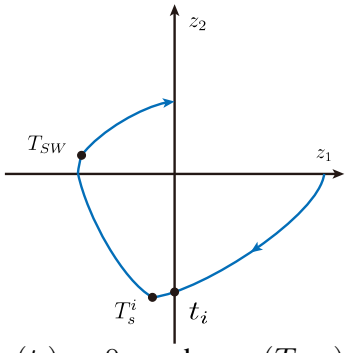

As shown in the left figure, the gain switching point for the twisting control occurs when the system trajectory crosses z_2-axis. Without loss of generality, suppose that at instant $t = t_i$ the system crosses z_2-axis for the i^{th} time, and at $t = T_s^i$ the i^{th} z_1-sign switching is detected. Given that the delay of the detection between t_i and T_s^i is less than one sampling step, consider the worst case, *i.e.* $T_s^i - t_i = T_e$. As shown in (3.35)-(3.36) , the large input u_H switches off just after the system trajectory crosses z_1-axis at instant $t = T_{SW}$.

If $z_2(t_i) < 0$ one has $z_2(T_{SW}) \geq 0$, otherwise $z_2(T_{SW}) \leq 0$ with $z_2(t_i) > 0$. It means that the length of the system trajectory projection on z_2-axis under large gain input is always larger than $|z_2(T_s^i)|$. It yields

$$\int_{T_s^i}^{T_s^i+\tau_i} K_M^*(t)dt \;\;\geq\;\; |z_2(t_i)| + K_m^{max} T_e \; . \tag{3.37}$$

According to Theorem 3.1, it is clear that the first line of condition (3.9) is satisfied. On the other hand, the time delay to detect the i^{th} sign switching of z_2 should also be less than one sampling step. So, one has $|z_2(T_{SW})| < K_M^{max} T_e$, which leads to

$$\int_{T_s^i}^{T_s^i+\tau_i} K_M^*(t)dt \;\;<\;\; |z_2(t_i)| + K_m^{max} T_e + K_M^{max} T_e \; . \tag{3.38}$$

If one considers the case where the system trajectory does not initially take place in a very vicinity of origin at instant t_i, it is reasonable to suppose that $|z_2(t_i)|$ is large enough such that $\Delta' > K_M^{max} T_e$. Then, the condition (3.9) in Theorem 3.1 is fulfilled, and the system trajectory will converge closer to origin. If it is not the case, it means that the system trajectories have already reached the vicinity of zero. This process can be repeated for the next gain commutation. Then, under the control of switching gain form TWC, the system trajectory reaches a vicinity of zero after a finite time. The system trajectories can no further converge to origin, when $\Delta' = K_M^{max} T_e$. Then, replacing this latter into (3.12), one gets that the final convergence domain for TWC is that

$$|z_2(t)| \leq \mu_1 T_e \tag{3.39}$$

where μ_1 is the positive solution of the second order equation

$$(\frac{1}{K_m^{max}} - \frac{1}{K_M^{min}})\mu_1^2 - 4\mu_1 - \frac{5}{2}K_m^{max} \;\;=\;\; (\frac{1}{K_m^{max}} - \frac{1}{K_M^{max}})K_M^{max^2} \; . \tag{3.40}$$

And the z_1 is also in the vicinity of zero with

$$|z_1(t)| \leq (\frac{\mu_1^2}{2K_M^{min}} + \mu_1 - \frac{1}{2}K_m^{min})T_e^2 \ . \tag{3.41}$$

The establishment of real second order sliding mode is verified.

3.4 Second order sliding mode output feedback control under switching gain form

As presented in the introduction of this part, the second order sliding mode output feedback control law (2SMOFC) Plestan et al. [2010a] has been designed to remove the use of time derivative of the sliding variable in the controller. This latter is applicable to systems with relative degree equal to 1 or 2. It ensures the establishment of a real second order sliding mode in a finite time, by using only the information of the sliding mode variable. In this section, the 2SMOFC is rewritten in the switching gain form and the convergence of system (2.3) under this control law is analyzed using Corollary 3.2.1.

3.4.1 Control algorithm

Consider the system (2.3), under Assumptions 2.2.1-2.2.3. The 2SMOFC algorithm Estrada and Plestan [2012] reads as [4]

$$u(kT_e) = -K(kT_e)\text{sign}(z_1(kT_e)) \tag{3.42}$$

with $k \in I\!N$, and K defined as

$$K(kT_e) = \begin{cases} K_m & \text{if} \quad kT_e \notin \mathcal{T}_{\mathcal{H}} \\ \gamma K_m & \text{if} \quad kT_e \in \mathcal{T}_{\mathcal{H}} \end{cases} \tag{3.43}$$

with

$$\mathcal{T}_{\mathcal{H}} = \{kT_e \mid \text{sign}(z_1((k-1)T_e)) \neq \text{sign}(z_1(kT_e))\}. \tag{3.44}$$

Theorem 3.4 (Estrada and Plestan [2012]). *Consider system (2.3) under Assumptions 2.2.1-2.2.3 and controlled by (3.1)-(3.2) with $\mathcal{T}_{\mathcal{H}}$ defined as (3.44). Then, with a sufficient large gain $K_m > a_M/b_m$ and $\gamma > 3$, a real second order sliding mode with respect to z_1 is established after a finite time.*

Duration of the large gain input: Given the definition of $\mathcal{T}_{\mathcal{H}}$ (3.44), the duration τ_i of the large gain application is constant and equal to T_e. Then, in the next section, the convergence of system (2.3) under the 2SMOFC, presented in Theorem 3.4, is proved.

3.4.2 Convergence analysis

In order to prove the convergence of the system trajectory the following assumption is required.

4. Note that the results in Plestan et al. [2010a] have been originally written under a switching gain control form.

Assumption 3.4.1. *Recalling that the sign switching of z_1 is detected at $T_s^i = k_i T_e$, $k_i \in \mathbb{N}$, $i \in \mathbb{N}$, one supposes that there exists $n > 1$ such that*

$$\forall i \in \mathbb{N} \cap [0; n],\ |z_2(T_s^i)| \geq K_M^{max} \cdot T_e. \tag{3.45}$$

It means that the system trajectory is not initially evolving in the vicinity of the origin. Otherwise, it is less interesting to analyze the convergence, when the system trajectories have already reached the vicinity of zero.
Knowing that the time delay to detect the z_1-sign switching is less than one sampling period, *i.e.* $T_s^i - t_i < T_e$, and for $t \in [t_i,\ T_s^i[$ the small gain control input is applied, it yields that

$$|z_2(T_s^i)| \ \leq \ |z_2(t_i)| + K_m^{max} T_e\ . \tag{3.46}$$

Consider also Assumption 3.4.1. One has

$$|z_2(T_s^i)| \ \geq \ K_M^{max} T_e\ . \tag{3.47}$$

From (3.46)-(3.47), one has

$$|z_2(t_i)| + K_m^{max} T_e \ \geq \ K_M^{max} T_e\ . \tag{3.48}$$

From the above inequality, it is obvious that

$$T_e K_M^{max} \ \leq \ |z_2(t_i)| + K_m^{max} T_e + \Delta' \tag{3.49}$$

holds with $\Delta' \geq 0$. Recalling that for 2SMOFC $\tau_i \equiv T_e$, one obtains

$$\tau_i = T_e \ \leq \ \frac{|z_2(t_i)| + K_m^{max} T_e + \Delta'}{K_M^{max}}. \tag{3.50}$$

Then, the right hand side of inequality(3.26) holds. According to expression (3.10), Δ increases if K_M^{min} increases. So, one can always find K_M large enough such that

$$T_e K_M^{min} \ \geq \ |z_2(t_i)| + K_m^{max} T_e - \Delta\ . \tag{3.51}$$

Then, one obtains

$$\tau_i = T_e \ \geq \ \frac{|z_2(t_i)| + K_m^{max} T_e - \Delta}{K_M^{min}}\ . \tag{3.52}$$

Then, the left hand side of inequality (3.26) holds. According to Corollary 3.2.1, the system trajectory tends to be closer towards the origin. By repeating this process at each time that the system trajectory crosses z_2-axis, the system finally converges to a vicinity of zero under the control of 2SMOFC. Moreover, in Estrada and Plestan [2014], the final convergence domain is given for a class of systems.

Lemma 3.4.1 (Estrada and Plestan [2014])**.** *Consider system (2.3), with $a = 0$ and $b = 1$, controlled by the 2SMOFC presented in Theorem 3.4. Then, for any $\gamma > 3$, $K_m > 0$, the final convergence domain is given by*

$$|z_1| < \tfrac{1}{2} K_m [\eta(\gamma) - 1]^2 T_e^2, \qquad |z_2| < K_m \eta(\gamma) T_e, \tag{3.53}$$

with

$$\eta \ = \ \frac{\gamma^2 - \gamma - 2}{2(\gamma - 3)}\ . \tag{3.54}$$

3.5 Summary

The main contributions of this chapter are summarized as follows :

- An unified switching gain form is proposed, in order to present several second order sliding mode controllers by a similar way.
- A convergence analysis tool is given, which is based on analytic analysis of system trajectories.
- The control input for the twisting control (TWC) switches between two magnitudes. Thanks to this feature, TWC is revisited in the switching gain form.
- For TWC, the large gain input is applied when z_1 and z_2 have the same sign. By proving that the duration τ_i satisfies the constraints given in Theorem 3.1, the convergence of system trajectories under TWC is verified.
- The key-point of the second order sliding mode output feedback control (2SMOFC) is the application of large gain input during a signal sampling period, after each detection of z_1 sign commutation. It can be also presented in the switching gain form.
- For 2SMOFC, the duration τ_i is always equal to T_e, and one can always find a large enough gain K_M, such that the convergence of system trajectory under 2SMOFC is ensured.

4

Twisting-like control

Contents

As presented in the previous chapter, the twisting control (TWC) and the second order sliding mode output feedback control (2SMOFC) can be reformulated in the switching gain form. The advantage of the 2SMOFC is that it is using only the sign of z_1, and requires no information on z_2. However, its main drawback is that the application of the high magnitude control during just one sampling period induces a low convergence rate. It means that the convergence time (which is finite) is large compared to the TWC.

Based on the 2SMOFC method, a possible improvement can be made, if the large scale control input is applied during a time varying duration longer than one sampling period. By this way, the dynamic performance of system (2.3) under this controller could be close to the performance of TWC. Furthermore, the use of derivative of the sliding variable is removed.

The main contribution of this chapter consists in the presentation of a new output feedback control law named "twisting-like" control Yan et al. [2016d] (denoted TWLC), which is written under the switching gain form and based on a time-varying duration τ_i. This control law only requires the sign of the sliding variable. Compared to TWC, this feature allows to avoid additional noise introduced by the differentiation. Moreover, by applying the large gain control for multiple sampling periods, the convergence time of this new controller is no longer sensitive to the sampling period and is strongly improved with respect to the 2SMOFC.

The TWLC requires only the measurement of the sliding variable, and this feature allows to use this controller as a differentiator to estimate the time derivative of a sampled signal. The design of the "twisting-like" differentiator is also presented in this chapter.

4.1 Control algorithm

As previously written, the design of the TWLC is based on the switching gain form (3.1)-(3.2). Compared to the 2SMOFC, instead of applying u_H during a constant duration T_e, a new algorithm for the computation of τ_i is given, which offers the possibility to apply u_H during multi sampling periods. Recall that for the TWC the duration τ_i is also time-varying, but its evaluation depends on both z_1 and z_2.
Consider the system (2.3), under Assumptions 2.2.1-2.2.3. The TWLC algorithm Yan et al. [2016d] reads as ($k \in I\!N$)

$$u(kT_e) = -K(kT_e)\text{sign}(z_1(kT_e)) \ , \tag{4.1}$$

with the gain K defined as

$$K(kT_e) \ = \ \begin{cases} K_m & \text{if} \quad kT_e \notin \mathcal{T}_{\mathcal{H}} \\ \gamma K_m & \text{if} \quad kT_e \in \mathcal{T}_{\mathcal{H}} \end{cases} \tag{4.2}$$

and the gain switching condition given by

$$\mathcal{T}_{\mathcal{H}} \ = \ \{kT_e \mid T_s^i \leq kT_e \leq T_s^i + \tau_i, i \in I\!N\} \tag{4.3}$$

As previously, T_s^i is the time at which the i^{th} z_1-sign switching is detected. The gain switching condition (4.3) depends on an online updated variable τ_i which is the duration of u_H for $t \in [T_s^i, \ T_s^{i+1}[$.

Duration of the large gain input: Recall that

$$\begin{aligned} K_m^{max} &= b_M K_m + a_M, \qquad K_m^{min} = b_m K_m - a_M \\ K_M^{max} &= \gamma b_M K_m + a_M, \qquad K_M^{min} = \gamma b_m K_m - a_M \ . \end{aligned}$$

If the gain is tuned such that $K_m > a_M/b_m$ and $\gamma > 2 + \frac{b_M}{b_m}$, one has

$$K_m^{min} > 0 \quad , \quad K_M^{min} > K_m^{max} \ . \tag{4.4}$$

Then, the computation of τ_i reads as

$$\tau_i = \max(\tau_i', T_e) \tag{4.5}$$

with

$$\tau_i' \ = \ T_e \cdot \text{floor}\left[2\alpha \frac{\tau_{i-1} K_M^{min} + \bar{\tau}_{i-1} K_m^{min}}{K_M^{max} T_e} - 1\right] \tag{4.6}$$

in which the function $\text{floor}(\cdot)$ rounds the element of the argument to the nearest integer towards minus infinity. α and $\bar{\tau}_i$ are defined as

$$\alpha \ = \ \frac{\sqrt{K_m^{min}}}{\sqrt{K_M^{max}} + \sqrt{K_m^{min}}} \tag{4.7}$$

and

$$\bar{\tau}_i \ = \ \max(0, \ T_s^{i+1} - T_s^i - \tau_i) \ . \tag{4.8}$$

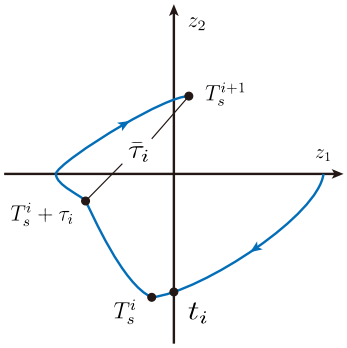

Remark that $\bar{\tau}_i$ is the duration of the small gain control $u = u_L$ for $t \in [T_s^i, \ T_s^{i+1}[$ (see Figure on the left). Then, τ_i can be computed by the iteration process (4.5)-(4.8), with the initial conditions $T_s^0 = 0$ and $\tau_0 = 0$. It is important to notice that in (4.5)-(4.8), only the information of z_1 and the bound of the perturbation are required. Then, this output feedback control law is summarized by the following theorem.

Theorem 4.1 (Yan et al. [2016d]). *Consider system (2.3) under Assumptions 2.2.1-2.2.3 and controlled by (4.1)-(4.2). Define $\mathcal{T}_{\mathcal{H}}$ as (4.3) with τ_i given by (4.5)-(4.8). Then, there always exist some large enough $K_m > a_M/b_m$ and $\gamma > 2 + b_M/b_m$, such that a real second order sliding mode is established with respect to z_1 in a finite time.*

4.2 Convergence analysis

In this section, the convergence analysis of TWLC is made thanks two lemmas. By a similar way than the convergence proof for 2SMOFC, one also supposes that the system trajectory is initially evolving outside a vicinity of the origin.

Assumption 4.2.1. *Recalling that the sign switching of z_1 is detected at instants $T_s^i = k_i T_e$, $i \in \mathbb{N}$, one supposes that there exists $n > 1$ such that*

$$\forall i \in \mathbb{N} \cap [0; n],\ |z_2(T_s^i)| \geq K_M^{max} \cdot T_e. \tag{4.9}$$

- The main result is given by Lemma 4.2.2 which proves that τ_i computed by (4.5)-(4.8) satisfies the condition (3.26) in Corollary 3.2.1.
- Lemma 4.2.1 can be viewed as a preliminary result of Lemma 4.2.2, which states that for the z_1-sign commutation detection points, $|z_2(T_s^i)|$ has a minimal value.

Lemma 4.2.1 (Yan et al. [2016d]). *Consider system (2.3) under Assumptions 2.2.1-2.2.3-4.2.1 and controlled by (4.1)-(4.3). Recalling that T_s^i is the time at which the i^{th} z_1-sign switching is detected, one has, for all $i > 2$,*

$$|z_2(T_s^i)| \ \geq \ \alpha L \tag{4.10}$$

with

$$\alpha \ = \ \frac{\sqrt{K_m^{min}}}{\sqrt{K_M^{max}} + \sqrt{K_m^{min}}} < 1 \tag{4.11}$$

and $L = |z_2(T_s^i) - z_2(T_s^{i-1})|$ being the vertical distance between two points at two successive instants T_s^{i-1} and T_s^i.

Proof. The objective is to identify the case for which one has the maximal convergence rate. Consider the Figure 4.1-Left describing the system trajectory in the phase plane. Some particular points are described by Table 4.1, particularly points B ($t_B = T_s^{i-1}$) and F ($t_F = T_s^i$) that are two successive z_1-sign switching detection points. The vertical distance between these two points is denoted L. Firstly, defining the convergence rate δ as

$$\delta \ = \ \frac{|z_2(T_s^{i-1})|}{|z_2(T_s^i)|},$$

one should admit that for a given $z_2(T_s^{i-1})$ the maximal value of δ is obtained when there is no delay for the sign switching detection (it is the case in Figure 4.1-Right). It is obvious that, if there is any delay between points E and F, one has $|z_2(t_F)| > |z_2(t_E)|$ and $\delta < \frac{|z_2(t_B)|}{|z_2(t_E)|}$. So, the first constraint in order to get surly maximal δ is that the sampling period T_e equals zero.
Next, one considers the effect of the switching gain to δ. As shown in Figure 4.1-Right, if

the gain commutation appears before that the trajectory crosses z_1-axis, then the trajectory will track the red dotted line. In another case, if the switching appears after that the trajectory crosses z_1-axis, then the trajectory will track the green dotted line. In these both cases, the convergence rate is not maximal given that $|z_2(T_s^i)|$ is larger.

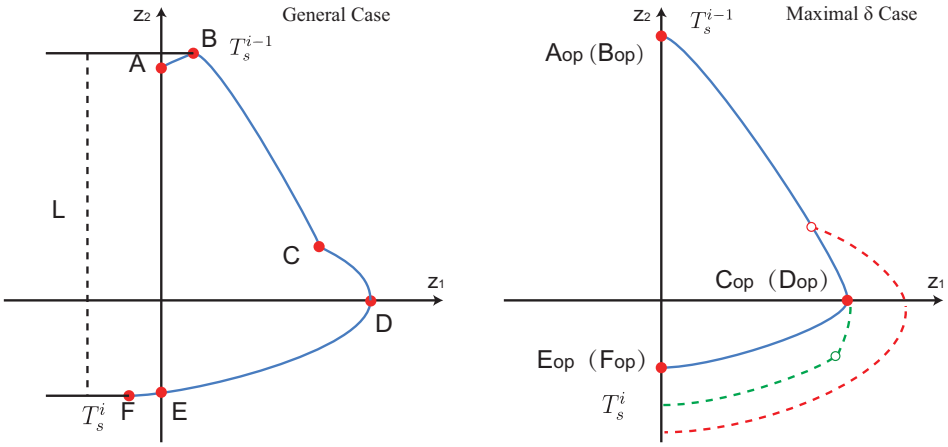

Figure 4.1 – **Left.** System trajectory in (z_1, z_2) phase plane in the general case; **Right.** System trajectory with maximal δ in (z_1, z_2) phase plane.

Point	Instant	Control u^*	Description
A	t_A	K_m^*	$z_1(t_A) = 0, z_2(t_A) > 0$
B	t_B	$-K_M^*$	$t_B - t_A \leq T_e$
C	t_C	$-K_m^*$	$t_C - t_B = \tau_{i-1}$
D	t_D	$-K_m^*$	$z_1(t_D) > 0, z_2(t_D) = 0$
E	t_E	$-K_m^*$	$z_1(t_E) = 0, z_2(t_E) < 0$
F	t_F	K_M^*	$t_F - t_E \leq T_e, t_F - t_C = \bar{\tau}_{i-1}$

Table 4.1 – Points describing the trajectory in (z_1, z_2) phase plane in case of real system (Figure 4.1-Left).

The maximal convergence rate δ_{Max} can actually be obtained only if

- there is no delay in the sign switching detections;
- the gain is switching from K_M^{max} to K_m^{min} when the trajectory crosses z_1-axis (point D_{op} in Figure 4.1-Right).

Remark that this latter item corresponds to the twisting algorithm in ideal conditions (*i.e.* the sampling period converges towards zero). In this case, one has

$$\begin{aligned} t_{C_{op}} - t_{B_{op}} &= \frac{z_2(t_{B_{op}})}{K_M^{max}} \\ z_1(t_{C_{op}}) &= \frac{1}{2} K_M^{max} (t_{C_{op}} - t_{B_{op}})^2 \end{aligned} \tag{4.12}$$

and

$$\begin{aligned} t_{F_{op}} - t_{C_{op}} &= \frac{-z_2(t_{F_{op}})}{K_m^{min}} \\ z_1(t_{C_{op}}) &= \frac{1}{2} K_m^{min} (t_{F_{op}} - t_{C_{op}})^2 \end{aligned} \tag{4.13}$$

Then, from (4.12)-(4.13), one gets

$$\delta_{Max} = \frac{|z_2(B_{op})|}{|z_2(F_{op})|} = \frac{\sqrt{K_M^{max}}}{\sqrt{K_m^{min}}} . \tag{4.14}$$

This maximal value only depends on the gain K_M^{max} and K_m^{min}. Now, considering the system trajectories in a general case, with L being the distance between B and F (see Figure 4.1-Left)). Because $\delta \leq \delta_{Max}$, for the general case, one has

$$\frac{|z_2(t_B)|}{|z_2(t_F)|} \leq \frac{\sqrt{K_M^{max}}}{\sqrt{K_m^{min}}} \tag{4.15}$$

Then, recalling $L = |z_2(t_F) - z_2(t_B)|$, one has

$$|z_2(t_F)| \geq \alpha L \tag{4.16}$$

with $\alpha = \dfrac{1}{1+\delta_{Max}}$. ■

Lemma 4.2.2 (Yan et al. [2016d]). *Consider system (2.3) under Assumptions 2.2.1-2.2.3 and 4.2.1, controlled by (3.1)-(3.2). Define $\mathcal{T}_{\mathcal{H}}$ as (4.3) with τ_i given by (4.5)-(4.8). Then, there always exist some large enough K_m and γ such that the condition (3.26) in Corollary 3.2.1 holds at every gain commutation point.*

Proof. The proof of Lemma 4.2.2 consists in considering two cases: first-of-all, one considers the minimal value of τ_i, which can be not lower than the sampling period T_e. The second case will be devoted to larger values of τ_i.

Case 1: $\tau_i = T_e$ [1].

Given that the time delay between t_i and T_s^i is less than one sampling step, one has

$$|z_2(T_s^i)| \leq |z_2(t_i)| + K_m^{max} T_e. \tag{4.17}$$

At $t = T_s^i$, one also supposes that the system trajectory does not reach a very vicinity of origin: then, under Assumption 4.2.1, one has

$$|z_2(T_s^i)| \geq K_M^{max} T_e . \tag{4.18}$$

It yields

$$|z_2(t_i)| + K_m^{max} T_e \geq K_M^{max} T_e. \tag{4.19}$$

It is now obvious that the inequality

$$T_e K_M^{max} \leq |z_2(t_i)| + K_m^{max} T_e + \Delta' \tag{4.20}$$

holds with $\Delta' \geq 0$. According to (3.10), the term Δ increases if K_M^{min} increases. So, one can always find a parameter γ large enough such that

$$T_e K_M^{min} \geq |z_2(t_i)| + K_m^{max} T_e - \Delta. \tag{4.21}$$

By this way, one proves that inequality (3.26) holds.

1. This is the case of the second order sliding mode output feedback control (2SMOFC), presented in Section 3.4

Case 2: $\tau_i > T_e$.

From (4.6), one has

$$\tau_i K_M^{max} \leq 2\alpha(K_M^{min}\tau_{i-1} + K_m^{min}\bar{\tau}_{i-1}) - K_M^{max}T_e. \tag{4.22}$$

Suppose that $z_2(t_i) < 0$ (one can get similar results with $z_2(t_i) > 0$). From (4.21), given that $\tau_i > T_e$, one can ensure

$$\tau_i K_M^{min} \geq |z_2(t_i)| + K_m^{max}T_e - \Delta \tag{4.23}$$

with large enough K_M. The left-hand side of inequality (3.26) is satisfied. On the other hand, according to Lemma 4.2.1, one has

$$z_2(t_i) - K_m^{max}T_e \leq z_2(T_s^i) \leq -\alpha L \tag{4.24}$$

which means that

$$|z_2(t_i)| + K_m^{max}T_e \geq \alpha L \tag{4.25}$$

with $L \geq K_M^{min}\tau_{i-1} + K_m^{min}\bar{\tau}_{i-1}$. Then, one gets

$$\tau_i K_M^{max} \leq 2(|z_2(t_i)| + K_m^{max}T_e) - K_M^{max}T_e. \tag{4.26}$$

From (4.21), it is obvious that there always exists K_M large enough such that

$$-T_e K_M^{max} \leq -T_e K_M^{min} \leq -|z_2(t_i)| - K_m^{max}T_e + \Delta \tag{4.27}$$

Then, by substituting $-T_e K_M^{max}$ by its upper bound into (4.26), one obtains

$$\tau_i K_M^{max} \leq |z_2(t_i)| + K_m^{max}T_e + \Delta. \tag{4.28}$$

From (3.10) and (3.11), one has

$$(\frac{1}{K_m^{min}} - \frac{1}{K_M^{min}})\Delta^2 = (\frac{1}{K_m^{max}} - \frac{1}{K_M^{max}})\Delta'^2. \tag{4.29}$$

Furthermore, one can always find K_M large enough such that

$$\frac{1}{K_m^{min}} - \frac{1}{K_M^{min}} \geq \frac{1}{K_m^{max}} - \frac{1}{K_M^{max}} \tag{4.30}$$

which gives $\Delta \leq \Delta'$. Then, from (4.28), one gets

$$\tau_i K_M^{max} \leq |z_2(t_i)| + K_m^{max}T_e + \Delta' \,. \tag{4.31}$$

The right-hand side of inequality (3.26) is satisfied: the proof of Lemma 4.2.2 is completed. ■

Remark 4.2.1. *Lemma 4.2.2 proves that thanks to the definition of τ_i by (4.5)-(4.8), the convergence condition given by Corollary 3.2.1 is fulfilled. It yields that under Assumption 4.2.1, the system trajectory is converging towards zero. The convergence process will stop when the system trajectory reaches in a finite time a vicinity of zero in the phase plane such that*

$$|z_2(T_s^i)| \leq K_M^{max}T_e. \tag{4.32}$$

So, there exists a finite time t_f such that

$$\forall t \geq t_f \qquad |z_2(t)| \leq K_M^{max}T_e \,. \tag{4.33}$$

Moreover, one has

$$|z_1(T_s^i)| \quad \leq T_d \cdot |z_2(T_s^i)| \tag{4.34}$$

with $T_d < T_e$ being the delay of the sign switching detection. Remarking that $z_1(t)$ reaches its maximum value when z_2 equals zero, one has

$$|z_1| \leq |z_1(T_s^i)| + |z_2(T_s^i)|^2/2K_m^{min}. \tag{4.35}$$

Then, using (4.32)-(4.34), one has

$$\forall t \geq t_f \qquad |z_1(t)| \leq (1 + \frac{K_M^{max}}{2K_m^{min}})K_M^{max}T_e^2 \ . \tag{4.36}$$

Then, according to Definition 2.2.1, the real second order sliding mode with respect to z_1 is established. For this final converged domain, the duration of the large gain input will be reduced as one sampling period. So, for the final stable stage, the TWLC and 2SMOFC will get similar behavior and convergence domain.

4.3 Twisting-like algorithm: a differentiation solution

For standard high order sliding mode control Levant [1993, 2003], the knowledge of the sliding variable and its time derivatives is required. In many practical cases, the sliding variable is derived from the measured output, whereas the differentiators are used to evaluate the derivatives of the sliding variable. Previous section has shown that the TWLC ensures the establishment of a real second order sliding mode with respect to the sliding variable in a finite time. Moreover this controller requires only the information of the sliding variable. This feature offers the possibility to use TWL algorithm as a differentiator. In this section, the design of the differentiator based on twisting-like algorithm is presented.

4.3.1 Differentiator design

Consider a signal $F(t)$ satisfying the following conditions:

- $F(t)$ is a locally bounded function defined on $[0, \infty)$;
- the second time derivative of $F(t)$, $\ddot{F}(t)$, is bounded by a known constant $L > 0$;
- $F(t)$ is measured with a sampling period T_e.

In order to estimate its first order time derivative, consider the system

$$\begin{array}{rcl} \dot{\xi}_1 & = & \xi_2 \\ \dot{\xi}_2 & = & u \end{array} \tag{4.37}$$

with the initial condition $\xi_1(0) = F(0)$, $\xi_2(0) = 0$. Then, define the sliding variable as $\sigma = \xi_1 - F(t)$. Denote $z_1 = \sigma$ and $z_2 = \dot{\sigma}$. One gets

$$\begin{array}{rcl} \dot{z}_1 & = & z_2 \\ \dot{z}_2 & = & -\dfrac{d^2F}{dt^2} + u \end{array} \tag{4.38}$$

System (4.38) is similar to system (2.3): therefore, by applying TWLC as the control input u, z_1 and z_2 converge to a vicinity of zero after a finite time. Then, from (4.37), ξ_2 can be viewed as an estimation of the time derivative of $F(t)$.

Theorem 4.2. *Consider system (4.38), with $z_1 = \xi_1 - F(t)$, $z_2 = \xi_2 - \frac{dF}{dt}$, and the control input u given in Theorem 4.1 with $a_M = L$ and $b_m = b_M = 1$. Then, there always exist some large enough $K_m > L$, $\gamma > 3$ and a finite time t_F, such that*

$$|\xi_2(t) - \frac{dF}{dt}| < \mu T_e \qquad \forall t \geq t_F \tag{4.39}$$

with $\mu > 0$.

Proof. According to Theorem 4.1, by applying TWLC to system (4.38), a real second order sliding mode with respect to z_1 is established after a finite time. Then, there exists a finite time t_F such that

$$|\dot{z}_1| \leq \mu T_e, \qquad \forall t \geq t_F \tag{4.40}$$

with $\mu > 0$, which gives

$$|\xi_2(t) - \tfrac{dF}{dt}| \leq \mu T_e \; . \tag{4.41}$$

■

4.3.2 Simulation

The objective of the subsection is to illustrate the previous result. Define the signal $F(t) = 20sin(t) + 5cos(2t)$, which is measured with a white noise of amplitude 5×10^{-3} under a sampling period $T_e = 0.001s$. The objective is to estimate its time derivative. Then, the TWLC is applied to system (4.38), with the parameters tuned as

$$\begin{aligned} a_M = L = 40 \qquad & b_m = b_M = 1 \\ K_m = 120 \qquad & \gamma = 6 \; . \end{aligned}$$

The performance of the twisting-like differentiator (denoted TWLD) is shown with Figure 4.2. It shows that, after a finite time, ξ_2 converges to the derivative of $F(t)$.

4.4 Summary

The main contributions of this chapter are summarized as follows :

- The twisting-like control (TWLC) is presented in the switching gain form. This control approach can be applied to systems with relative degree equal to two, and only the sign of the sliding variable is required in the controller.
- The key-point for TWLC is the time varying duration τ_i of the large gain input. Compared to the second order sliding mode output feedback control (2SMOFC) presented in Section 3.4, the large gain input for TWLC is applied during a time varying duration τ_i. Its computation depends on the control gain K_m, K_M and the time gap between two successive z_1-sign commutations. Thanks to the application of u_H during multiple sampling periods, the performance of system (2.3) under TWLC is close to the performance of twisting control. Furthermore, the use of time derivative of the sliding variable is removed.
- Thanks to the definition of τ_i by (4.5)-(4.8), the convergence condition given by Corollary 3.2.1 is fulfilled. So, the establishment of a real second order sliding mode is ensured after a finite time for system (2.3) under TWLC.

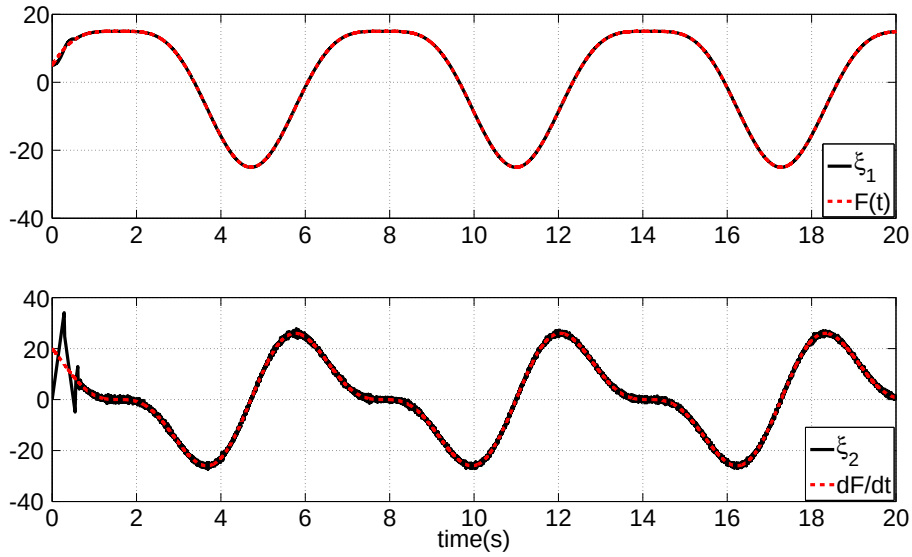

Figure 4.2 – **Simulations - use of TWLD algorithm. Top.** Signal $F(t)$ (red dotted line) and $\xi_1(t)$ versus time (sec); **Bottom.** Signal $\frac{dF}{dt}$ (red dotted line) and $\xi_2(t)$ versus time (sec).

- The TWL algorithm also offers a solution to estimate the time derivative of a sample measured signal.

5

Comparison between TWC, 2SMOFC and TWLC

Contents

In Chapter 4, the twisting control (TWC), the second order sliding mode output feedback control (2SMOFC) and the new twisting-like control algorithm (TWLC), have been formulated in an unified switching gain form (3.1)-(3.2). For this class of control laws, the control gain is switching between a large magnitude and a smaller one. The large input is applied when the commutation of the sliding variable sign is detected. The main difference between each control law is the duration of the large gain input. In this chapter, detailed comparisons about the performances between these three control laws are firstly made through a simulation example. Then, these control laws are applied to a pendulum system in order to compare their performances.

5.1 Academic example

Consider system (2.3) with the functions a and b defined respectively as $a = 5\sin(\omega t)$ and $b = 1$ *i.e.*

$$\begin{aligned} \dot{z}_1 &= z_2 \\ \dot{z}_2 &= u + 5\sin(\omega t) \end{aligned} \tag{5.1}$$

with $\omega = 0.2\pi$ and initial conditions being $z_0 = [10\ 10]^T$. The simulations have been made with a control input sampling time $T_e = 0.01sec$, which is 10 times higher than the integration step (10^{-3} s) used to simulate the system. A comparison is made between the three methods TWC, 2SMOFC and TWLC. These control laws are written in the switching gain form (3.1)-(3.2), and the domain $\mathcal{T}_{\mathcal{H}}$ is defined for each control law as

- Twisting controller (TWC):

$$\mathcal{T}_{\mathcal{H}} = \{kT_e \mid \text{sign}(z_1(kT_e)) \cdot \text{sign}(z_2(kT_e)) = 1\} \ . \tag{5.2}$$

- Second order output feedback controller (2SMOFC):

$$\mathcal{T}_{\mathcal{H}} = \{kT_e \mid \text{sign}(z_1((k-1)T_e)) \neq \text{sign}(z_1(kT_e))\} \ . \tag{5.3}$$

- Twisting-like controller (TWLC):

$$\mathcal{T}_{\mathcal{H}} = \{kT_e \mid T_s^i \leq kT_e \leq T_s^i + \tau_i, i \in I\!N\} \tag{5.4}$$

  with τ_i representing the duration of the large gain input for $t \in [T_s^i,\ T_s^{i+1}[$, computed by (4.5)-(4.8).

The parameters for these three controllers are tuned uniformly as $K_m = 15$, $T_e = 0.01$sec and $\gamma = 5$. Then, the single difference between these three control laws is the duration of the large gain input τ_i defined by $\mathcal{T}_{\mathcal{H}}$. The performances of system (5.1) obtained with these three controllers are displayed in Figures 5.1-5.2-5.3. Furthermore, the mean value of the tracking accuracy $|z_1|$ and the input u for the last ten seconds are calculated in Table 5.1.
Figure 5.1 represents z_1 and z_2 (Top and Middle), and the control input u (Bottom). The system trajectories in the phase plane (z_1, z_2) are shown by Figure 5.2. From these two figures, one can conclude that, with OFTWC, z_1 and z_2 converge to a vicinity of zero in a finite time. Based on a more detailed data comparison in Table 5.1, the tracking accuracy for these three control laws are at the same level. With the TWC, one gets a faster convergence time. However, in this case both z_1 and its derivative z_2 are required. For the TWLC, with the convergence of the system trajectories towards the vicinity of zero, the duration τ_i will be also reduced (see (4.5)-(4.8)). Consider the final stable phase where τ_i is equal to one sampling period. Then, the performance of TWLC is identical to the performance of 2SMOFC. So, for the stable phase, one obtains similar $mean(|z_1|)$ and $mean(|u|)$ for TWLC and 2SMOFC. For these two latter control laws, the large gain input is applied during one sampling period, which explains the smaller $mean(|u|)$ compared to TWC. For this stage, the application of the large gain input for one sampling period has been sufficient to maintain the system trajectories in the vicinity of origin. Furthermore, the oversize control magnitude for TWC causes a less accuracy. Moreover, considering the convergence phase, the TWLC induces a much faster convergence time, compared to the 2SMOFC.
In order to make a further comparison, define the "energy" applied by the i^{th} large gain control (which starts at instant T_s^i and ends at instant T_{end}^i) as

$$E_i = \int_{T_s^i}^{T_{end}^i} |u_H| dt \ . \tag{5.5}$$

Remark that for the three controllers, the gain K_m is constant and has the same value. Then, the "energy" of the large gain control only depends on its duration.
The "energy" applied by the three controllers is plotted in Figure 5.3. It shows that the "energy" used by 2SMOFC is impulsive with constant amplitude. For TWC, during the convergence phase, high "energy" is sent by u_H; then, the "energy" is reduced once the convergence is achieved. The "energy" sent by TWLC during the convergence phase is not as high as TWC, but much larger than 2SMOFC. From the energy distribution scheme, one can also conclude that the performance of TWLC is close to the one of TWC.
This test has been repeated with different sampling periods, and the control accuracies are evaluated for $t \in [70sec, 80sec]$ (see Table 5.2). Basically, when the sampling period is multiplied

2, the accuracy of z_1 is multiplied by 4 and z_2 by 2. It proves that a real second order sliding mode has been established. To summarize, the proposed new algorithm, TWLC, ensures the establishment of a real second order sliding mode for system (5.1), using only the information of z_1. This control law inherits output feedback feature from 2SMOFC and also the advantage of fast convergence time from TWC.

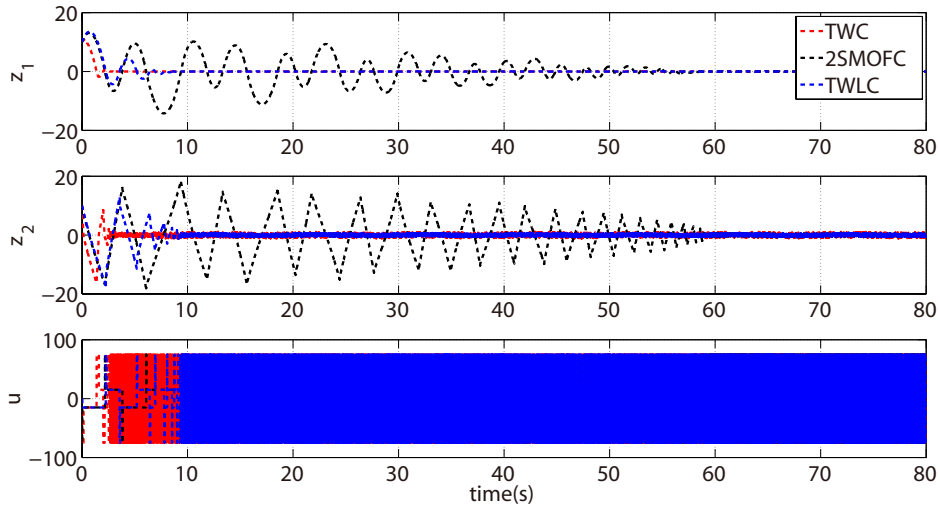

Figure 5.1 – System states and control input. **Top.** z_1 versus time (sec); **Middle.** z_2 versus time (sec); **Bottom.** control input u versus time (s).

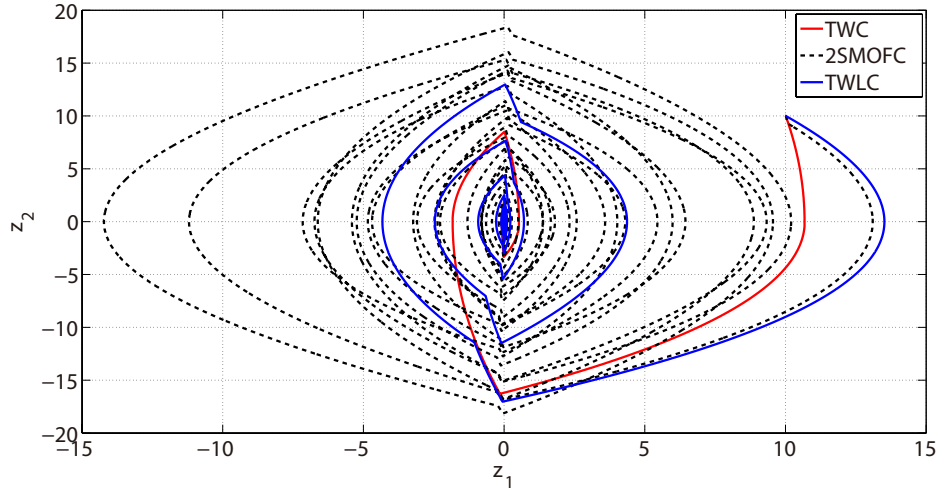

Figure 5.2 – System trajectory in the phase plane (z_1, z_2).

	$mean(\|z_1\|)$	$mean(\|u\|)$	Convergence time
TWC	0.0059	44.4631	<5s
2SMOFC	0.0035	34.2581	>50s
TWLC	0.0035	34.2581	<10s

Table 5.1 – Comparison between TWC, 2SMOFC and TWLC

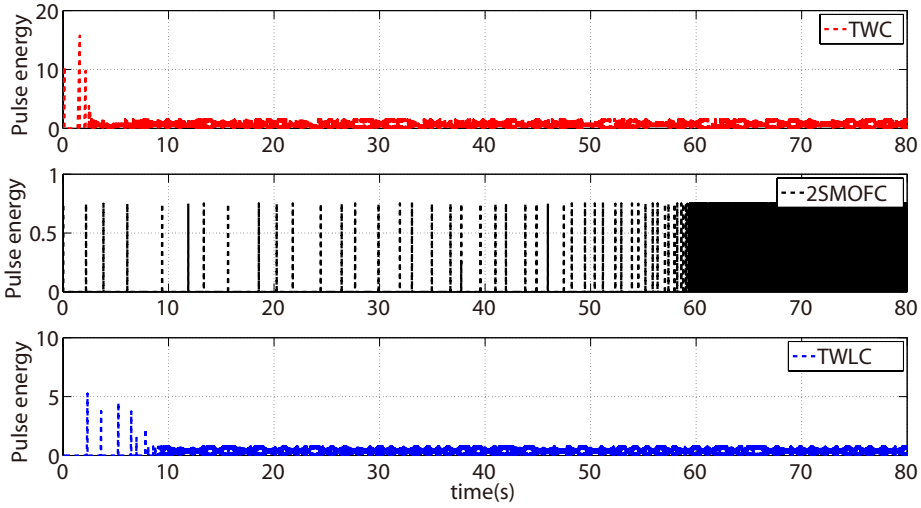

Figure 5.3 – Large gain control energy E versus time (s).

		$T_e = 0.01$s	$T_e = 0.02$s	$T_e = 0.04$s	$T_e = 0.08$s
TWC	$mean(\|z_1\|)$	0.0059	0.0211	0.0765	0.2576
	$mean(\|z_2\|)$	0.4893	0.8585	1.5196	2.8701
2SMOFC	$mean(\|z_1\|)$	0.0035	0.0132	0.0506	0.1876
	$mean(\|z_2\|)$	0.3091	0.6107	1.2067	2.3701
TWLC	$mean(\|z_1\|)$	0.0035	0.0132	0.0506	0.1876
	$mean(\|z_2\|)$	0.3091	0.6107	1.2067	2.3701

Table 5.2 – Tracking accuracies under different sampling periods.

5.2 Control of a pendulum system

In this section, the three controllers are applied to a pendulum system and their performances are compared.

5.2.1 System description

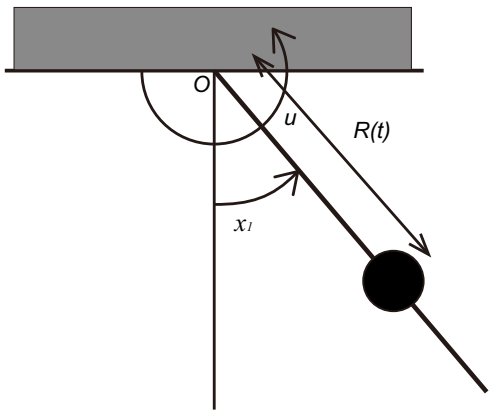

Figure 5.4 – Pendulum scheme Levant [2007]

Figure 5.4 shows the scheme of a variable-length pendulum system Levant [2007] evolving

in a vertical plane. The system dynamics reads as

$$\begin{aligned} \dot{x_1} &= x_2 \\ \dot{x_2} &= -2\frac{\dot{R}(t)}{R(t)}x_2 - \frac{g}{R(t)}sin(x_1) + \frac{1}{mR(t)^2}u \end{aligned} \tag{5.6}$$

with x_1, x_2 respectively the angular position and velocity of the rod, $m = 1kg$ the load mass, $g = 9.81ms^{-2}$ the gravitational constant, $R(t)$ the distance from the fix point O and the mass, and u the control torque. $R(t)$ is a non-measured disturbance and reads as $R(t) = 1 + 0.01\sin(8t) + 0.02\cos(4t)$. Function $R(t)$ and its time derivative $\dot{R}(t)$ are such that $0.974 \leq R(r) \leq 1.026$ and $-0.1601 \leq \frac{\dot{R}(t)}{R(t)} \leq 0.0887$.

5.2.2 Control design

Define the sliding variable $\sigma(x,t) = x_1 - x_c$, with the reference trajectory $x_c = 0.5\sin(0.5t) + 0.5\cos(t)$. The system is initialized such that $\sigma(0) = -0.5\text{rads}^{-1}$. One has

$$\ddot{\sigma} = \left[-\frac{2\dot{R}(t)}{R(t)}x_2 - \frac{g}{R(t)}\sin(x_1) - \ddot{x}_c\right] + \left[\frac{1}{mR(t)^2}\right]u\ . \tag{5.7}$$

Then, defining $z_1 = \sigma$ and $z_2 = \dot{\sigma}$, one obtains a system under the form (2.3)

$$\begin{aligned} \dot{z}_1 &= z_2 \\ \dot{z}_2 &= a(x,t) + b(x,t)\cdot u \end{aligned} \tag{5.8}$$

with

$$\begin{aligned} a(x,t) &= -\frac{2\dot{R}(t)}{R(t)}x_2 - \frac{g}{R(t)}\sin(x_1) - \ddot{x}_c \\ b(x,t) &= \frac{1}{mR(t)^2}\ . \end{aligned} \tag{5.9}$$

For $|x_2| \leq 10$rad/s , the functions a and b are bounded with $|a(t)| < 13.898$ and $0 < 0.950 \leq b(t) \leq 1.0541$. The angle x_1 is supposed to be measured with a white noise of amplitude 10^{-5}, whereas x_2 is estimated by using a first order Levant differentiator Levant [1998] from the measurement of x_1. The simulations have been made with a control input sampling time $T_e = 0.001$s, which is 100 times higher than the integration step (10^{-5} s). The three SOSM control laws, TWC, 2SMOFC and TWLC are applied to system (5.8). The gain K_m has to fulfill $K_m > a_M/b_m$, which leads to $K_m > 14.63$. In the simulations, the parameters for the three control laws are uniformly chosen as $K_m = 100$, $\gamma = 5$.

5.2.3 Comparison results

The performances of these control laws are presented in Figures 5.5-5.7. More detailed comparisons can be made from Table 5.3, including the mean value of $|\sigma|$, $|\dot{\sigma}|$ and u, as well as the standard deviation of σ, calculated for the last 5 seconds of the simulations. The simulation results show that these three control laws make the system trajectories converging, in a finite time, in a neighborhood of desired trajectories. However, due to the noisy measurement, the use of differentiator in TWC causes an accuracy degradation. The tracking accuracies of 2SMOFC and TWLC reach the same level, but the large gain duration τ_i in 2SMOFC, being only one sampling step, leads to a longer convergence time. Not affected by the estimation quality of z_2, TWLC has a shorter convergence time than TWC.

The simulations are repeated with a reduced sampling period $T_e = 10^{-4}$s, and the comparison between the three control laws is shown in Figure 5.8. According to Table 5.3, the tracking accuracy with TWC has been improved thanks to a better estimation of x_2 from the differentiator. Due to the fact that the final convergence domain has been reduced, the convergence time for TWC slightly increases. However, due to a too small sampling period, the large gain duration τ_i of 2SMOFC has been also reduced, the convergence rate becomes very low, and its convergence time is finally over 30 seconds. Moreover, the performance of TWLC is improved due to a lower delay for the σ-sign switching detection. Furthermore, its convergence time does not depend on the sampling period.

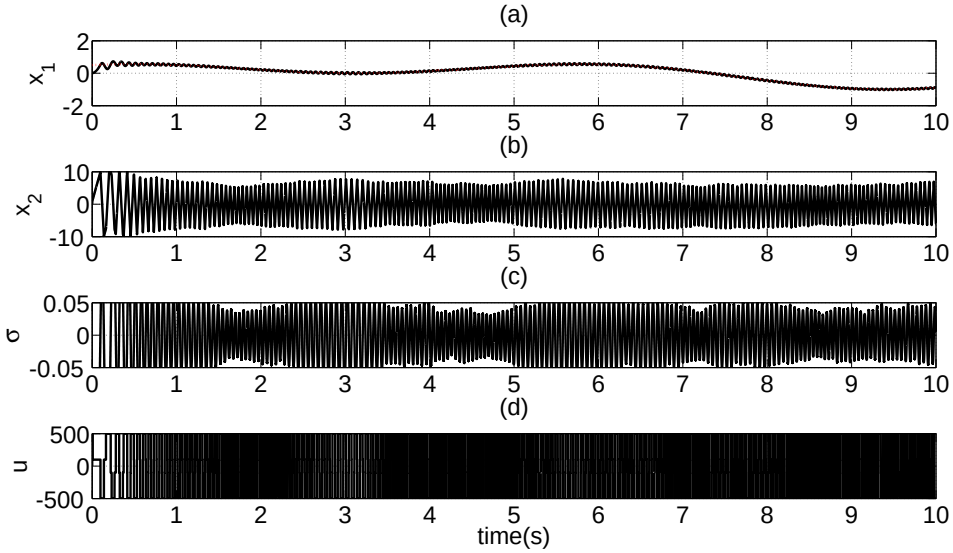

Figure 5.5 – **TWC** : State variables of system (5.8), sliding variable and control input. **(a).** x_1 versus time (sec); **(b).** x_2 versus time (sec) **(c).** σ versus time (sec); **(d).** u versus time (sec).

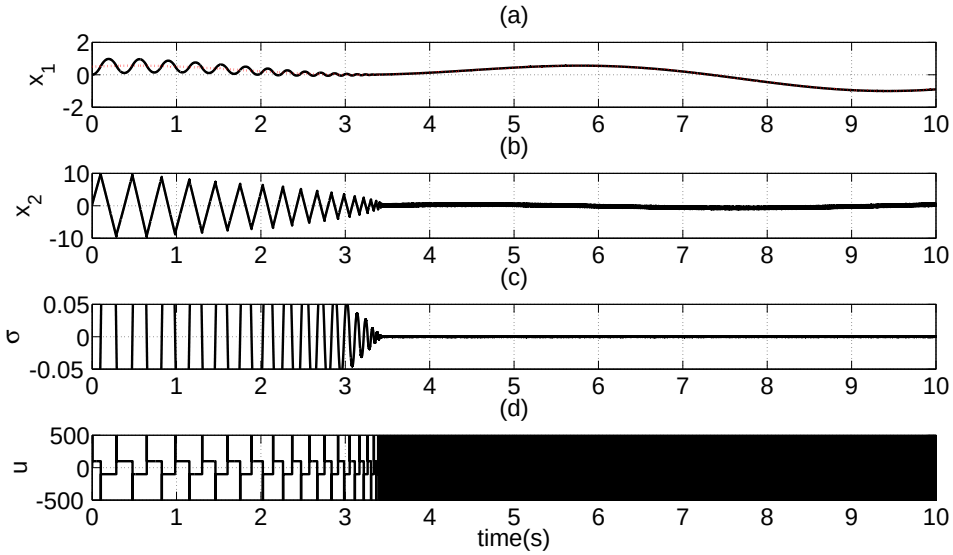

Figure 5.6 – **2SMOFC** : State variables of system (5.8), sliding variable and control input. **(a).** x_1 versus time (sec); **(b).** x_2 versus time (sec); **(c).** σ versus time (sec); **(d).** u versus time (sec).

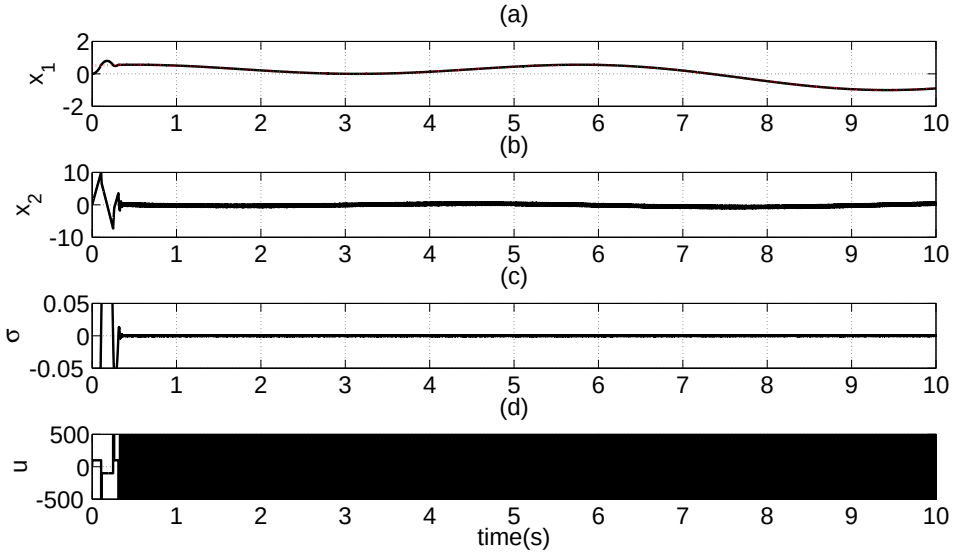

Figure 5.7 – **TWLC** : State variables of system (5.8), sliding variable and control input. **(a).** x_1 versus time (sec); **(b).** x_2 versus time (sec); **(c).** σ versus time (sec); **(d).** u versus time (sec).

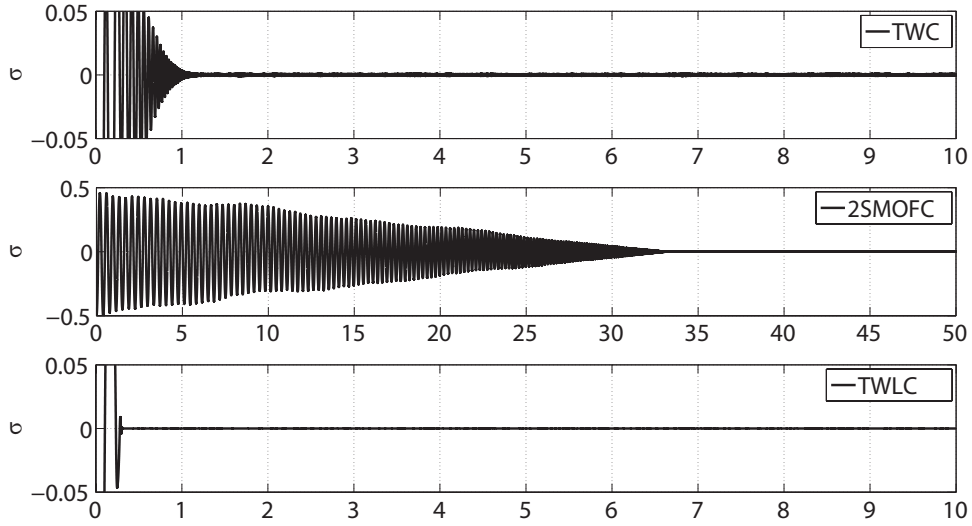

Figure 5.8 – **Sampling period** $T_e = 10^{-4}$s : Sliding variable σ versus time (sec) for the three control laws. **Top.** TWC; **Middle.** 2SMOFC; **Bottom.** TWLC.

	TWC	2SMOFC	TWLC
$mean(\|\sigma\|)$	0.031	1.88×10^{-4}	1.87×10^{-4}
$std(\sigma)$	0.034	2.25×10^{-4}	2.23×10^{-4}
$mean(\|\dot{\sigma}\|)$	1.24	0.10	0.11
$mean(\|u\|)$	480.56	252.64	253.04
Convergence Time (CT)	<0.6s	>3s	<0.4s
$mean(\|\sigma\|)$ for $T_e = 10^{-4}$s	4.32×10^{-4}	7.64×10^{-6}	7.62×10^{-6}
CT for $T_e = 10^{-4}$	<1.2s	>30s	<0.5s

Table 5.3 – Comparison between TWC, 2SMOFC and TWLC.

Conclusion

The main contributions of this part are summarized as following:

- The switching gain form is presented, which is an unified formalism of a class of second order sliding mode control laws.
- The twisting control and the second order sliding mode output feedback control are reformulated in the switching gain form. This reformulation is interesting because it allows to compare these both controllers with a new one named twisting-like controller.
- The twisting-like controller ensures the establishment of a real second order sliding mode with respect to the sliding variable in a finite time. The main features of this control law can be summarized as follows
  - Only the measurement of σ is required but not its derivative;
  - The performances (convergence time and accuracy) of this control law are close to those obtained with twisting control;
  - A gain switching strategy is used for this control law and the switching conditions depend on the detection of the sign commutations of σ and an online updated variable τ_i.
- The twisting-like control can be used as a differentiator, which offers an estimation of the first time derivative of a measured signal.
- Comparisons between TWC, 2SMOFC and TWLC, have been shown that the convergence time of TWLC has been strongly improved with respect to 2SMOFC and is closed to the one obtained with TWC. Moreover, thanks to the remove of the use of time derivative of the sliding variable, the additional disturbance caused by the differentiator is reduced for TWLC.

Adaptive high order sliding mode control

6

Introduction

In the previous part, an unified switching gain control form has been presented and three strategies of second order sliding mode control, Twisting control (TWC), Second order sliding mode output feedback control (2SMOFC) and Twisting-like control (TWLC) have been formulated in this framework. A common feature of these control laws is that the control gain switches between two constants: a large value and a small one.
The robustness of these control laws against matched perturbations is directly related to the value of their control gain. Overestimated perturbations bounds lead to large control gains, and then large chattering amplitude. An adaptation mechanism of the control gain allows to reduce the gain according to the actual perturbations (avoiding the assumption of the "worst" case scenario). The idea of reducing the chattering and relaxing the requirement of perturbation bounds knowledge has played a crucial role in the interest to develop SM controllers with adaptive or time-varying gain. Adaptive controllers based on sliding mode theory have been developed since several years Estrada and Plestan [2012]; Estrada et al. [2013]; Taleb et al. [2014]. An adaptive version of twisting control has been presented in Taleb et al. [2013]. The first contribution of this part consists in presenting the adaptive version of the second order sliding mode control laws 2SMOFC and TWLC. Moreover, the extension of adaptive 2SMOFC towards third order sliding mode is also introduced in this part.
In Estrada and Plestan [2014], a gain adaptation law is proposed for the 2SMOFC. Due to the feature that only the sign of the sliding variable is measured, an original mechanism is used to adjust the gain. Such mechanism is based on the time elapsed between two successive sign commutations of the sliding variable. This gain adaptation does not only simplify the gain tuning process, but also reduces the chattering caused by an overestimated large gain.
Considering the TWLC presented in Chapter 4, the z_1-sign commutation is the trigger to apply the large gain control $u = u_H$. Due to this latter feature, a drawback of this controller is that, if the system trajectory is initially far from the origin, there will be a quite long time until that the first z_1-sign commutation occurs. It means that, during this time interval, no large gain will be applied, which may lead to a long convergence time.
In Yan et al. [2016d], an adaptation law is proposed for TWLC. This gain adaptation mechanism allows not only to reduce the gain when a real sliding mode is established, but also to reduce the convergence time.
With the adaptive version of 2SMOFC and TWLC, the establishment of the real 2SM is ensured after a finite time. Moreover, compared to the TWC, the use of the time derivatives of the

sliding variable has been removed. Then, in this work, the effort has been made to extend the 2SMOFC to the higher order sliding mode (more than two) approaches.
In Yan et al. [2016c], a third order sliding mode control approach (denoted 3SMC) has been proposed and is presented in the sequel. This new 3SMC is based on the 2SMOFC . Compared to the standard third order sliding mode controller (for example, Defoort et al. [2009]; F.Dinuzzo and A.Ferrara [2009]; Trivedi and Bandyopadhyay [2012]), the main advantage of this new method is that only the sliding variable and its first order derivative are required. Moreover, an adaptation gain law is proposed which allows to reduce the gain (and then the chattering) and to simplify the tuning.

6.1 Organization

This part is organized as follows: Chapter 7 focuses on the adaptive second order sliding mode control: adaptive versions of 2SMOFC and TWLC are presented. In Chapter 8, an adaptive new third order sliding mode controller is proposed, for which the design of the control law and the parameter tuning are presented.

6.2 System presentation

Consider the uncertain nonlinear system

$$\dot{x} = f(x,t) + g(x,t) \cdot u \tag{6.1}$$

with $x \in \mathcal{X} \subset \mathbb{R}^n$ the system state ($\mathcal{X}$ being a bounded subset of $\mathbb{R}^n$) and $u \in \mathbb{R}$ the control input. Functions $f(x,t)$ and $g(x,t)$ are differentiable partially known vector-fields.

7

Adaptive second order sliding mode control

Contents

7.1 Problem statements

The two control laws, 2SMOFC and TWLC, are applicable to systems with a relative degree equal to two. Consider the system (6.1) and define from the control objective the sliding variable $\sigma(x,t)$, with relative degree equal to 2. It means that the control objectives are fulfilled when $\sigma = 0$ and

$$\ddot{\sigma} = a(x,t) + b(x,t) \cdot u \tag{7.1}$$

with functions $a(x,t)$ and $b(x,t)$ supposed to be uncertain. Then, the control problem of system (6.1) is equivalent to the finite time stabilization around the origin of

$$\begin{aligned} \dot{z}_1 &= z_2 \\ \dot{z}_2 &= a(x,t) + b(x,t) \cdot u \end{aligned} \tag{7.2}$$

with $z_1 = \sigma$, $z_2 = \dot{\sigma}$. Suppose that the following assumptions are fulfilled

Assumption 7.1.1. *The system trajectories are supposed to be infinitely extendible in time for any bounded Lebesgue measurable input;*

Assumption 7.1.2. *The controller is updated in discrete-time with the sampling period T_e which is a strictly positive constant. The control input u is constant between two successive sampling steps i.e*

$$\forall t \in [kT_e \;\; (k+1)T_e[\;\; u(t) \;\; = \;\; u(kT_e)\,; \tag{7.3}$$

Assumption 7.1.3. *Function a is a bounded uncertain function and b is positive and bounded. Thus, there exist positive constants a_M, b_m, b_M such that*

$$\begin{array}{l} |a(x,t)| \leq a_M \\ 0 < b_m \leq b(x,t) \leq b_M \end{array} \tag{7.4}$$

for $x \in \mathcal{X}$ and $t > 0$.

7.2 Adaptive version of second order sliding output feedback control

In Section 3.4, a first version of 2SMOFC is given by Theorem 3.4. In this case, the gain K_m is supposed to be a constant. In this section, the gain K_m becomes a time-varying function which allows to simplify the tuning process and to reduce the chattering, by adjusting the gain magnitude.

7.2.1 Recall of the non-adaptive control law

Consider the system (7.2), under Assumptions 7.1.1-7.1.3. The 2SMOFC algorithm Estrada and Plestan [2012] reads as

$$u(kT_e) \;\; = \;\; -K(kT_e)\text{sign}(z_1(kT_e)) \tag{7.5}$$

with $k \in I\!N$, K being defined as

$$K(kT_e) \;\; = \;\; \left\{ \begin{array}{ll} K_m & \text{if} \;\; kT_e \notin \mathcal{T}_{\mathcal{H}} \\ \gamma K_m & \text{if} \;\; kT_e \in \mathcal{T}_{\mathcal{H}} \end{array} \right. \tag{7.6}$$

and

$$\mathcal{T}_{\mathcal{H}} = \{kT_e \mid \text{sign}(z_1((k-1)T_e)) \neq \text{sign}(z_1(kT_e))\}. \tag{7.7}$$

In Section 3.4, it has been proved that with some large enough constant K_m and γ, a real second order sliding mode with respect to z_1 is ensured in a finite time. A necessary condition for the tuning of K_m is that it must be larger than a_M/b_m. From a practical point of view, the bound of the uncertainty could not be known precisely, and the "worst" case may never happen. Then, an oversized gain K_m induces large control magnitude and then can increase the chattering. In the sequel, a novel version of 2SMOFC with gain adaptation is presented.

Remark 7.2.1. *Compared to the constant gain version of 2SMOFC presented in Theorem 3.4, in this chapter, the control gain K_m is no longer a constant, but becomes a time varying function $K_m(t)$, whose computation is detailed next.*

7.2.2 Gain adaptation law

The gain adaptation algorithm developed for the 2SMOFC should answer to the following requirements:

- with the adaptation law, the gain $K_m(t)$ should be reduced when the system trajectories have converged to a vicinity of the origin;
- the gain $K_m(t)$ increases when the system trajectories have left or have not reached a vicinity of the origin;
- the detection of whether the system has reached the vicinity of the origin, must be based on z_1.

In Yan et al. [2016a] a mechanism satisfying the above requirements is proposed which is based on the time elapsed between two successive z_1-sign commutations. Recall that T_s^i ($i \in \mathbb{N}, i > 0$) is the time at which the i^{th} z_1-sign switching is detected. *i.e.*

$$\text{sign}(z_1(T_s^i)) \quad \neq \quad \text{sign}(z_1(T_s^i - T_e)) \tag{7.8}$$

and set $T_s^0 = 0$. Then, the gain adaptation algorithm is summarized by the following theorem.

Theorem 7.1 (Yan et al. [2016a])**.** *Consider the system (7.2), under Assumptions 7.1.1-7.1.3. The control input u is defined by (7.5)-(7.6) (where the constant K_m is replaced by time varying function $K_m(t)$) with $\gamma > 1$, by $\mathcal{T}_{\mathcal{H}}$ defined as (7.7) and by the gain $K_m(t)$ fulfilling the following rules*

- *$K_m(t)$ is constant over each sampling period T_e i.e. $\forall t \in [kT_e, (k+1)T_e[,\ K_m(t) = K_m(kT_e)$;*
- *$K_m(0) > 0$;*
- *the adaptation law of K_m reads as*

$$\forall t \in [T_s^i, T_s^{i+1}[, \quad \dot{K}_m(t) = \Gamma \cdot \text{sign}(t - T_s^i - \beta T_e) \tag{7.9}$$

with $\Gamma > 0$ and $\beta > 1$ ($\beta \notin \mathbb{N}$).

Then, the establishment of a real second order sliding mode with respect to z_1 is ensured.

Remark 7.2.2.

- *This gain adaptation law helps to simplify the tuning process for K_m, it allows to adjust the gain without knowing the bound of the perturbations and uncertainties.*
- *The duration between two successive z_1-sign commutations is a key-point of the gain adaptation law. Denote $\eta_i \in \mathbb{N}$ the number of sampling periods between T_s^i and T_s^{i+1}*

$$T_s^{i+1} - T_s^i \ = \ \eta_i T_e.$$

If $\eta_i = 1$, no commutation between K_m and γK_m would take place and no convergence can be ensured Plestan et al. [2010a]. On the other hand, when a real second order sliding mode is established, the sliding variable is changing its sign at high frequency Bartolini et al. [2002], which implies that η_i is bounded.

- *The main idea of the gain adaptation law consists in counting the number of sampling periods between two successive z_1-sign commutations, and checking if this number is lower than a value fixed by the parameter β: if it is the case, it means that a real second order sliding mode is established, then the gain can be reduced; if it is not the case, the detection fails and the gain is increasing.*
- *The parameter β allows to evaluate if the trajectory in (z_1, z_2)-phase plane is evolving with a relative high frequency around the origin. This latter feature of trajectories dynamics is directly connected to the establishment of a real second order sliding mode.*

Proof. Without loss of generality, suppose that the $i+1$-th z_1-sign commutation occurs at a time larger than $T_s^i + \text{Ceil}(\beta)T_e$ [1]. If it not the case, it means that the number of sampling period between T_s^i and T_s^{i+1} have been smaller than β then, the convergence to a vicinity of the origin is considered to be obtained: given (7.9), the gain K_m is decreasing.
From equation (7.9), for $t \in [T_s^i, T_s^i + \text{Ceil}(\beta)T_e[$, one has

$$\dot{K}_m(t) = -\Gamma \tag{7.10}$$

which gives

$$K_m(T_s^i + \text{Ceil}(\beta)T_e) = K_m(T_s^i) - \Gamma \cdot \text{Ceil}(\beta)T_e \tag{7.11}$$

By a similar way, for $t \in [T_s^i + \text{Ceil}(\beta)T_e, T_s^{i+1}[$, one has

$$\dot{K}_m(t) = \Gamma \tag{7.12}$$

which gives

$$K_m(T_s^{i+1}) = K_m(T_s^i + \text{Ceil}(\beta)T_e) + \Gamma \cdot (T_s^{i+1} - T_s^i - \text{Ceil}(\beta)T_e) \tag{7.13}$$

Then, from (7.11)-(7.13), one gets

$$\begin{aligned} K_m(T_s^{i+1}) &= K_m(T_s^i) + \Gamma \cdot (T_s^{i+1} - T_s^i) - 2\Gamma\text{Ceil}(\beta)T_e \\ &= K_m(T_s^i) + \eta_i T_e \Gamma - 2\Gamma\text{Ceil}(\beta)T_e \end{aligned} \tag{7.14}$$

Denote $T_s^{i+1} - T_s^i = \eta_i T_e$ then, by comparing η_i to $2\text{Ceil}(\beta)$,

- if $\eta_i > 2\text{Ceil}(\beta)$, it means that the switching frequency of the sign of the sliding variable is at a relative low level. The system trajectories have not yet converged: it could be due to the fact that the gain is not large enough and then has to be increased, *i.e.*

$$\eta_i > 2\text{Ceil}(\beta) \Rightarrow K_m(T_s^{i+1}) > K_m(T_s^i); \tag{7.15}$$

- in the opposite case, it means that the switching frequency of the sign of the sliding variable is at a relative high level. It means that the system trajectories have converged: the gain can be considered large enough and then can be decreased, *i.e.*

$$\eta_i < 2\text{Ceil}(\beta) \Rightarrow K_m(T_s^{i+1}) < K_m(T_s^i). \tag{7.16}$$

From K_m-dynamics (7.9), it is clear that, until the convergence to a vicinity of the origin of the (z_1, z_2)-phase plane is not detected, the gain is increasing. Given its dynamics, it is obvious that K_m is reaching in a finite time a sufficiently large gain with respect to uncertainties and perturbations, in order to make the closed-loop system (7.2) converging to a vicinity of the origin. Once this convergence is detected, K_m-dynamics allows to reduce the gain which could become too small with respect to uncertainties and perturbations: then, the detection of the convergence statement fails inducing that the gain is increasing again, and so on. ■

1. The function Ceil is defined as follows: given $\alpha \in \mathbb{R}$ and $\alpha^* \in \mathbb{N}$, $\text{Ceil}(\alpha) = \min\{\alpha^* \in \mathbb{N} | \alpha^* \geq \alpha\}$.

Remark 7.2.3. *The tuning rule of β is given as $\beta > 1$. If $0 < \beta \leq 1$, the single possibility to reduce the gain would be to have $\eta_i \in \{0, 1\}$. In this case, there is no more interval time to apply the large gain γK_m; knowing that the application of γK_m is absolutely necessary to make the system converge Plestan et al. [2008b], one concludes that, if $0 < \beta \leq 1$, the system trajectories are diverging.*

7.2.3 Simulations

Some simulations are presented in this section. Consider system (7.2) with

$$\begin{aligned} a(t) &= 6\sin(10t) + 0.5\text{sign}(\sin(10\text{t})) \\ b(t) &= 1 + 0.1\sin(40t) \end{aligned}$$

which gives

$$b_m = 0.9, \quad b_M = 1.1, \quad a_M = 6.5. \tag{7.17}$$

Assumption 7.1.3 is fulfilled: recall that these bounds are unknown. The system is controlled by (7.5)-(7.6) with adaptation law (7.9). The sampling period is $T_e = 0.01\,\text{sec}$. The initial conditions are set as $z(0) = [1\ 0]^T$. Then, the comparison between standard 2SMOFC and its adaptive version is made, the parameter configurations being detailed by Table 7.1. The control gain for adaptive 2SMOFC is time varying with $\Gamma = 100$, and the gain K_m for standard 2SMOFC is tuned equal to the average value of adaptive gain. The simulation result is plotted in Figure 7.1, and detailed comparisons are made in Table 7.2. The convergence time is defined as the time when $T_s^{i+1} - T_s^i < 2\text{Ceil}(\beta)T_e$ fulfilled. It shows that thanks to the gain increasing before the establishment of 2SM, the convergence time obtained with adaptive 2SMOFC is improved with respect to its standard version. Moreover, comparing their absolute means values and standard deviations, the gain adaptation algorithm improves the tracking accuracy for both z_1 and z_2.

2SMOF	Adp 2SMOF
$\gamma = 10,\ K_m = 17$	$\gamma = 10,\ K_m(0) = 100$ $\Gamma = 100,\ \beta = 3.1$

Table 7.1 – Parameter configurations of 2SMOF and adaptive 2SMOF.

	2SMOFC	Adp 2SMOFC
Convergence time	2s	0.3s
mean($\lvert z_1 \rvert$)	0.064	0.017
std(z_1)	0.171	0.074
mean($\lvert z_2 \rvert$)	0.917	0.673
std(z_2)	1.253	1.766
mean(K_m)	17	17.14

Table 7.2 – Comparison between standard 2SMOFC and adaptive 2SMOFC.

Then, the simulation is repeated, in order to investigate the effect of parameter β in the gain adaptation algorithm (7.9). Figure 7.2 displays simulation results with several values of $\beta = \{0.9, 1.1, 2.1, 3.1\}$.

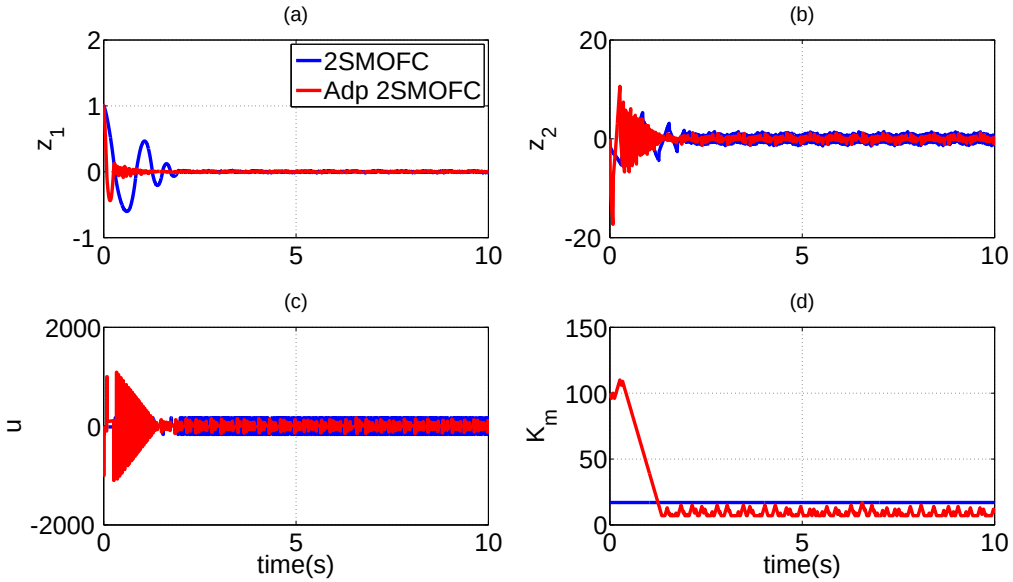

Figure 7.1 – **Standard 2SMOFC vs Adaptive 2SMOFC**: **(a).** z_1 versus time (sec); **(b).** z_2 versus time (sec); **(c).** control input u versus time (sec); **(d).** gain $K_m(t)$ versus time (sec).

Remark 7.2.4. *The "sign" function not being defined at 0, the values of β are not chosen as integers: then, in (7.9), there is no ambiguity on the sign value. However, note that, for a nonzero sampling period T_e, the behavior of K_m is the same for $\beta \in]k\ , k+1[$, $k \in \mathbb{N}$.*

The convergence of z_1 in a vicinity of 0 is obtained for $\beta > 1$. However, when $\beta < 1$, the system is diverging given that the gain K_m is always increasing. In order to show the influence of the tuning of β and T_e, Table 7.3 presents root mean square (rms) values of z_1 and K_m once the real 2SM is established. It appears that the accuracy is improved when the sampling period T_e is reduced. Furthermore, when the parameter β is increased, according to (7.16), the gain K_m is reduced. However, for the final sliding mode phase, the duration between two successive z_1-sign switching is longer, which leads to a lower accuracy. Then, it is necessary to get a compromise between T_e and β.

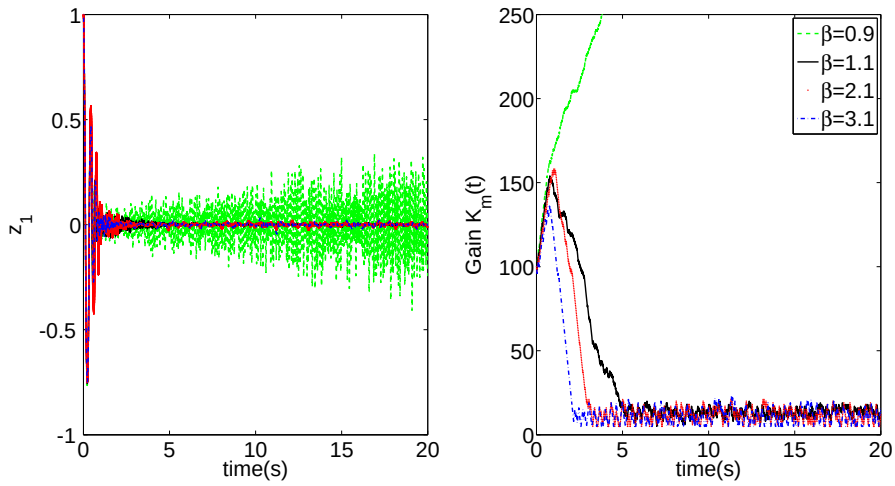

Figure 7.2 – $z_1(t)$ (left) and $K_m(t)$ (right) versus time (sec) with $\beta = \{0.9, 1.1, 2.1, 3.1\}$.

	$\beta = 1.1$		$\beta = 2.1$		$\beta = 3.1$	
T_e	$\text{rms}(z_1)$	$\text{rms}(K_m)$	$\text{rms}(z_1)$	$\text{rms}(K_m)$	$\text{rms}(z_1)$	$\text{rms}(K_m)$
0.01s	4.8×10^{-3}	13.51	7.2×10^{-3}	12.10	9.9×10^{-3}	12.00
0.001s	5.3×10^{-5}	15.67	5.4×10^{-5}	8.91	5.8×10^{-5}	7.84

Table 7.3 – Root mean squares of z_1 and K_m in steady state, for different values of T_e and β

7.3 Adaptive version of twisting-like control

The twisting-like control law (TWLC) introduced in Chapter 4 (see Theorem 4.1) is an improvement control strategy based on the 2SMOFC, the TWLC allowing a faster convergence. The following features are shared by these two control laws:

- applicable to systems with relative degree equal to one or two;
- only the measurement of the sign of the sliding variable is required;
- a real second order sliding mode with respect to the sliding variable is ensured in a finite time.

In the previous section, an adaptation gain law has been developed for the 2SMOFC. In this section, an adaptation gain algorithm is developed for the TWLC in Theorem 7.2.Similar to Theorem 7.1, these both gain adaptation laws are using the time gap between two successive sign switching of the sliding variable as a sliding mode detector.

7.3.1 Recall of the non adaptive control law

Consider the system (7.2), under Assumptions 7.1.1-7.1.3. The TWLC algorithm Yan et al. [2016d] reads as ($k \in I\!N$)

$$u(kT_e) = -K(kT_e)\text{sign}(z_1(kT_e)) \tag{7.18}$$

with the gain K defined as

$$K = \begin{cases} K_m & \text{if} \quad kT_e \notin \mathcal{T}_{\mathcal{H}} \\ \gamma K_m & \text{if} \quad kT_e \in \mathcal{T}_{\mathcal{H}} \end{cases} \tag{7.19}$$

and the domain $\mathcal{T}_{\mathcal{H}}$ defined as

$$\mathcal{T}_{\mathcal{H}} = \{kT_e \mid T_s^i \leq kT_e \leq T_s^i + \tau_i, i \in I\!N\} \tag{7.20}$$

The value of τ_i is obtained from

$$\tau_i = \max(\tau_i', T_e) \tag{7.21}$$

with

$$\tau_i' = T_e \cdot \text{floor}\left[2\alpha \frac{\tau_{i-1} K_M^{min} + \bar{\tau}_{i-1} K_m^{min}}{K_M^{max} T_e} - 1\right] \tag{7.22}$$

and

$$\begin{aligned} K_m^{max} &= b_M K_m + a_M, \qquad K_m^{min} = b_m K_m - a_M \ , \\ K_M^{max} &= \gamma b_M K_m + a_M, \qquad K_M^{min} = \gamma b_m K_m - a_M \ . \end{aligned}$$

The parameters α and $\bar{\tau}_i$ are respectively defined as

$$\alpha = \frac{\sqrt{K_m^{min}}}{\sqrt{K_M^{max}} + \sqrt{K_m^{min}}} \tag{7.23}$$

and

$$\bar{\tau}_i = \max(0,\ T_s^{i+1} - T_s^i - \tau_i)\ . \tag{7.24}$$

As the 2SMOFC, the main difficulty for the development of a gain adaptation algorithm for TWLC is that only the sign of the sliding variable is available. The gain adaptation algorithm introduced in Section 7.2 could offer a solution for such class of control laws. This mechanism is based on the time elapsed between two successive z_1-sign commutations. However, with a finite gain, there exists also an additional problem. Indeed, for the TWLC, the z_1-sign commutation is the trigger to apply the large gain control $u = u_H$. Therefore, if the system trajectory is initially far from the origin, there would be a quite long time until the first z_1-sign commutation occurs. It means that during this time interval no large gain would be applied, which may leads to a long convergence time. This is the main reason to develop a new gain adaptation algorithm in order to reduce the convergence time.

7.3.2 Gain adaptation law

A gain adaptation law is developed for the TWLC. Under this adaptation mechanism, the gain K_m should satisfy the following requirements

- K_m should be reduced when the system trajectories have converged to a vicinity of the origin;
- the gain K_m increases when the system trajectories have left or have not reached a vicinity of the origin;
- if during a given time interval, no sign commutation of the sliding variable is detected, the gain K_m should increase in order to reduce the convergence time.

Then, a new gain adaptation algorithm is described in the following theorem.

Theorem 7.2 (Yan et al. [2016d]). *Consider the system (7.2) with Assumptions 7.1.1-7.1.3 fulfilled and under the control law (7.18)-(7.24) (with the constant gain K_m replaced by the time varying function $K_m(t)$). Denote T_s^i the time of the i-th detected change of z_1-sign. The adaptation mechanism for gain $K_m(t)$ reads as*

$$K_m(t) = \begin{cases} K_m^i & \text{if} \quad t \in [T_s^i, T_s^{i+1}[\text{ and } t - T_s^i \leq \varepsilon(T_s^i - T_s^{i-1}) \\ K_{max} & \text{if} \quad t \in [T_s^i, T_s^{i+1}[\text{ and } t - T_s^i > \varepsilon(T_s^i - T_s^{i-1}) \end{cases} \tag{7.25}$$

$$K_m^i = \min\left(\max\left(K_m^{i-1} + \Gamma \cdot (T_s^i - T_s^{i-1} - \beta T_e)\ , 0\right)\ , K_{max}\right)$$

with $\beta \in \mathbb{N}^\star$, $\varepsilon \geq 1$, $\Gamma > 0$ and $K_{max} > a_M/b_m$. Using this adaptation law, the controller (7.18)-(7.24) ensures the establishment of a real second order sliding mode with respect to z_1.

Remark 7.3.1.

- *The gain K_m is updated when the switching of z_1-sign is detected; K_m is constant between two successive z_1-sign switching points.*
- *As Theorem 7.1, the idea consists in counting the number of sampling periods between two successive z_1-sign commutations. It has been presented in Yan et al. [2016a], that the establishment of real second order sliding mode can be detected through the comparison between $T_s^i - T_s^{i-1}$ and βT_e. If a real second order sliding mode is established then, $T_s^i - T_s^{i-1} \leq \beta T_e$, and the gain is reduced. If it is not the case, the gain increases.*
- *The parameter β allows to evaluate if the trajectory in (z_1, z_2)-phase plane is evolving with a relative high frequency around the origin. This latter feature of trajectories dynamics is directly connected to the establishment of a real second order sliding mode. From this evaluation, the gain is increased or decreased.*
- *The gain is forced to have its maximum value if, since the latest detection time T_s^i, no z_1-sign switching is detected for a "relatively" long time. This latter is defined by the parameter ε: the smaller ε is, the faster convergence time is, but with a larger gain.*

Proof. Consider the system (7.2) under the control law (7.18)-(7.24) and Assumptions 7.1.1-7.1.3 fulfilled. The adaptation law for $K_m(t)$ reads as (7.25). This gain adaptation strategy can be summarized by Figure 7.3.

- The gain is forced to have its maximum value if, since the latest detection instant T_s^i, no z_1-sign switching can be detected for a relatively long time which is defined by ε.
  Set $T_s^0 = T_s^{-1} = 0$. Then, if $t - T_s^i > \varepsilon(T_s^i - T_s^{i-1})$, with $i \in \mathbb{N}$ and $\varepsilon > 1$, one has $K_m = K_{max}$. According to Theorem 4.1, the system converges closer to zero. It yields that $T_s^{i+1} - T_s^i \leq T_s^i - T_s^{i-1}$.
- If $T_s^{i+1} - T_s^i \geq \beta T_e$, it means that the sign switching frequency of the sliding variable is at a relative low level. In other words, the system trajectories have not yet converged to the final vicinity of zero: the gain should be increased to shorten the convergence time, *i.e.*
  $$K_m^{i+1} = \min(K_m^i + \Gamma \cdot (T_s^{i+1} - T_s^i - \beta T_e), K_{max}) \tag{7.26}$$
  which yields $K_{max} \geq K_m^{i+1} \geq K_m^i$.
- In the opposite case, if $T_s^{i+1} - T_s^i < \beta T_e$, it means that the sign switching frequency of the sliding variable is at a relative high level: the system trajectories have converged. Therefore, the gain can be considered large enough and then can decrease, *i.e.*
  $$K_m^{i+1} = \max(K_m^i + \Gamma \cdot (T_s^{i+1} - T_s^i - \beta T_e), 0) \tag{7.27}$$
  which yields $0 \leq K_m^{i+1} \leq K_m^i$.

■

7.3.3 Simulations

Consider system

$$\begin{aligned} \dot{x}_1 &= x_2 \\ \dot{x}_2 &= a(t) + b(t)u \\ y &= x_1 \end{aligned} \tag{7.28}$$

with

$$\begin{aligned} a(t) &= 6\sin(10t) + 0.5\text{sign}(\sin(10t)) \\ b(t) &= 1 + 0.1\sin(40t)\ . \end{aligned} \tag{7.29}$$

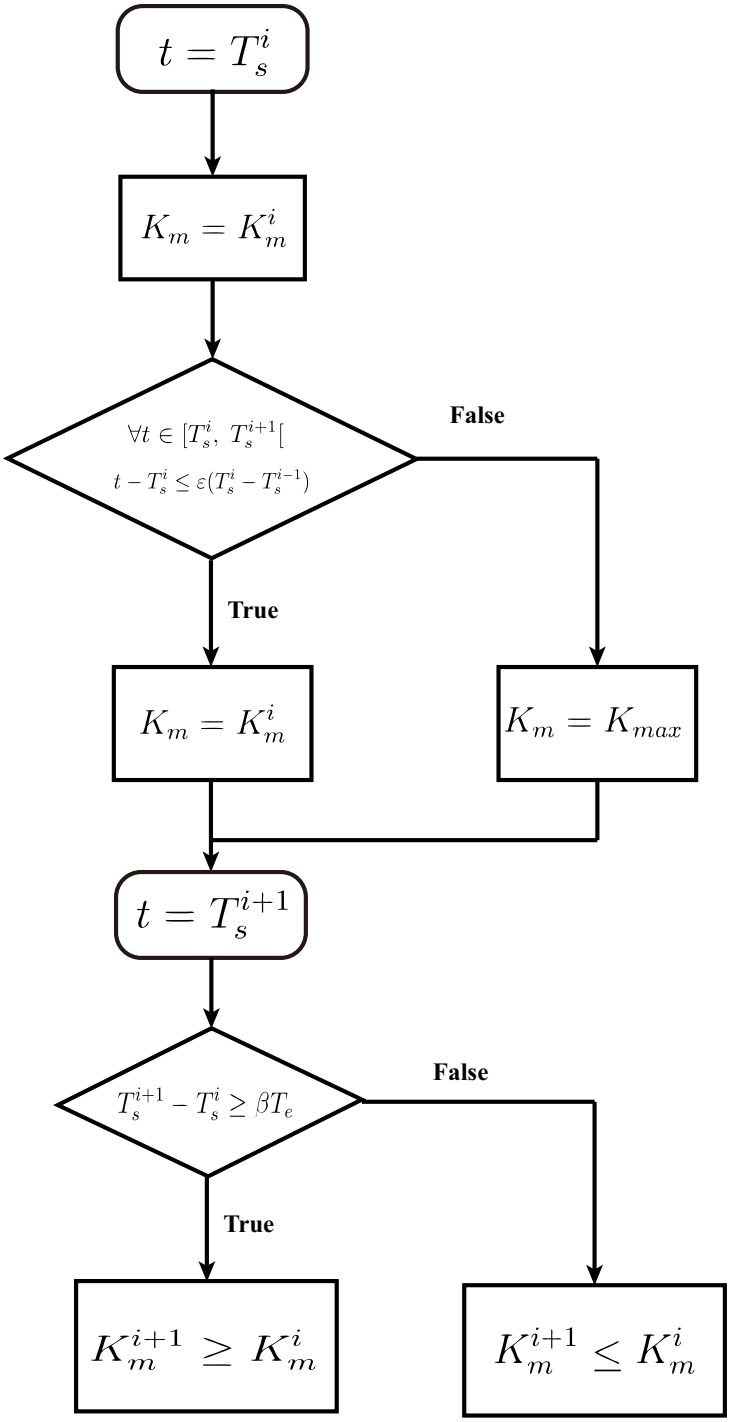

Figure 7.3 – Scheme of adaptive TWLC

The main advantage of the adaptation gain law for the TWLC consists in reducing the convergence time, when there is no sign commutation of the sliding variable. In order to highlight the contribution of this improved adaptation algorithm, in the simulation example, the state variable x_1 is forced to track a square form reference signal $x_{1_{ref}} = -5\text{sign}(\sin(0.2\pi t))$ (see Figure 7.4 (a)). It means that, periodically, the system trajectories will be far from the objectives. Then, the control objective is to force the output y to track a constant reference 5 or -5. The points for which $x_{1_{ref}}$ changes, can be treated as a reinitialization of the system. So, in this case, consider $\dot{x}_{1_{ref}} = 0$. Define the sliding variable σ as

$$\sigma \ = \ x_1 - x_{1_{ref}} \ . \tag{7.30}$$

Denote $z_1 = \sigma$, $z_2 = \dot{\sigma}$; then, the control problem is equivalent to stabilize

$$\begin{array}{rcl} \dot{z}_1 & = & z_2 \\ \dot{z}_2 & = & a(t) + b(t)u \ . \end{array} \tag{7.31}$$

Function $a(t)$ is bounded by $a_M = 6.5$. Function $b(t)$ satisfies $0.9 \leq b(t) \leq 1.1$. The simulation test is made with sampling period $T_e = 0.01$s, and the initial conditions are set as $x_1(0) = 1$, $x_2(0) = 0$. The performance of the standard TWLC and the adaptive TWLC are compared. The parameter tuning of these two control laws are detailed in Table 7.4. For the adaptive TWLC, the gain $K_m(t)$ is time-varying, and its dynamics depends on the parameter Γ. The constant gain K_m for standard TWLC is chosen close to the average value of the time varying one in the adaptive controller. The performance of standard TWLC is displayed by Figure 7.4. Figure 7.4 (a) shows that when the reference signal jumps, the sliding variable will be pushed far away from zero. During a relative long time, there is no sign switching for the sliding variable, which leads to a longer convergence time. The performance of the adaptive version TWLC is presented in Figure 7.5. Thanks to the gain adaptation algorithm (7.25), after the discontinuous point of the reference signal, the gain K_m is forced to its maximum value K_{max}, which allows to reduce the convergence time. A real second order sliding mode is said to be established, if $T_s^{i+1} - T_s^i < \beta T_e$ fulfills. Then, the convergence time can be calculated around the points $t = 0, t = 5, t = 10, t = 15$. A detailed comparison is made in Table 7.5. The average convergence time obtained with adaptive TWLC is improved with respect to standard version. Then, this reduction of the convergence time leads to the smaller tracking error for x_1.

TWLC	Adp TWLC
$\gamma = 10,\ K_m = 100$	$\gamma = 10,\ K_m(0) = 20$ $\Gamma = 100,\ \beta = 3.1$ $\varepsilon = 10,\ K_{max} = 200$

Table 7.4 – Parameters of standard and adaptive TWLC.

	TWLC	Adp TWLC
Average convergence time	2.12s	1.32s
mean($\lvert\sigma\rvert$)	1.26	0.97
std(σ)	2.60	2.4
mean(K_m)	100	99.99

Table 7.5 – Comparison between standard and adaptive TWLC.

7.4 Summary

The main contributions of this chapter are summarized as follows :

- A gain adaptation algorithm is proposed for 2SMOFC. It is based on the time elapsed between two successive sign commutations of the sliding variable.
- It has been proved that, under this adaptive mechanism, the gain K_m decreases when the system trajectory reaches a vicinity of zero, and increases in the opposite case.
- Through the simulations, it shows that the convergence time and the tracking accuracy obtained with adaptive 2SMOFC are improved with respect to its standard version.

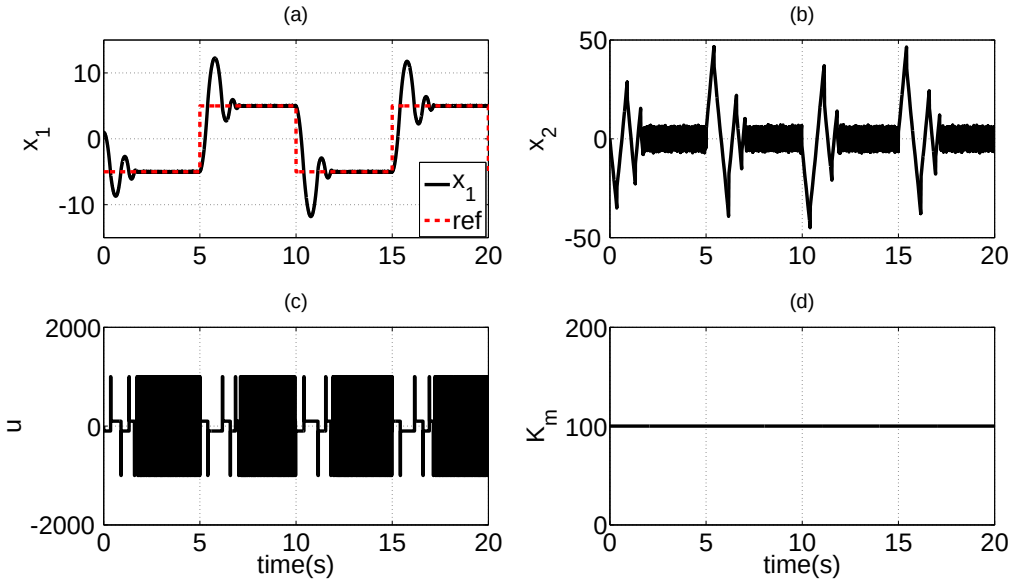

Figure 7.4 – **Standard TWLC: (a).** x_1 and $x_{1_{ref}}$ versus time (sec); **(b).** x_2 versus time (sec); **(c).** control input u versus time (sec); **(d).** gain $K_m(t)$ versus time (sec).

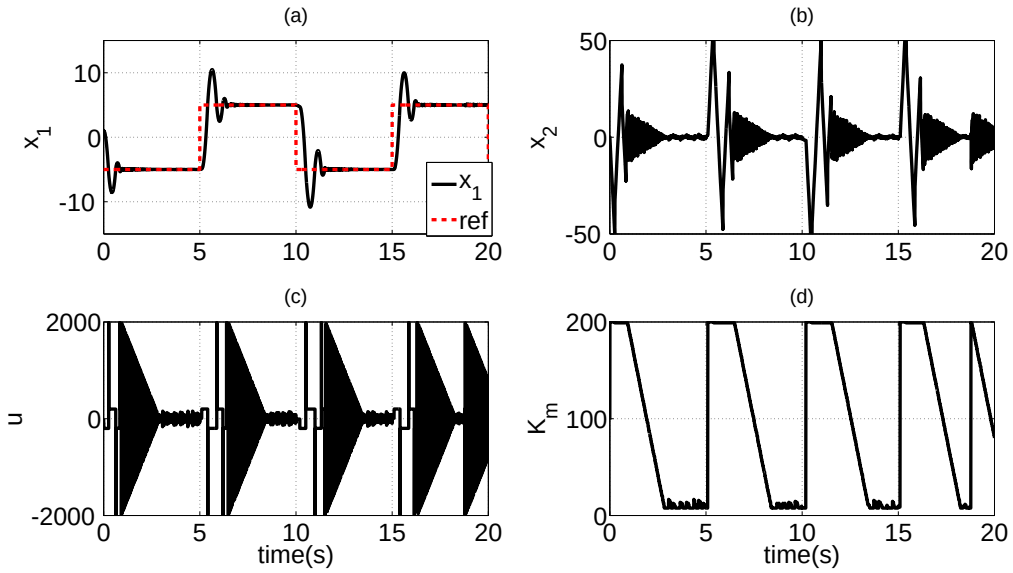

Figure 7.5 – **Adaptive TWLC: (a).** x_1 and $x_{1_{ref}}$ versus time (sec); **(b).** x_2 versus time (sec); **(c).** control input u versus time (sec); **(d).** gain $K_m(t)$ versus time (sec).

- Analyzing the roles played by the parameter β, it appears that, when the parameter β is increased, the gain K_m is reduced but the accuracy is lower.
- A gain adaptation algorithm is developed for TWLC. Under this adaptive mechanism the gain K_m decreases when the system trajectory reaches a vicinity of zero, and increases in the opposite case. Moreover, a jump of the gain is designed, if no sign commutation of the sliding variable is detected during a predefined time interval.
- According to the simulation results, the gain adaptation law allows to further improve the tracking accuracy and the convergence time, compared to the standard TWCL.

8

Adaptive third order sliding mode control

Contents

In Chapter 3 and 4, two second order sliding mode control laws 2SMOFC and TWLC have been presented under an unified formalism, based on gain switching strategy. These control laws are applicable to systems with relative degree equal to one or two and the use of time derivative of the sliding variable is not required. Then, in Chapter 7, gain adaptation algorithms have been developed for these two control laws respectively. The objective of this chapter is to extend these methods to higher order sliding mode (more than two). The study is based on the concept used for 2SMOFC, and the extension is made for third order sliding mode control (denoted 3SMC). This new controller can be applied directly to systems with relative degree equal to three with respect to the sliding variable, but it is also applicable to the cases of relative degree equal to one or two.

8.1 Problem statement

Consider the system (6.1) and define, from the control objective, the sliding variable $\sigma(x,t)$ with relative degree equal to three, *i.e.*

$$\sigma^{(3)} = a(x,t) + b(x,t) \cdot u \tag{8.1}$$

with functions $a(x,t)$ and $b(x,t)$ deduced from (6.1). Then, the control problem is equivalent to the finite time stabilization of the system

$$\begin{array}{rcl} \dot{z}_1 & = & z_2 \\ \dot{z}_2 & = & z_3 \\ \dot{z}_3 & = & a(x,t) + b(x,t) \cdot u \end{array} \tag{8.2}$$

with $z = [z_1, z_2, z_3]^T = [\sigma, \dot{\sigma}, \ddot{\sigma}]^T$. Suppose that the following assumptions hold

Assumption 8.1.1. *The trajectories of system (8.2) are supposed to be infinitely extendible in time for any bounded Lebesgue measurable input.*

Assumption 8.1.2. *For $x \in \mathcal{X}$ and $u \in \mathbb{R}$, the vector z is evolving in a bounded open subset of $\mathbb{R}^3$, i.e. $z \in \mathcal{Z} \subset \mathbb{R}^3$.*

Assumption 8.1.3. *The control input u is updated in discrete-time with the positive sampling period T_e. The control input u is constant between two successive sampling steps i.e*

$$\forall t \in [kT_e,\ (k+1)T_e[,\quad u(t) \ = \ u(kT_e)\,. \tag{8.3}$$

Assumption 8.1.4. *Functions a and b are bounded uncertain functions, and there exist positive constants $a_M > 0$, $b_m > 0$ and $b_M > 0$ such that*

$$|a(x,t)| \leq a_M,\quad 0 < b_m < b(x,t) < b_M \tag{8.4}$$

for $x \in \mathcal{X}$ and $t > 0$.

The objective is here to develop a new controller, based on high order sliding mode concept, for the system (8.2), which meets the following requirements

- a real third order sliding mode with respect to z_1 should be ensured in a finite time;
- the use of time derivatives of the sliding variable used in the control law has to be reduced with respect to the full state feedback HOSM controller Levant [2003].

Definition 8.1.1. *Levant [1993] The system (8.2) is said to perform a real third order sliding mode with respect to z_1 if the system trajectory satisfies in a finite time $|z_1| \leq \mu_0 T_e^3$, $|z_2| \leq \mu_1 T_e^2$ and $|z_3| \leq \mu_2 T_e$ with T_e the sampling period used for control application, and μ_0, μ_1, μ_2 positive constants independent of T_e.*

8.2 Presentation of the control law

In Yan et al. [2016c], a new third order sliding mode controller is proposed. Its main feature is that only the sliding variable and its first order time derivative are required. It means that, considering system (8.2), this 3SMC requires only the informations of z_1 and z_2, which meets the requirements mentioned just above.

The idea of the new control law is to stabilize the system (8.2) *step-by-step*. Firstly, the controller forces z_1 to converge to a vicinity of zero. Then, the next step is to vanish z_2 and z_3 without breaking the accuracy of z_1. The design of this new 3SMC is composed by three main steps

1. definition of two "layers";
2. definition of "internal sliding" variable $\bar{\sigma}$;
3. design of the control law.

8.2.1 Definition of two layers

The convergence of system (8.2) to a vicinity of the origin is made in two steps: firstly the convergence of z_1; then, the convergence of z_2 and z_3. Starting from this fact two layers $\mathcal{L}_1$ and $\mathcal{L}_2$ are defined according to z_1 such that

$$\begin{aligned} \mathcal{L}_1 &= \{z \in \mathcal{Z} \mid |z_1| > \mu K_m T_e^3\} \\ \mathcal{L}_2 &= \{z \in \mathcal{Z} \mid |z_1| \leq \mu K_m T_e^3\} \end{aligned} \tag{8.5}$$

with T_e the sampling step and μ a positive constant (see Figure 8.1). Note that the definition of these both layers is linked to Definition 8.1.1 of real third order sliding mode.

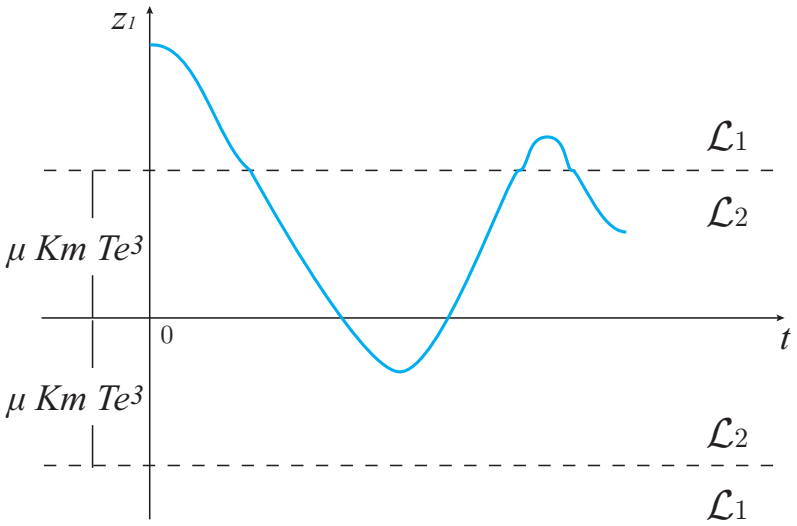

Figure 8.1 – Definition of the layers $\mathcal{L}_1$ and $\mathcal{L}_2$.

The control objectives are defined with respect to the both layers

- **Layer $\mathcal{L}_1$.** When $z \in \mathcal{L}_1$, the main control objective is to force z_1 to converge to a vicinity of zero, which makes the system trajectory reach $\mathcal{L}_2$.
- **Layer $\mathcal{L}_2$.** Once z_1 belongs to $\mathcal{L}_2$, the main task is no longer the control of z_1, but to force z_2 and z_3 to reach a vicinity of 0, in order to ensure the establishment of a real third order sliding mode.

8.2.2 Definition of the sliding variable

The control objectives are different for the two layers: so, an "internal" sliding variable $\bar{\sigma}$ (different from the sliding variable σ defined for system (6.1)) is defined respectively for both $\mathcal{L}_1$ and $\mathcal{L}_2$ layers.

- **Layer $\mathcal{L}_1$.** When system trajectories are evolving in $\mathcal{L}_1$, according to the control objective, the definition of the internal sliding variable $\bar{\sigma}$ must lead to the finite time convergence of z_1. The definition of $\bar{\sigma}$ is based on the terminal sliding mode control concept Feng et al. [2002] and reads as (with $\alpha > 0$)

$$\bar{\sigma} = z_2 + \alpha z_1^{2/3} \text{sign}(z_1). \tag{8.6}$$

- **Layer $\mathcal{L}_2$.** The objective of the control law in $\mathcal{L}_2$ is now to vanish z_2 and z_3. Then, by defining the internal sliding variable as

$$\bar{\sigma} = z_2, \tag{8.7}$$

the establishment of a real 2SM with respect to $\bar{\sigma}$ leads to the convergence of $z_2 = \sigma$ and $z_3 = \dot{\sigma}$ to a vicinity of zero.

Note that $\bar{\sigma}$ depends on z_1 and z_2, but not on z_3. Given that $\mathcal{L}_1$ and $\mathcal{L}_2$ are also defined only by z_1, the control law proposed here is independent on $\ddot{\sigma}$.

8.2.3 Control design

Once the internal sliding variable $\bar{\sigma}$ defined, the 2SMOFC (see Section 3.4) is used to ensure the convergence of $\bar{\sigma}$. Recalling that the 2SMOFC requires only the knowledge of $\bar{\sigma}$, it means that only σ and $\dot{\sigma}$ are required. The scheme of the 3SMC can be presented by Figure 8.2. The 3SMC is basically composed by

1. the layer detection (8.5);
2. the construction of internal sliding variable $\bar{\sigma}$;
3. the 2SMOFC (presented in Theorem 3.4).

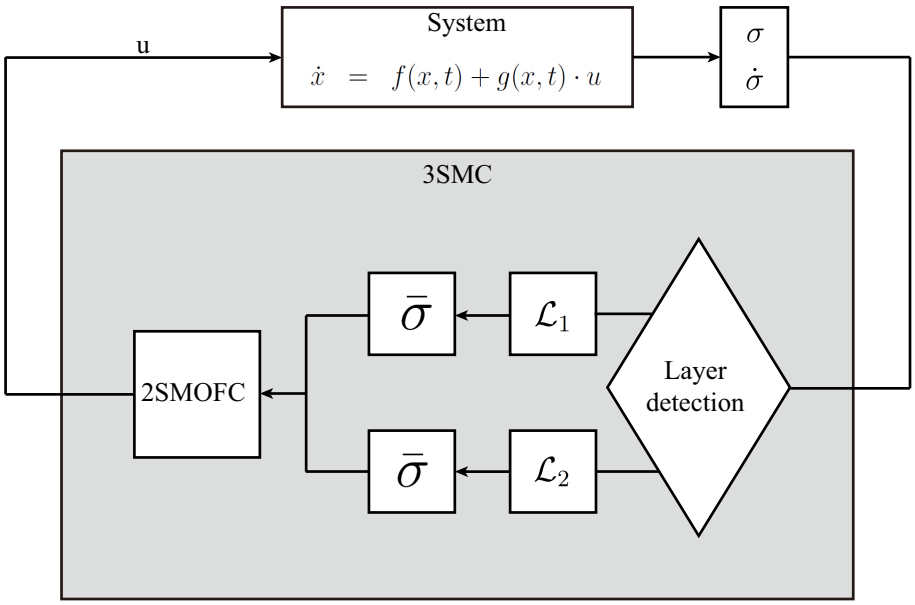

Figure 8.2 – 3SMC scheme.

Theorem 8.1 (Yan et al. [2016c]). *Consider system (8.2) under Assumption 8.1.1-8.1.4, and the internal sliding mode variable defined as*

$$\bar{\sigma} = z_2 + \alpha z_1^{2/3} \Gamma(z_1) \tag{8.8}$$

with $\alpha > 0$ and the function $\Gamma(z_1)$ defined as

$$\Gamma(z_1) = \begin{cases} \text{sign}(z_1) & \text{if} \quad z \in \mathcal{L}_1 \\ 0 & \text{if} \quad z \in \mathcal{L}_2 \end{cases} \tag{8.9}$$

with $\mathcal{L}_1$ and $\mathcal{L}_2$ defined by (8.5). Consider the control input defined as

$$u(kT_e) = -K(kT_e)\text{sign}(\bar{\sigma}(kT_e)) \tag{8.10}$$

with $K(t)$ defined as

$$K(kT_e) = \begin{cases} K_m & \text{if } kT_e \notin \mathcal{T}_{\mathcal{H}} \\ \gamma K_m & \text{if } kT_e \in \mathcal{T}_{\mathcal{H}} \end{cases} \tag{8.11}$$

and

$$\mathcal{T}_{\mathcal{H}} = \{kT_e \,|\text{sign}(\bar{\sigma}((k-1)T_e)) \neq \text{sign}(\bar{\sigma}(kT_e))\} \tag{8.12}$$

Then, there exist a sufficiently large but finite gain K_m, a sufficiently large $\gamma > 3$, a positive parameter α and a large enough parameter μ such that, under the control law (8.8)-(8.12), a real third order sliding mode with respect to z_1 is established in a finite time.

8.3 Convergence analysis

The convergence analysis for the 3SMC proposed in Theorem 8.1. is based on four Lemmas.

- Lemma 8.3.1 shows that the control law (8.8)-(8.12) ensures the establishment of a real second order sliding mode (2SM) with respect to the internal sliding variable $\bar{\sigma}$ in a finite time.
- Lemma 8.3.2 ensures that, if $z \in \mathcal{L}_1$, then one gets $z \in \mathcal{L}_2$ in a finite time.
- Lemma 8.3.3 and 8.3.4 claim that, once the system trajectories are evolving in $\mathcal{L}_2$ and once a real 2SM with respect to $\bar{\sigma}$ has been established, then z_2 and z_3 converge to a vicinity of zero in a finite time. A 3SM with respect to z_1 is then established.

Lemma 8.3.1 (Yan et al. [2016c]). *Consider system (8.2) under Assumption 8.1.1-8.1.4. There always exist sufficiently large but finite gain K_m and a sufficiently large parameter γ such that, under the control law (8.8)-(8.12), a real 2SM with respect to $\bar{\sigma}$ is established in a finite time.*

Proof. Consider the internal sliding variable $\bar{\sigma}$ defined by (8.8); one has, if $z \in \mathcal{L}_1$

$$\ddot{\bar{\sigma}} = a(x,t) + b(x,t)u + \alpha[-\tfrac{2}{9}z_1^{-4/3}z_2^2 + \tfrac{2}{3}z_1^{-1/3}z_3]\text{sign}(z_1)\ , \tag{8.13}$$

and, if $z \in \mathcal{L}_2$, $\ddot{\bar{\sigma}} = a(x,t) + b(x,t)u$. Then, by defining a^* as

$$a^* = \begin{cases} \alpha[-\frac{2}{9}z_1^{-4/3}z_2^2 + \frac{2}{3}z_1^{-1/3}z_3]\text{sign}(z_1) & \text{if } z \in \mathcal{L}_1 \\ 0 & \text{if } z \in \mathcal{L}_2 \end{cases} \tag{8.14}$$

one has

$$\ddot{\bar{\sigma}} = a(\cdot) + a^*(\cdot) + b(\cdot)u \tag{8.15}$$

Remarking that $\mathcal{Z}$ is a bounded open subset of $\mathbb{R}^3$, for $z \in \mathcal{Z}$ and $x \in \mathcal{X}$, there exists a positive a_M^* such that $|a^*(\cdot)| < a_M^*$. It yields that $|a + a^*| < a_M + a_M^*$. By tuning the gain K_m as $K_m > (a_M + a_M^*)/b_m$ and according to Theorem 3.4, a real 2SM with respect to $\bar{\sigma}$ is established in a finite time. ■

Remark 8.3.1. *The function a^* is bounded, but its bound a_M^* depends on the bound of z_3. In order to avoid the use of the information of z_3 in the gain tuning process, a gain adaptation law will be presented in the next section. It allows to adjust the gain to satisfy $K_m > (a_M + a_M^*)/b_m$ without any information on z_3.*

Lemma 8.3.2 (Yan et al. [2016c]). *Suppose that the trajectories of system (8.2) are evolving in $\mathcal{L}_1$. Then, under the control law (8.8)-(8.12) with K_m, γ and μ sufficiently large, once the real 2SM with respect to $\bar{\sigma}$ is established, the system trajectories will pass from $\mathcal{L}_1$ to $\mathcal{L}_2$ in a finite time.*

Lemma 8.3.2 does not claim that, once they reach $\mathcal{L}_2$, the system trajectories are maintained inside it and never escape out. Due to perturbations, uncertainties and intrinsic features of the controller, the trajectories may leave $\mathcal{L}_2$. But, thanks to the control law, they will be force to reach back $\mathcal{L}_2$ in a finite time. It means that the convergence domain may be slightly wider than $\mathcal{L}_2$, this domain being given by Lemma 8.3.4.

Proof. From Lemma 8.3.1, suppose that a real 2SM with respect to $\bar{\sigma}$ is established, then, there exists a constant $k_0 > 0$ such that

$$|\bar{\sigma}| < k_0 T_e^2. \tag{8.16}$$

If the trajectories of system (8.2) are evolving in $\mathcal{L}_1$, from (8.8), and given that $\dot{z}_1 = z_2$, one has

$$\dot{z}_1 \;=\; -\alpha z_1^{2/3}\text{sign}(z_1) + \bar{\sigma}. \tag{8.17}$$

Then, consider the following candidate Lyapunov function $V = \frac{1}{2}z_1^2$. Differentiating V with respect to time, one gets

$$\dot{V} = z_1\dot{z}_1 = |z_1|(-\alpha z_1^{2/3} + \bar{\sigma}\cdot\text{sign}(z_1)). \tag{8.18}$$

Define $\delta(z_1, t) = \alpha z_1^{2/3} - \bar{\sigma}\cdot\text{sign}(z_1)$. If $z \in \mathcal{L}_1$, then, from (8.5)-(8.16), there always exists a sufficient large μ such that $\delta(z_1, t) > \delta^* > 0$, with δ^* a positive number defined by $\delta^* = \alpha\mu^{2/3}K_m^{2/3}T_e^2 - k_0T_e^2$. Finally, one gets $\dot{V} = z_1\dot{z}_1 < -\delta^*|z_1| < 0$ which yields that z_1 will converge to a vicinity of zero in a finite time. In other words, z will reach $\mathcal{L}_2$ in a finite time. ■

Lemma 8.3.3 (Yan et al. [2016c]). *Denote t_i^* ($i = 1, 2, \ldots$) the instants for which $z_2(t_i^*) = 0$ (see Figure 8.3). Suppose that at instant $t = t_i^*$, the system trajectories are evolving in $\mathcal{L}_2$ and a real second order sliding mode with respect to $\bar{\sigma}$ has been established. Then, there always exists a $L > 0$ independent from T_e, such that*

$$|z_1(t_i^*) - z_1(t_{i+1}^*)| \leq LK_mT_e^3 \tag{8.19}$$

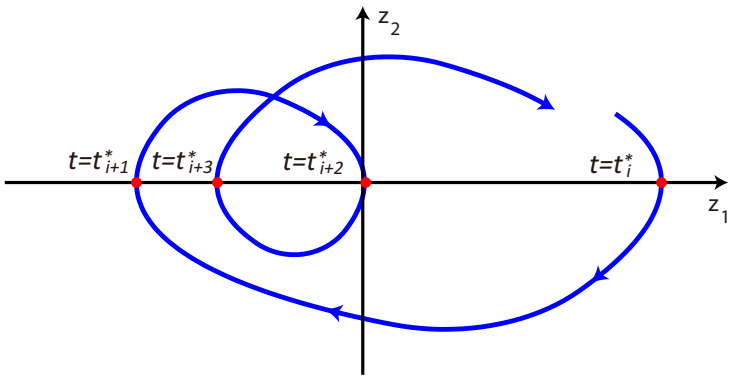

Figure 8.3 – Definition of t_i^* in the phase plane (z_1, z_2).

Proof. From Lemmas 8.3.1 and 8.3.2, suppose that under the control law (8.8)-(8.12), a real second order sliding mode with respect to $\bar{\sigma}$ is established and the system trajectories are evolving in $\mathcal{L}_2$. The system performs a series of "spiral lines" in the phase plane (z_1, z_2) and a series of "quadrangle" lines in the phase plane (z_2, z_3) (see Figure 8.4). In order to describe the state

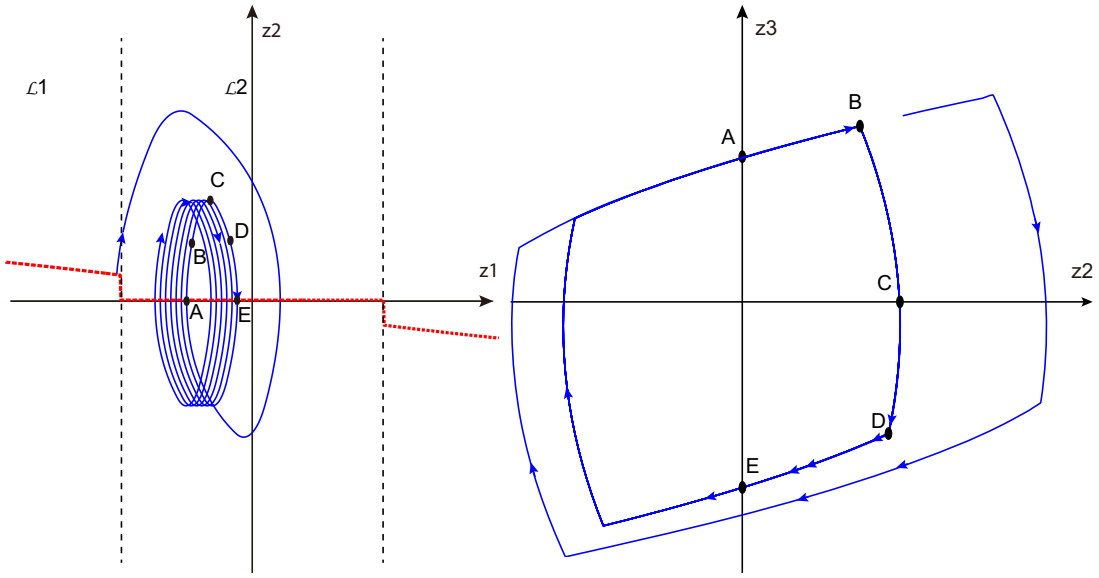

Figure 8.4 – **Left.** System trajectory in phase plane (z_1, z_2) (blue) and switching surface $S = 0$ (red dotted); **Right.** System trajectory in phase plane (z_2, z_3).

Point	Instant	Control	Description
A	$t_A = t_i^*$	K_m	$z_2(t_A) = 0$ and $z_3(t_A) > 0$
B	t_B	$-\gamma K_m$	switch of the gain
C	t_C	$-\gamma K_m$	$z_3(t_C) = 0$
D	t_D	$-K_m$	switch of the gain
E	$t_E = t_{i+1}^*$	$-K_m$	$z_2(t_E) = 0$ and $z_3(t_E) < 0$

Table 8.1 – Points describing the state trajectory

trajectories, once the system has reached $\mathcal{L}_2$, a succession of points classified in chronological order are defined (see Table 8.1 and Figure 8.4). Without loss of generality, denote $t_i^* = t_A$ and $t_{i+1}^* = t_E$. Remark that

- $T_e \geq t_B - t_A \geq 0$: the delay to detect the sign switching of z_2 can not be longer than one sampling step;
- $t_D - t_B = T_e$: the duration of K_M application is only one sampling step.

Denote $\Sigma = |z_1(t_i^*) - z_1(t_{i+1}^*)|$ as the distance between points A and E in the phase plane (z_1, z_2). In the sequel, Σ is evaluated in two cases : ideal and perturbed system.

Ideal system. Assume that system (8.2) fulfills $a = 0$, $b = 1$. When the system trajectories are evolving in $\mathcal{L}_2$, only z_2 and z_3 are controlled : system (8.2) can then be reformulated as

$$\begin{array}{rcl} \dot{z}_2 & = & z_3 \\ \dot{z}_3 & = & u(z_2, t) \end{array} \tag{8.20}$$

Considering this reduced second order system, according to Lemma 3.4.1, after a finite time z_2 and z_3 satisfy

$$|z_2| < \tfrac{1}{2} K_m [\eta(\gamma) - 1]^2 T_e^2, \quad |z_3| < K_m \eta(\gamma) T_e, \tag{8.21}$$

with $\eta = \frac{\gamma^2-\gamma-2}{2(\gamma-3)}$. Then, the task is to estimate the maximum value of Σ. The worst case (*i.e.* the largest value for Σ) occurs when $z_3(t_B) = \eta K_m T_e$ and when $t_B - t_A$ tends to one sampling step. Then, in the sequel, one takes $t_B - t_A = T_e$. Given that between t_A and t_B, $\dot{z}_3 = K_m$, one gets

$$\begin{array}{rcl} z_3(t_A) & = & z_3(t_B) + K_m(-T_e) = (\eta - 1)K_m T_e \\ z_2(t_B) & = & T_e(z_3(t_B) + z_3(t_A))/2 \\ & = & (\eta - 0.5)K_m T_e^2 \\ z_1(t_B) & = & z_1(t_A) + 1/2 z_3(t_A) T_e^2 + 1/6 K_m T_e^3 \\ & = & z_1(t_A) + (0.5\eta - 1/3)K_m T_e^3 \end{array} \tag{8.22}$$

By a similar way, since between t_B and t_D, $\dot{z}_3 = -\gamma K_m$, it comes

$$\begin{array}{rcl} z_3(t_D) & = & z_3(t_B) - \gamma K_m T_e = (\eta - \gamma)K_m T_e \\ z_2(t_D) & = & z_2(t_B) + z_3(t_B)T_e - 1/2\gamma K_m T_e^2 \\ & = & (2\eta - 0.5\gamma - 0.5)K_m T_e^2 \\ z_1(t_D) & = & z_1(t_B) + z_2(t_B)T_e + 1/2 z_3(t_B) T_e^2 \\ & - & 1/6\gamma K_m T_e^3 \\ & = & z_1(t_A) + (2\eta - 1/6\gamma - 5/6)K_m T_e^3 \ . \end{array} \tag{8.23}$$

Between D and E, the control input equals to $-K_m$, which gives

$$t_E - t_D \ = \ \frac{z_3(t_E) - z_3(t_D)}{-K_m} \ . \tag{8.24}$$

Then, one has

$$z_2(t_E) - z_2(t_D) = z_3(t_D)(t_E - t_D) - \frac{K_m}{2}(t_E - t_D)^2 \tag{8.25}$$

Replacing (8.23) and (8.24) in (8.25), one gets

$$z_3^2(t_E) = (\eta^2 + 4\eta - 2\gamma\eta + \gamma^2 - \gamma - 1)K_m^2 T_e^2 \ . \tag{8.26}$$

After reductions and remarking that $z_3(t_E) < 0$, one gets

$$z_3(t_E) = -(\eta - 1)K_m T_e = -z_3(t_A) \tag{8.27}$$

and

$$t_E - t_D \ = \ (2\eta - \gamma - 1)T_e \ . \tag{8.28}$$

Given that, in the case $\gamma > 3$,

$$2\eta - \gamma - 1 = \frac{\gamma + 1}{\gamma - 3} \ ,$$

one has $t_E - t_D > 0$, which enables to write :

$$\begin{array}{rcl} z_1(t_E) & = & z_1(t_D) + z_2(t_D)(t_E - t_D) \\ & + & 1/2 z_3(t_D)(t_E - t_D)^2 - 1/6 K_m (t_E - t_D)^3 \ . \end{array} \tag{8.29}$$

It implies $\Sigma = |z_1(t_i^*) - z_1(t_{i+1}^*)| \leq L K_m T_e^3$ with

$$\begin{array}{rcl} L & = & 1/6(4\eta^3 - 12\eta^2\gamma + 24\eta^2 + 9\eta\gamma^2 \\ & - & 12\eta\gamma - 9\eta - 2\gamma^3 + 5\gamma - 1) \ . \end{array} \tag{8.30}$$

Lemma 8.3.3 is proved for non perturbed case.

Perturbed system. Consider now the system (8.2) under Assumptions 8.1.1-8.1.4 and define $u^* = a(\cdot) - b(\cdot)u$. Then, when the system trajectories are evolving in $\mathcal{L}_2$, the control of system (8.2) can be reduced as

$$\dot{z}_2 = z_3, \quad \dot{z}_3 = u^*. \tag{8.31}$$

System (8.31) has a similar form to (8.20). Define the small and large gains for the input u^* as

$$\begin{array}{rcl} K_m^* & = & bK_m - a \cdot sign(z_2) \\ K_M^* & = & \gamma bK_m - a \cdot sign(z_2). \end{array} \tag{8.32}$$

One has

$$\begin{array}{rcl} K_m^* & \in & [b_m \cdot K_m - a_M, b_M \cdot K_m + a_M] \\ K_M^* & \in & [\gamma b_m \cdot K_m - a_M, \gamma b_M \cdot K_m + a_M] \end{array} \tag{8.33}$$

Define γ^* as

$$\gamma^* = \frac{K_M^*}{K_m^*} \in [\gamma_{min}, \gamma_{max}] \tag{8.34}$$

with γ_{min} and γ_{max} deduced from (8.33)-(8.34). Define also

$$\eta^* = \frac{\gamma^{*2} - \gamma^* - 2}{2(\gamma^* - 3)} . \tag{8.35}$$

Replace γ and η respectively by γ^* and η^* in (8.30) and introduce the following function

$$\begin{array}{l} \Sigma^*(\gamma^*) = 1/6(4\eta^{*3} - 12\eta^{*2}\gamma^* + 24\eta^{*2} + 9\eta^*\gamma^{*2} - 12\eta^*\gamma^* \\ -9\eta^* - 2\gamma^{*3} + 5\gamma^* - 1) . \end{array} \tag{8.36}$$

Then, $\Sigma^*(\gamma^*) \cdot K_m^* T_e^3$ can be viewed as the approximation of $|z_1(t_i^*) - z_1(t_{i+1}^*)|$ for the perturbed system, and one has

$$|z_1(t_i^*) - z_1(t_{i+1}^*)| < L^* K_m T_e^3 \tag{8.37}$$

with $L^* = (b_M + \frac{a_M}{K_m}) \cdot \sup_{\gamma^*} \Sigma^*$.

Lemma 8.3.3 is proved for perturbed system. ■

Lemma 8.3.4 (Yan et al. [2016c]). *Suppose that the trajectories of system (8.2) are evolving in $\mathcal{L}_2$, and a real 2SM with respect to $\bar{\sigma}$ has been established. Then, under the control law (8.8)-(8.12) with K_m, γ and μ sufficiently large, a 3SM with respect to z_1 is established in a finite time. Moreover, the accuracy of the states is given by*

$$|z_1| \leq \mu_0 K_m T_e^3, \quad |z_2| \leq 2\mu_0 K_m T_e^2, \quad |z_3| \leq 4\mu_0 K_m T_e$$

with $\mu_0 = \mu + L$.

Proof. From Lemma 8.3.1 and 8.3.2, one admits, that under the control law (8.8)-(8.12), a real 2SM with respect to $\bar{\sigma}$ is established and the system trajectories are evolving in $\mathcal{L}_2$. Then, two cases may happen:

Case 1 : The system trajectories are maintained in $\mathcal{L}_2$. In this case, given that $z \in \mathcal{L}_2$, which implies $|z_1| \leq \mu K_m T_e^3$, it is obvious that a real third order sliding mode with respect to z_1 is established, and the accuracy satisfies

$$|z_1| \leq \mu K_m T_e^3, \ |z_2| \leq 2\mu K_m T_e^2 \ |z_3| \leq 4\mu K_m T_e.$$

Case 2 : Due to perturbations and non-zero sampling time, the system trajectory may transiently pass to $\mathcal{L}_1$ and according to Lemma 8.3.2, the trajectory will go back to $\mathcal{L}_2$ in a finite time. Consider the worst case : the system trajectory reaches $\mathcal{L}_1$ at instant $t = t_i^*$ with $|z_1(t_i^*)| = \mu K_m T_e^3$ and $z_2(t_i^*) = 0$. After a "half circle", at instant $t = t_{i+1}^*$, z_1 reaches its maximum. From Lemma 8.3.3, there exists some positive L such that $|z_1(t_i^*) - z_1(t_{i+1}^*)| \leq L K_m T_e^3$; it gives $|z_1| \leq \mu_0 K_m T_e^3$ with $\mu_0 = \mu + L$. It implies that the accuracy of z_2 and z_3 satisfies at least $|z_2| \leq 2\mu_0 K_m T_e^2$ and $|z_3| \leq 4\mu_0 K_m T_e$. The real third order sliding mode with respect to z_1 is proved. ■

8.4 Gain adaptation law

In order to ensure the convergence, the gain has to be tuned large enough *w.r.t.* the perturbations. In practice, the bound of the perturbations is hard to determine. And as mentioned in Remark 8.3.1, the tuning condition for the gain depends on the bound of z_3. So, instead of a constant gain, a self tuning rule of K_m is proposed. This gain adaptation law helps to improve the performance of the controller and avoids using any information of z_3.

Proposition 8.4.1 (Yan et al. [2016c]). *Consider the system (8.2) with Assumptions 8.1.1-8.1.4 fulfilled, under the control law (8.8)-(8.12). Consider the adaptation law of K_m:*

- *if $K_m \leq K_{mm}$, $\dot{K}_m = K_{mm}$,*
- *if $K_m > K_{mm}$*

$$\dot{K}_m = \begin{cases} -\Lambda & \text{if} \quad z(t) \in \mathcal{L}_2 \\ \Lambda & \text{if} \quad z(t) \in \mathcal{L}_1 \end{cases} \tag{8.38}$$

with $K_{mm} > 0$ and $\Lambda > 0$.

The concept can be described as follows:

- if $z \in \mathcal{L}_1$, it means that there is no 3SM, which could be due to a too low gain. Then, the gain is forced to increase;
- given that perturbation is bounded, and the system state z is evolving in a bounded subset, the gain will become large enough in a finite time. Then the condition $K_m > (a_M + a_M^*)/b_m$ holds, the convergence is ensured. Then, thanks to (8.8)-(8.12), $z \in \mathcal{L}_2$ in a finite time;
- if $z \in \mathcal{L}_2$, 3SM is established: the gain is decreasing in order to avoid the escaping from $\mathcal{L}_2$ due to an oversized gain.

8.5 Parameter tuning rules

8.5.1 Tuning of γ

Consider system (8.2) under Assumptions 8.1.1-8.1.4; in order to establish a 2SM with respect to $\bar{\sigma}$, from Theorem 3.4, the parameter γ has to be also tuned large enough. Define u^* as

$$u^* = a(x,t) + a^*(z) + b(x,t)u \ . \tag{8.39}$$

where the function a^* is defined by (8.14). Then, dynamics of $\bar{\sigma}$ reads as

$$\ddot{\bar{\sigma}} \ = \ u^* \tag{8.40}$$

Firstly, consider $kT_e \notin \mathcal{T}_{\mathcal{H}}$. One has

$$u^* = -K_m \cdot \text{sign}(\bar{\sigma}(kT_e)) \cdot b(x,t) + a(x,t) + a^*(z) \tag{8.41}$$

Now, introduce K_m^* defined by

$$K_m^* = K_m \cdot b(x,t) - (a(x,t) + a^*(z)) \cdot \text{sign}(\bar{\sigma}(kT_e)) \ . \tag{8.42}$$

Then, the control input u^* takes the following form

$$u^* = -K_m^* \cdot \text{sign}(\bar{\sigma}(kT_e)) \quad \text{if} \quad kT_e \notin \mathcal{T}_H \tag{8.43}$$

and

$$\theta = \frac{a_M + a_M^*}{K_m} . \tag{8.44}$$

with $K_m^* \in [(b_m - \theta)K_m, (b_M + \theta)K_m]$. One supposes that under the adaptation law (8.38) the gain K_m is large enough such that $\theta < b_m$, which yields $K_m^* > 0$. Consider now $kT_e \in \mathcal{T}_H$, which gives

$$u^* = -\gamma K_m \cdot \text{sign}(\bar{\sigma}(kT_e)) \cdot b(x,t) + a(x,t) + a^*(z). \tag{8.45}$$

As previously, one gets

$$u^* = -K_M^* \cdot \text{sign}(\bar{\sigma}(kT_e)) \quad \text{if} \quad kT_e \in \mathcal{T}_H \tag{8.46}$$

with

$$K_M^* = \gamma K_m \cdot b(x,t) - (a(x,t) + a^*(z)) \cdot \text{sign}(\bar{\sigma}(kT_e)) . \tag{8.47}$$

In this case, one has

$$K_M^* \in [(\gamma b_m - \theta)K_m, (\gamma b_M + \theta)K_m] . \tag{8.48}$$

Defining γ^* as

$$\gamma^* = \frac{K_M^*}{K_m^*}, \tag{8.49}$$

one gets

$$\gamma^* \in \left[\frac{\gamma b_m - \theta}{b_M + \theta}, \frac{\gamma b_M + \theta}{b_m - \theta}\right] . \tag{8.50}$$

According to Estrada and Plestan [2012], the establishment of a real 2SM is ensured by setting $\gamma^* > 3$. Then, the tuning rule of γ is given by

$$\gamma > \frac{3b_M + 4\theta}{b_m} . \tag{8.51}$$

Moreover, under the gain adaptation law (8.38), if the system trajectories keep evolving in $\mathcal{L}_1$, in a finite time the gain will increase large enough such that $K_m > (a_M + a_M^*)/b_m$ holds. Then, one has $\theta/b_m < 1$ and tuning rule of γ can be given by the following proposition.

Proposition 8.5.1 (Yan et al. [2016c]). *Consider system (8.2) under Assumptions 8.1.1-8.1.4, and controlled by (8.8)-(8.12) with the gain adaptation law (8.38). Then, a sufficient condition on the parameter γ to ensure the establishment of a 3SM with respect to z_1 is*

$$\gamma > \frac{3b_M}{b_m} + 4 \tag{8.52}$$

8.5.2 Tuning of μ

The role of μ is to define $\mathcal{L}_1$ and $\mathcal{L}_2$. Theoretically, with a smaller μ, one could get better accuracy with respect to z_1. However, in practice, the output is usually measured with noise, and it is obvious that the width of $\mathcal{L}_2$ should be at least larger than the noise amplitude. The following proposition gives a necessary condition for this parameter.

Proposition 8.5.2 (Yan et al. [2016c]). *Consider system (8.2) under Assumptions 8.1.1-8.1.4, controlled by (8.8)-(8.12), and suppose that the state is measured with noise, $\bar{z}_1 = z_1 + \varepsilon$, where ε is a bounded white noise. Then, the width of $\mathcal{L}_2$ should be tuned large enough thanks to μ such that*

$$\mu K_{mm} T_e^3 > |\varepsilon| .$$

8.6 Simulations

Consider the system

$$\begin{array}{rcl} \dot{z}_1 & = & z_2 \\ \dot{z}_2 & = & z_3 \\ \dot{z}_3 & = & (\sin(z_1)+2)\,u + 20\sin(t) \end{array} \tag{8.53}$$

One has $b_m = 1$, $b_M = 3$, $a_M = 20$. The objective is to stabilize $z = [z_1\ z_2\ z_3]^T$ in a vicinity of the origin. The simulation is made with sampling period $T_e = 0.01s$, and the initial condition is stated as $z(0) = [5\ 0\ -10]^T$. The 3SMC (8.8)-(8.12) with gain adaptation law (8.38), is applied with the parameters tuned as follows

$$\begin{array}{ll} \alpha = 2 & \mu = 55 \\ \gamma = 10 & K_m(0) = 100 \\ K_{mm} = 20 & \Lambda = 500 \end{array} \tag{8.54}$$

The gain $K_m(t)$ is such that, after a finite time, the gain will increase large enough such that $K_m > (a_M + a_M^*)/b_m$ holds. Then, the parameter $\gamma = 10$ is tuned according to Proposition 8.5.1. The parameters α and μ are tuned to get the best performance.
The performance of the 3SMC is presented through Figure 8.5-8.6. Figure 8.5 displays the system state variables, which show that z_1 firstly converges towards zero, then z_2 and z_3 reach a vicinity of zero after a finite time as well. In Figure 8.6(a), it is shown that the system trajectories initially take place in layer $\mathcal{L}_1$, and during two seconds, the controller forces the trajectories to get into layer $\mathcal{L}_2$. Then, a high frequency switching between the two layers appears, which means that the system trajectories are maintained around the boundary of $\mathcal{L}_2$. Moreover, once the system trajectories reach layer $\mathcal{L}_2$ (see Figure 8.6(b)), the gain K_m is reduced, that allows to relax the control input and to reduce the chattering.
This simulation test is repeated under different sampling periods. The ratio between the mean tracking error $mean(|z|)$ and the mean value of the control gain $mean(K_m)$ are calculated once the steady state is established ($t \in [15, 20]$s). From the results in Table 8.2, one can notice that, when the sampling period is multiplied by two, $mean(|z_1|)/mean(K_m)$ is multiplied by eight, $mean(|z_2|)/mean(K_m)$ by four and $mean(|z_3|)/mean(K_m)$ by two. According to Definition 8.1.1, it shows that a real third order sliding mode with respect to z_1 is established, with μ_0, μ_1, μ_2 depending on the control gain K_m.

	$T_e = 0.01$s	$T_e = 0.02$s	$T_e = 0.04$s
$mean(\|z_1\|)/mean(K_m)$	6.34×10^{-5}	4.94×10^{-4}	0.0041
$mean(\|z_2\|)/mean(K_m)$	0.0022	0.0084	0.032
$mean(\|z_3\|)/mean(K_m)$	0.12	0.24	0.46

Table 8.2 – Tracking accuracy under different sampling periods

8.7 Summary

The main contributions of this chapter are summarized as follows :

- A third order sliding mode control law (3SMC) is proposed.
- The main feature of this new control law is that only the information of the sliding variable and its first order time derivative are required, which allows to reduce the use of time derivatives with respect to standard 3SMC.

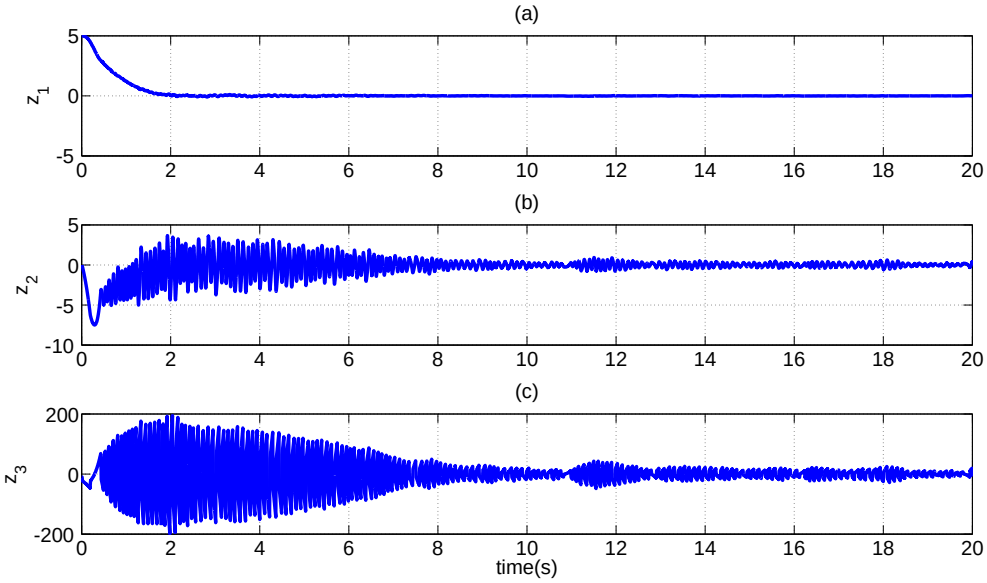

Figure 8.5 – **Adaptive 3SMC: (a).** z_1 versus time (sec); **(b).** z_2 versus time (sec); **(c).** z_3 versus time (sec).

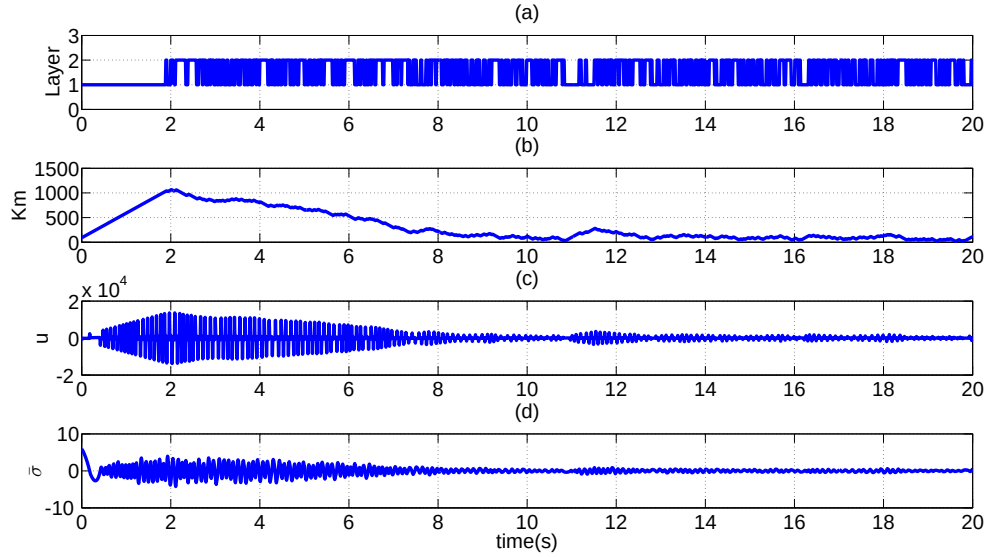

Figure 8.6 – **Adaptive 3SMC: (a).** Layer detection versus time (sec); **(b).** K_m versus time (sec); **(c).** Control input u versus time (sec); **(d).** Internal sliding variable $\bar{\sigma}$ versus time (sec).

- It has been proved that, this 3SMC ensures the establishment of a real third order sliding mode after a finite time.
- In order to simplify the tuning and improve the performance, a gain adaptation law has been proposed for this control law. It allows to relax the control gain when the system trajectories reach a vicinity of the origin, and to increase the gain when the system trajectories are far from the origin.
- Some tuning rules are given for two parameters of the new controller.

Conclusion

The main contributions of this part are summarized as following:

- Adaptive version of second order sliding mode output feedback control (2SMOFC) and Twisting-like control (TWLC) have been presented.
- Compared to their standard versions of 2SMOFC and TWLC presented in Part I, the adaptive versions allow to reduce the convergence time, to improve the accuracy and to reduce the chattering.
- A new third order sliding mode control law (3SMC) is proposed. This new control law only requires the information of the sliding variable and its first order time derivative.
- This 3SMC ensures the establishment of a real third order sliding mode in a finite time.
- A gain adaptation law is designed for this proposed 3SMC, which helps to simplify the parameter tuning and to improve the accuracy as well.

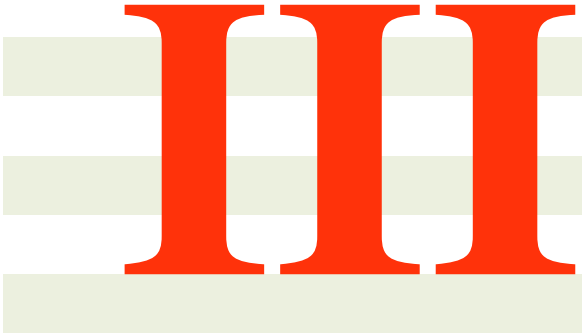

Experimental applications

9

Application to an electropneumatic system

Contents

9.1 Introduction

Pneumatic actuators are widely used in the field of industry, due to their advantages in high power-weight ratio and low cost. However, the pneumatic actuator is a system which is quite difficult to control in an accurate way. Its dynamics is usually described by a fourth order non-linear model Belgharbi et al. [1999] and with unavoidable uncertainties. These latter are caused by friction, (external) perturbations and parametric uncertainties (for example, the mass flow rate, which is a key-data to estimate the pressure in the actuator chamber, is very difficult to be estimated). This work is motivated by the control problem of a pneumatic actuator position. The control laws applied to pneumatic system must not only guarantee the high accuracy but have to ensure the robustness with respect to uncertainties and perturbations.
From the last century, many robust control laws have been proposed to deal with the pneumatic system control. In Brun et al. [1999], Morioka et al. [2000], Girin and Plestan [2009], experimental electropneumatic actuator systems have been designed, and state feedback control laws

have been developed from a nonlinear model of electropneumatic systems. Due to the presence of perturbation and uncertainties, robust control is required. In Smaoui et al. [2006], Smaoui et al. [2001], a nonlinear robust control strategy based on backstepping method is developed for the electropneumatic system. In Bouri and Thomasset [2001], Girin and Plestan [2009], Paul et al. [1994], sliding mode control laws have been applied to electropneumatic systems. In Chillari et al. [2001], experimental comparisons have been made between several control methods. The sliding mode control shows its advantages due to its robustness features and the guarantee of finite time convergence. The objective of this chapter is to address the control problem of pneumatic system using the new control strategies developed in this thesis.
Recall that, in Part I, different types of second order sliding mode control methods have been presented, including the second order sliding mode output feedback control (2SMOFC) and the twisting-like control (TWLC). In Chapter 8, a third order sliding mode controller (3SMC) has been introduced. Compared to the standard HOSM controller, the maximal differentiation order of the sliding variable used in the controller is reduced. For the electropneumatic system control, the position can be measured, but the velocity and acceleration (if necessary in the controllers) are usually deduced from the position by using numerical differentiators. Thanks to the reduced differentiation order, controllers developed in the sequel for the electropneumatic system could improve "standard" control approaches by reducing the introduction of noise in the controller. By this way, the twisting-like approach proposed in Chapter 4 is firstly adapted to be the basis of the control, but also to be qualified in order to estimate the velocity of the actuator. Moreover, the gain adaptation algorithms presented in Part II, can also be applied in order to improve the accuracy and simplify the tuning process.
All the experimental applications have been made on the electropneumatic system of *IRCCyN* lab (see Figure 9.1), Nantes, France, which is described in the sequel.

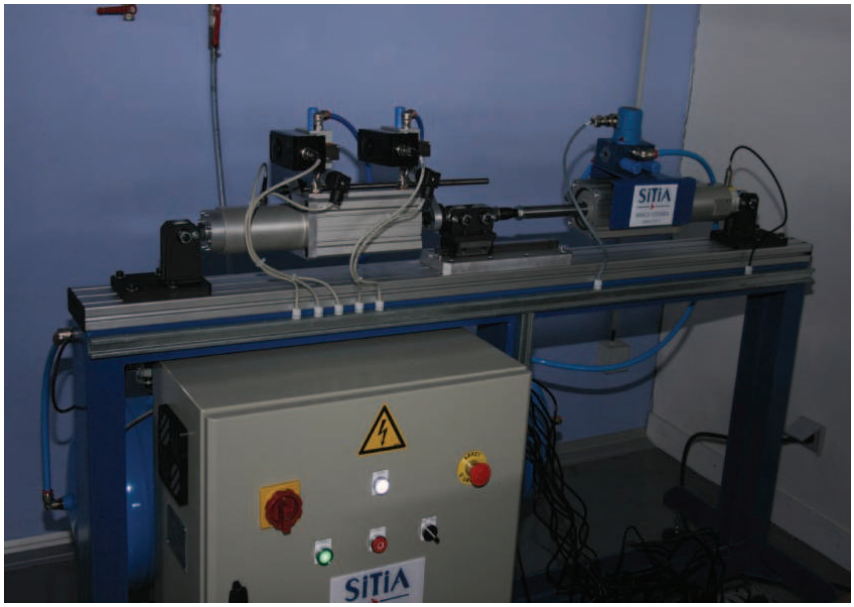

Figure 9.1 – Photo of electropneumatic system

9.2 Description of electropneumatic system

The pneumatic system (see Figure 9.2) is composed of two actuators. The first one, named the "main actuator", is a double acting pneumatic actuator and is composed of two chambers denoted P and N. The piston diameter is $80\ mm$ and the rod diameter is $25\ mm$. It is controlled

by two servodistributors, which can hold high frequency discontinuous inputs. The source pressure is 7 bar and the maximum force developed by the actuator is 2720 N. The air mass flow rates entering in the chambers are modulated by two three-way servodistributors. The pneumatic jack horizontally moves a load carriage of mass M. This carriage is coupled with the second pneumatic actuator, referred as the "perturbation actuator". This latter has the same mechanical characteristics as the main one, but the air mass flow rate is modulated by a single five-way servodistributor, and produces a dynamical load force on the main actuator. The pneumatic system has a software architecture based on a dSpace board. In the sequel, only the control of the main actuator position is considered. The "perturbation" one is controlled by a force PID controller provided by the experimental set-up constructor.

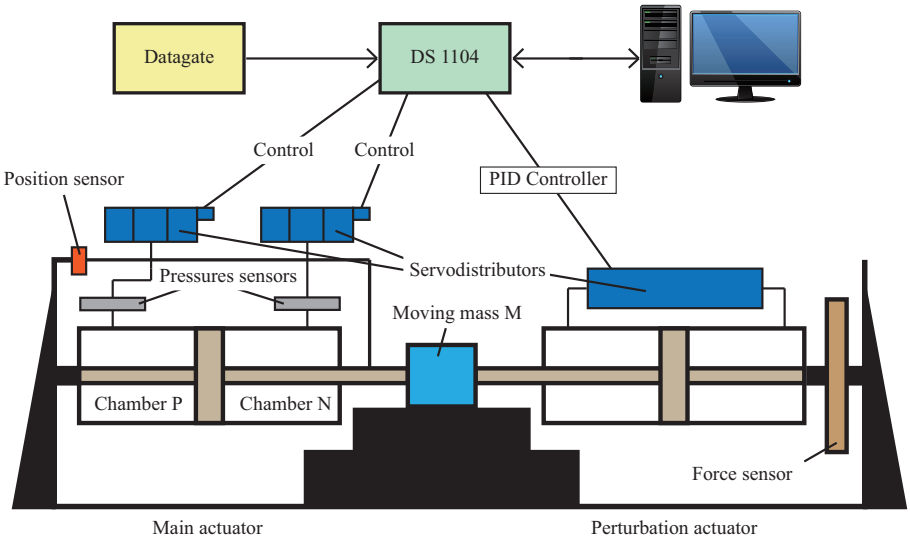

Figure 9.2 – Scheme of pneumatic system.

The model of the experimental set-up reads as Taleb et al. [2013]

$$\begin{aligned} \dot{p}_P &= \frac{krT}{V_P(y)}[\alpha_P + \beta_P \cdot w - \frac{S}{rT} p_P v] \\ \dot{p}_N &= \frac{krT}{V_N(y)}[\alpha_N - \beta_N \cdot w + \frac{S}{rT} p_N v] \\ \dot{v} &= \frac{1}{M}[S(p_P - p_N) - b_v v - F_{ext}(t)] \\ \dot{y} &= v \end{aligned} \tag{9.1}$$

with y the main actuator piston position, v its velocity, p_P and p_N the pressures in the both chambers (respectively P and N chambers). F_{ext} is the external force produced by the "perturbation" actuator. w is the control input of the system. The volume of each chamber is defined as

$$\begin{aligned} V_P(y) &= V_0 + S \cdot y \\ V_N(y) &= V_0 - S \cdot y \end{aligned} \tag{9.2}$$

Table 9.1 displays the values of the physical parameters of the experimental set-up.
The functions α_X and β_X ($X = \{P, N\}$) are defined as 5^{th}-order polynomials *w.r.t.* chamber pressure p_X Belgharbi et al. [1999] such that the functions q_{m_X}, defined by

$$\begin{aligned} q_{m_P} &= \alpha(p_P) + \beta(p_P, \text{sign}(w))\, w = \alpha_P + \beta_P \cdot w \\ q_{m_N} &= \alpha(p_N) - \beta(p_P, \text{sign}(w))\, w = \alpha_N - \beta_N \cdot w \end{aligned} \tag{9.3}$$

Parameters	Notation	Value
Mass	M	$3.4\ kg$
Piston surface	S	$0.0045\ m^2$
Half-cylinder volume	V_0	$3.40\ 10^{-4}\ m^3$
Perfect gas constant	r	$287\ J.kg^{-1}.K^{-1}$
Temperature	T	$293°K\ =\ 20°C$
Polytropic constant	k	1.2
Viscous friction coeff.	b_v	50

Table 9.1 – Physical parameters of the experimental set-up.

represent the mass flow rate in each chamber of the actuator. Define $\mathcal{X}$ as the physical domain

$$\begin{aligned}\mathcal{X} = \{x \,|&1 \text{ bar} \leq p_P \leq 7 \text{ bars}, 1 \text{ bar} \leq p_N \leq 7 \text{ bars},\\ &-72 \text{ mm} \leq y \leq 72 \text{ mm},\ |v| \leq 1 \text{ m/s}\}.\end{aligned}$$

with $x = [p_P\ p_N\ v\ y]^T$. According to previous works Taleb et al. [2013], one can admit the following assumptions

- the uncertainty terms are supposed to be bounded, sufficiently smooth, *small with respect to the nominal value* and *unknown*;
- F_{ext} and its time derivatives are supposed to be bounded;
- only y, p_P and p_N are measured by sensors.

9.3 Experimental tests environment

The experimental tests are made with a sampling period $T_e = 1\ ms$. The initial conditions of the electropneumatic system are

$$y(0) = 0.07\ m,\ \ v(0) = 0\ m \cdot s^{-1},\ \ p_P(0) = 1 \text{ bar},\ \ p_N(0) = 1 \text{ bar}. \tag{9.4}$$

As shown in Figure 9.3, the main actuator is forced by the control law to track a reference signal $y_{ref}(t)$ under the perturbation force $F_{ext}(t)$. The objective of the benchmark is to evaluate the performances of 2SMOFC, TWLC and 3SMC, in case of trajectory tracking and in presence of time varying perturbations. The position trajectory reference $y_{ref}(t)$ is composed by two sinusoidal signals with different frequencies and is formally defined as

$$\begin{array}{lll} y_{ref}(t) = 0.04\cos(0.2\pi t) & \text{for} & 0 \geq t \geq 20\ s \\ y_{ref}(t) = 0 & \text{for} & 20 < t < 30\ s \\ y_{ref}(t) = 0.04\cos(0.4\pi t) & \text{for} & 30 \geq t \geq 50\ s \end{array} \tag{9.5}$$

The objective consists in evaluating the performances of the control solution, in case of slow/fast dynamics with presence of perturbation. The perturbation force has a sinus form with frequency of 0.1 Hz and magnitude of 500 N.
In the experimental tests, the velocity v is estimated from the position, by the twisting-like differentiator (TWLD) presented in Section 4.3. The acceleration a required by the Twisting control (but not by the other controllers), is also estimated by a TWLD from the estimated velocity. The parameters of TWLD are tuned as

$$\begin{array}{ll} K_m = 0.5, & \gamma = 6 \\ b_m = b_M = 1, & a_M = 0.1 \end{array} \tag{9.6}$$

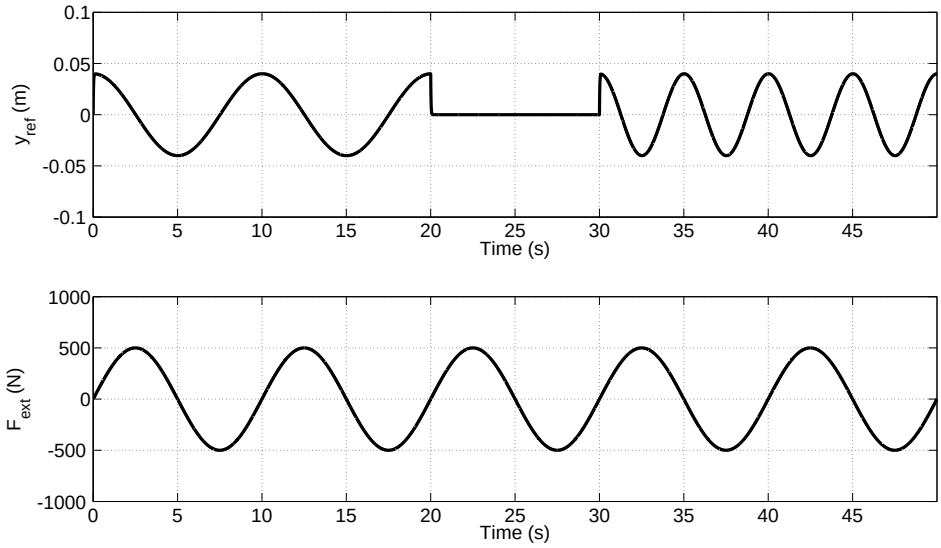

Figure 9.3 – **Top.** Position reference y_{ref} (m) versus time (sec); **Bottom.** Perturbation force F_{ext} (N) versus time (sec).

9.4 Second order sliding mode control

In Part I, two second order sliding mode control methods have been presented, the second order sliding mode output feedback control (2SMOFC) and the twisting-like control (TWLC). These methods can be applied to systems with relative degree equal to one or two. Their main feature is that only the sign of the sliding variable is required. Compared to the classic twisting control, the use of time derivative of the sliding variable is removed. In this section, the 2SMOFC and TWLC are applied to IRCCyN electropneumatic system and their performances are compared to the twisting control. Furthermore, the adaptive version of 2SMOFC and TWLC are also tested.

9.4.1 Control design

The problem is to design a control law w based on standard or adaptive 2SMOFC and TWLC that make the output (the position y) of the pneumatic actuator follow a prescribed profile $y_{ref}(t)$ in spite of the disturbance $F_{ext}(t)$ and uncertainties. The sliding variable $\sigma(x,t)$ is defined as

$$\sigma(x,t) \quad = \quad v - \dot{y}_{ref}(t) + \lambda\left(y - y_{ref}(t)\right) \tag{9.7}$$

with $\lambda > 0$. From (9.1)-(9.7), one gets

$$\ddot{\sigma} \quad = \Psi(t,x) + \Phi(x,t)w \tag{9.8}$$

with

$$\begin{aligned}
\Psi &= \frac{krTS}{M}\left(\frac{\alpha_P}{V_P}-\frac{\alpha_N}{V_N}\right)-\frac{kS^2}{M}\left(\frac{p_P}{V_P}+\frac{p_N}{V_N}\right)v+\frac{1}{M}\left(-b_v\dot{v}-\dot{F}_{ext}-M\cdot y_{ref}^{(3)}\right)\\
&\quad +\lambda\left(\dot{v}-\ddot{y}_{ref}\right)\\
&= \frac{krTS}{M}\left(\frac{\alpha_P}{V_P}-\frac{\alpha_N}{V_N}\right)-\frac{kS^2}{M}\left(\frac{p_P}{V_P}+\frac{p_N}{V_N}\right)v-\frac{1}{M}\left(\dot{F}_{ext}+M\cdot y_{ref}^{(3)}\right)\\
&\quad +\frac{M\lambda-b_v}{M^2}[S(p_P-p_N)-b_v v-F_{ext}]-\lambda\ddot{y}_{ref}\\
\Phi &= \frac{krTS}{M}\left(\frac{\beta_P}{V_P}+\frac{\beta_N}{V_N}\right).
\end{aligned} \tag{9.9}$$

Given that some parameters are uncertain (for example, additional mass ΔM can load the actuator whereas the control has been designed for a mass M) and given that there are external perturbations, one rewrite the functions Ψ and Φ as

$$\begin{aligned}
\Psi &= \Psi_{Nom}+\Delta\Psi,\\
\Phi &= \Phi_{Nom}+\Delta\Phi,
\end{aligned} \tag{9.10}$$

that is, there is a nominal term and an uncertain term. In Taleb et al. [2013], it has been numerically shown that, under current operating conditions, the bounded functions Ψ_{Nom} and Φ_{Nom} only depend on the measured or estimated variables, and $\Phi_{Nom}>0$. Then, consider the following control law

$$w = {\Phi_{Nom}}^{-1}\left(-\Psi_{Nom}+u\right) \tag{9.11}$$

with u being the "new" control input of σ-dynamics. Substituting (9.10) and (9.11) in (9.8), one gets

$$\ddot{\sigma} = \underbrace{\Delta\Psi-\Delta\Phi\Phi_{Nom}^{-1}\Psi_{Nom}}_{a}+\underbrace{\left(1+\Delta\Phi\Phi_{Nom}^{-1}\right)}_{b}\cdot u\ . \tag{9.12}$$

For the electropneumatic system (9.1),

- The system trajectories are supposed to be infinitely extendible in time for any bounded Lebesgue measurable input;
- the servodistributors are controlled by microprocessors, and the control input is updated in discrete-time with the sampling period T_e which is a strictly positive constant. The control input u is constant between two successive sampling steps *i.e*

$$\forall t\in[kT_e,\ (k+1)T_e[\ \ u(t) = u(kT_e)\,; \tag{9.13}$$

- under the operating conditions, the functions Ψ and Φ are bounded with $\Phi_{Nom}>0$, then, according to (9.12), there exist positive constants a_M, b_m, b_M such that

$$\begin{aligned}
&|a(x,t)|\le a_M\\
&0<b_m\le b(x,t)\le b_M
\end{aligned} \tag{9.14}$$

  for $x\in\mathcal{X}$ and $t>0$. In the experimental tests the estimated bounds are given as $a_M=500$, $b_m=0.99$, $b_M=1.01$.

Thus, consider equation (9.12) which can be easily rewritten in the form of system (2.3) with $z_1=\sigma$ and $z_2=\dot{\sigma}$. Assumptions 2.2.1-2.2.3 are satisfied. Then, the three types of second order sliding mode control methods presented in Chapter 3 and 4 (TWC, 2SMOFC and TWLC) can be applied.

Remark 9.4.1. *Remark that the three control methods (TWC, 2SMOFC and TWLC) do not have the same features. Therefore, the control scheme used for TWC (see Figure 9.4) needs two differentiators (TWL differentiator introduced in Section 4.3) while 2SMOFC and TWLC (Figure 9.5) require only a single differentiator. More precisely, one has*

- *if the control u appearing in (2.3) is TWC, then $z_1 = \sigma$ and $z_2 = \dot{\sigma}$ are required; therefore it is necessary to use two first order differentiators, a first one to obtain an estimation of v (which appears in definition (9.7) of σ), and a second one for $\dot{v}$ (see Figure 9.4);*
- *in the case of 2SMOFC and TWLC, only $z_1 = \sigma$ is required; only one differentiator is used to compute v (see Figure 9.5).*

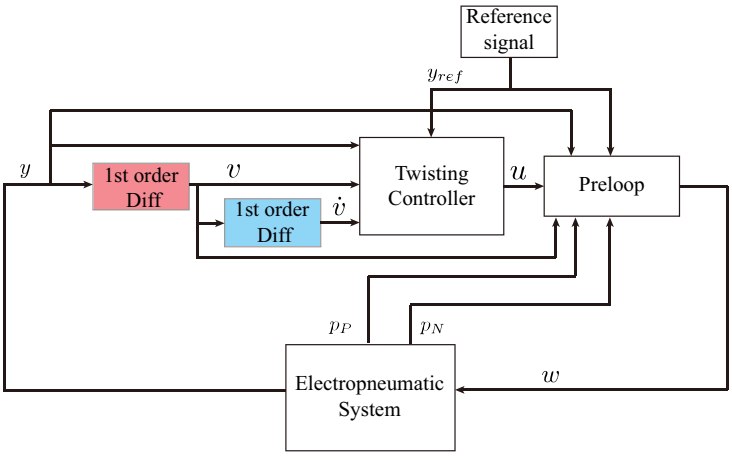

Figure 9.4 – Control scheme for TWC

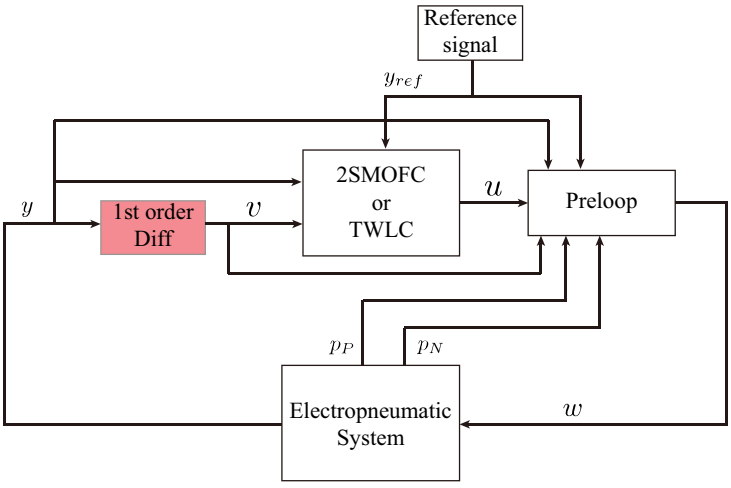

Figure 9.5 – Control scheme for 2SMOFC and TWLC

9.4.2 Experimental results

2SMC without adaptation

Firstly, the 2SMOFC and TWLC without gain adaptation are applied to the electropneumatic system. Furthermore a comparison with TWC is also made. In order to make a reasonable comparison, the same definition of the sliding variable is used for TWC, 2SMOFC and TWLC.

TWC	2SMOFC	TWLC
$K_1 = 7500, \quad K_2 = 5000$ $\lambda = 40$	$K_m = 2500 \quad \gamma = 5$ $\lambda = 40$	$K_m = 2500, \quad \gamma = 5$ $\lambda = 40,$

Table 9.2 – Parameters for the three 2SM controllers.

The parameters for these control laws are tuned such that their control gains have the same amplitude. The final configuration of the three control laws are detailed in Table 9.2.
Then, performances of these three control laws are shown by Figure 9.6-9.8. It shows that, under these three sliding mode control laws, the main actuator can track the reference signal with high accuracy after a finite convergence time. Figure 9.6 represents the performance of TWC. As mentioned previously, both the sliding variable and its first time derivative are required by TWC; so, an other TWLC differentiator is used to estimate the acceleration a from v. However, according to Yan et al. [2014b], for a noisy measured signal, the use of high order differentiator may introduce disturbance into the controller: from the detailed comparison in Table 9.3, the degradation of tracking accuracy for TWC is obvious. Compared to TWC, the 2SMOFC and TWLC require only the information of the sliding variable. Without using the second differentiator, one gets with these both latter controllers a better tracking accuracy. And comparing the average control magnitude $mean(|w|)$ and the pressure P_p, these two latter controllers cost less energy. However, for 2SMOFC, the large gain input is applied during only one sampling period, this feature inducing a relatively longer convergence time (see Figure 9.7). Assume that the convergence of the system trajectories is finished, when the tracking error is stable at an accuracy less than 5mm. Then, the response time can be calculated from sub-plots (b), when the reference changes its wave form. In Table 9.3, $\mathrm{mean(resptime)}$ represents the average response time, which is calculated right after each point of discontinuity (0 sec, 20 sec and 30 sec). Thanks to the online computed τ_i (see equations (4.5)-(4.8)), with TWLC, the duration of the large gain input could be more than one sampling period. From Figure 9.8,and the comparison in Table 9.3, one can see that TWLC inherits both the fast convergence time of TWC and the high tracking accuracy of 2SMOFC.

	TWC	2SMOFC	TWLC
$mean(\|y - y_{ref}\|)$	3.5×10^{-3}	2.8×10^{-3}	2.2×10^{-3}
$std(y - y_{ref})$	0.012	0.011	0.011
$mean(\|w\|)$	5.97	1.95	2.14
mean(resp time)	0.87	1.73	0.58

Table 9.3 – Experimental results for 2SMC without adaptation

Adaptive 2SMC

A key point of these experimental tests is that the reference signal is composed by signals with different frequency. In order to track the reference signal with higher frequency, a large gain is usually required, which is not the case when the frequency is lower. So, there is a real interest to use the gain adaptation laws. In the sequel, the adaptive versions of 2SMOFC and TWLC (see Section 7.2-7.3) are applied to system (9.12). Note that there exist other adaptive sliding mode control strategies which have been applied to the electropneumatic system, such as the adaptive twisting control Taleb et al. [2013] and the adaptive super-twisting control Taleb

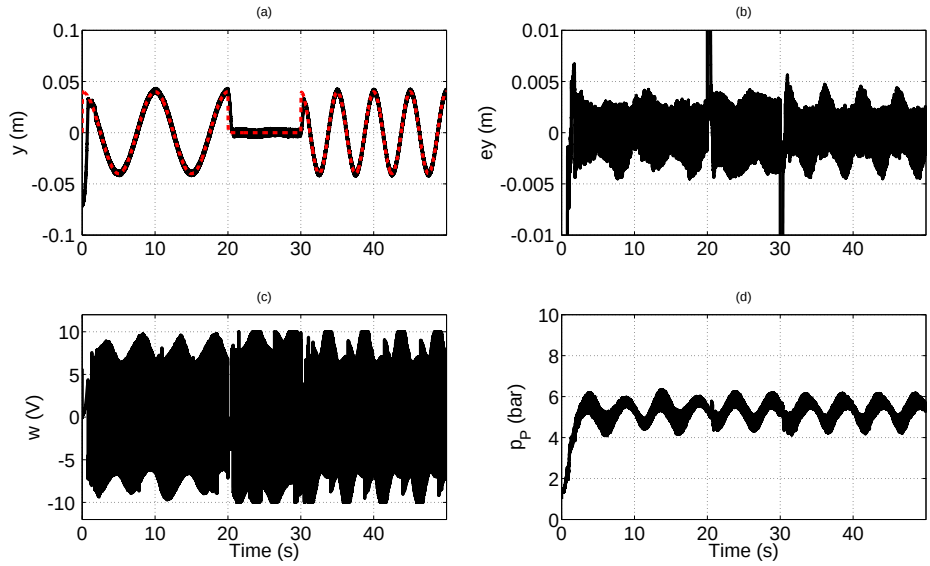

Figure 9.6 – **Experimental results of TWC. (a).** Reference position (red dotted) and measured position $y\ (m)$ (black solid) versus time (sec); **(b).** Position tracking error (m) versus time (sec); **(c).** Control input $w\ (V)$ versus time (sec); **(d).** Pressure in chamber P $p_P\ (bar)$ versus time (sec).

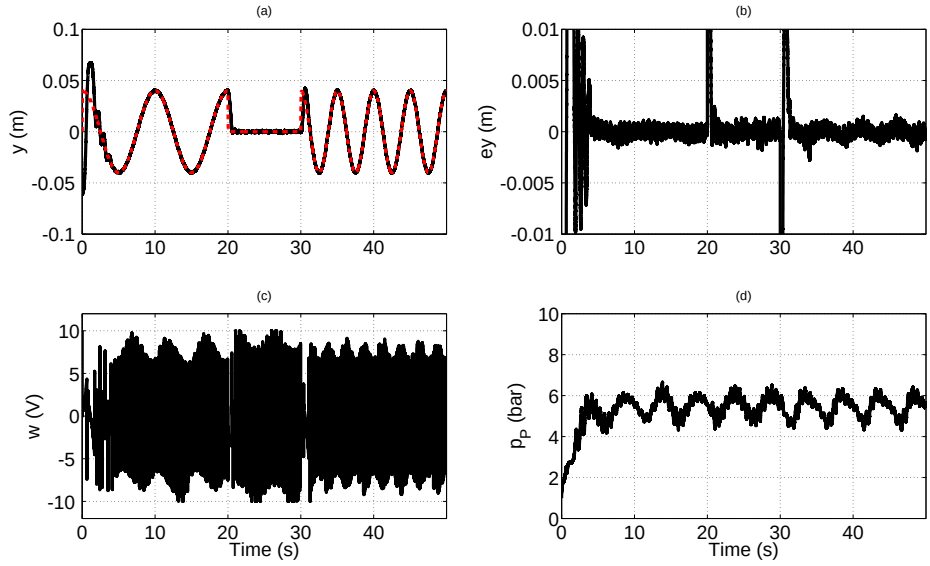

Figure 9.7 – **Experimental results of 2SMOFC.(a).** Reference position (red dotted) and measured position $y\ (m)$ (black solid) versus time (sec); **(b).** Position tracking error (m) versus time (sec); **(c).** Control input $w\ (V)$ versus time (sec); **(d).** Pressure in chamber P $p_P\ (bar)$ versus time (sec).

and Plestan [2012]. However, the super-twisting method is only applicable to the system with relative degree equal to one with respect to the sliding variable. For the twisting control, both the sliding variable and its time derivatives should be known, and the gain adaptation law is developed based on a different concept. So, for a sake of clarity, the comparison is made only between adaptive versions of 2SMOFC and TWLC. For these two methods, their initial gain has been fixed at $K_m(0) = 2000$. The parameters of 2SMOFC are tuned as Table 9.4, in order

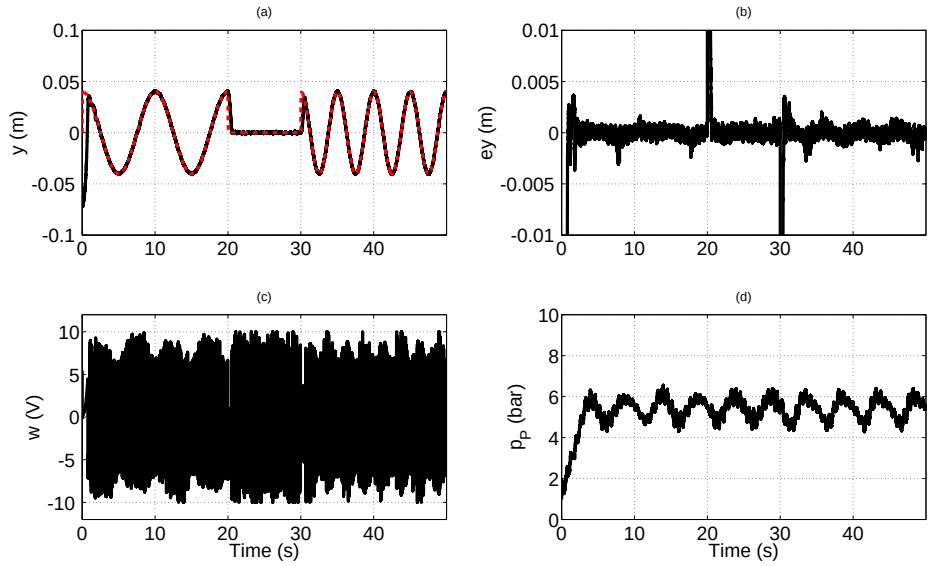

Figure 9.8 – **Experimental results of TWLC. (a).** Reference position (red dotted) and measured position $y\ (m)$ (black solid) versus time (sec); **(b).** Position tracking error (m) versus time (sec); **(c).** Control input $w\ (V)$ versus time (sec); **(d).** Pressure in chamber P $p_P\ (bar)$ versus time (sec).

to get its best performances (in the term of tracking accuracy and convergence time). Then, parameters for TWLC are tuned in order to get the similar dynamics for the gain adaptation as 2SMOFC.

Adaptive 2SMOFC	$\lambda = 40 \quad \gamma = 5$ $\Gamma = 800 \quad \beta = 4.1$ $K_m \in [0, \quad 3500]$
Adaptive TWLC	$\lambda = 40 \quad \gamma = 5$ $\Gamma = 800 \quad \beta = 8$ $\varepsilon = 100$ $K_m \in [0, \quad 3500]$

Table 9.4 – Parameters for adaptive 2SMOFC and TWLC.

Then, the performances of the closed-loop system under the adaptive 2SMOFC and TWLC are presented by Figure 9.9-9.10. It shows that, at the initial point, the position y is far from the target then, the control gain K_m is growing (for the adaptive TWLC, the gain $K_m(t)$ instantly reaches 3500 in $\varepsilon T_e = 0.1$ sec). Once the position reaches the reference signal and the real second order sliding mode is established, the gain starts to reduce in order to improve the tracking accuracy. If one compares the average gain firstly for $t \in [0,\ 20]$ and secondly for $t \in [30,\ 50]$, it shows that, with the increasing of the reference signal frequency, the gain K_m also increases by taking into account the higher frequency of the reference. As previously, assume that the convergence phase is finished when the tracking error is stable with an accuracy less than 5mm. Through the detailed comparison in Table 9.5, one can say that the adaptation gain law helps to improve the tracking accuracy and also the convergence time compared with Table 9.3. Moreover, the adaptive version of the TWLC keeps its advantages on the faster convergence time and better accuracy compared to the 2SMOFC.

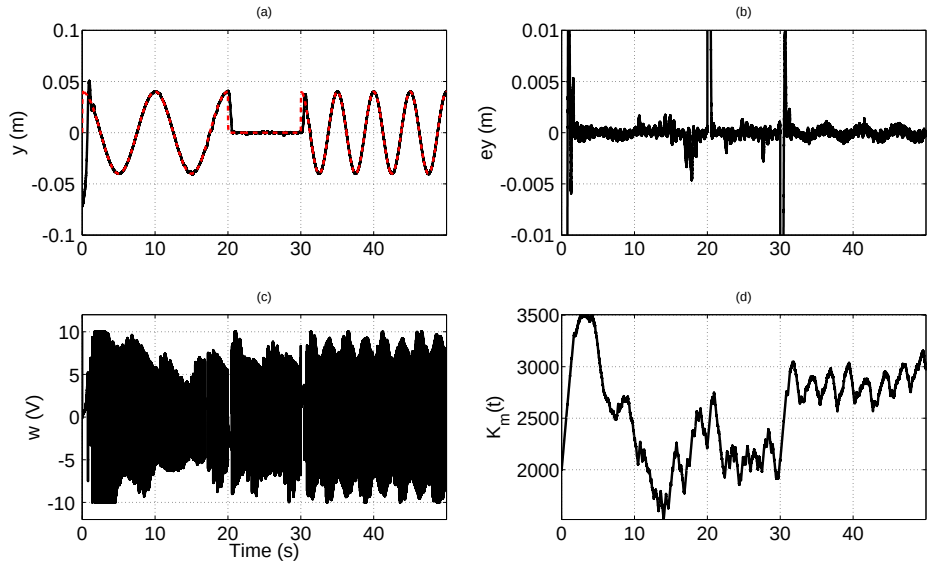

Figure 9.9 – **Experimental results of adaptive 2SMOFC.(a).** Reference position (red dotted) and measured position $y\ (m)$ (black solid) versus time (sec); **(b).** Position tracking error (m) versus time (sec); **(c).** Control input $w\ (V)$ versus time (sec); **(d).** Control gain K_m versus time (sec).

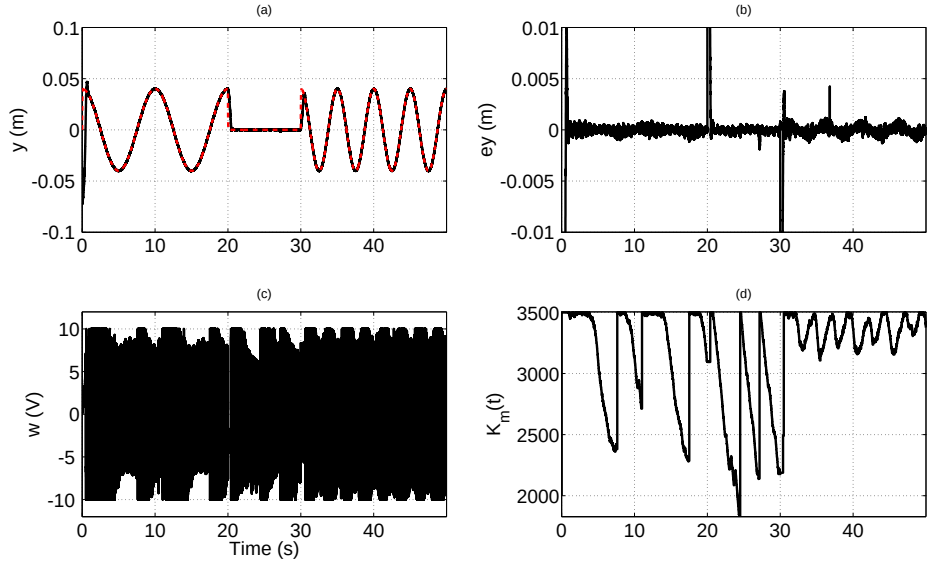

Figure 9.10 – **Experimental results of adaptive TWLC. (a).** Reference position (red dotted) and measured position $y\ (m)$ (black solid) versus time (sec); **(b).** Position tracking error (m) versus time (sec); **(c).** Control input $w\ (V)$ versus time (sec); **(d).** Control gain K_m versus time (sec).

9.5 Third order sliding mode control

In the context of electropneumatic system control, the objective is to force the position of the actuator to track a reference signal. According to (9.1), the position tracking error $e_y = y - y_{ref}$ has a relative degree equal to three. Then, in this section, the third order sliding mode control presented in Chapter 8 is applied to the electropneumatic system. A comparison is also made

	Adp 2SMOFC	Adp TWLC
$mean(\|y - y_{ref}\|)$	2.4×10^{-3}	1.5×10^{-3}
$std(y - y_{ref})$	0.011	0.009
$mean(K_m)$	2606	3137
mean(resp time)	0.97	0.49

Table 9.5 – Experimental results for adaptive 2SMOFC and TWLC

between this 3SMC and a higher order sliding mode controller (HOSMC) proposed in Levant [2005b].

9.5.1 Control design

Define the sliding variable from the control objective as

$$\sigma = y - y_{ref}(t). \tag{9.15}$$

The relative degree of system (9.1) with respect to σ (9.15) equals three and is constant. From (9.1) and (9.15), one gets

$$\sigma^{(3)} = \Psi'(x,t) + \Phi'(x,t) \cdot w \tag{9.16}$$

with

$$\begin{aligned} \Psi' &= \frac{krTS}{M}\left(\frac{\alpha_P}{V_P} - \frac{\alpha_N}{V_N}\right) - \frac{kS^2}{M}\left(\frac{p_P}{V_P} + \frac{p_N}{V_N}\right)v - \frac{1}{M}\left(\dot{F}_{ext} + M \cdot y_{ref}^{(3)}\right) \\ &\quad - \frac{b_v}{M^2}[S(p_P - p_N) - b_v v - F_{ext}] \\ \Phi' &= \frac{krTS}{M}\left(\frac{\beta_P}{V_P} + \frac{\beta_N}{V_N}\right). \end{aligned} \tag{9.17}$$

Furthermore, for $x \in \mathcal{X}$, Ψ' and Φ' have a nominal known part (named $\Psi'_N(x,t)$ and $\Phi'_N(x,t)$ respectively) and an unknown bounded uncertain part (named $\Delta\Psi'$ and $\Delta\Phi'$ respectively) such that

$$\Psi' = \Psi'_{Nom} + \Delta\Psi' \qquad \Phi' = \Phi'_{Nom} + \Delta\Phi' \ . \tag{9.18}$$

Note that the function Φ' fullfills $\Phi'_{Nom} > 0$ and $|\Delta\Phi'|/\Phi'_{Nom} < 1$. Define the control input (with u the "new" control input)

$$w = \frac{1}{\Phi'_{Nom}}\left(-\Psi'_{Nom} + u\right) \ . \tag{9.19}$$

Note that only measured or estimated states are used in (9.19). Then, applying w (9.19) to (9.16), one gets

$$\sigma^{(3)} = \underbrace{\Delta\Psi' - \Delta\Phi'{\Phi'_{Nom}}^{-1}\Psi'_{Nom}}_{a} + \underbrace{\left(1 + \Delta\Phi'{\Phi'_{Nom}}^{-1}\right)}_{b} u \ . \tag{9.20}$$

For the electropneumatic system (9.1),

- the system trajectories are supposed to be infinitely extendible in time for any bounded Lebesgue measurable input;

- for the current operating conditions, $x \in \mathcal{X}$ and $u \in I\!R$, the vector z is evolving in a bounded open subset of $I\!R^3$

$$z \in \mathcal{Z} \subset I\!R^3 \tag{9.21}$$

- the control input u is updated in discrete-time with the positive sampling period T_e. The control input u is constant between two successive sampling steps *i.e*

$$\forall t \in [kT_e,\ (k+1)T_e[,\ \ u(t) \ = \ u(kT_e)\,; \tag{9.22}$$

- according to (9.20), there exist positive constants $a_M > 0$, $b_m > 0$ and $b_M > 0$ such that

$$|a(x,t)| \leq a_M,\ \ 0 < b_m < b(x,t) < b_M \tag{9.23}$$

for $x \in \mathcal{X}$ and $t > 0$.

Then, a 3^{rd}-order sliding mode controller for system (9.1) with respect to sliding variable σ (9.15) is equivalent to the finite time stabilization of (8.2) with $z = [z_1\ z_2\ z_3]^T = [\sigma\ \dot{\sigma}\ \ddot{\sigma}]^T$ and Assumption 8.1.1-8.1.4 fulfils. The third order sliding mode control law (8.8)-(8.12) can be applied to the electropneumatic system.

9.5.2 Experimental results

The controller (8.8)-(8.12) and adaptation law (8.38) are tested on this set-up. The parameters are tuned as follows in order to get the best performance in term of tracking accuracy and convergence time

$$\begin{array}{lllllll} K_m(0) & = & 2000 & K_{mm} & = & 100 \\ \mu & = & 150 & \alpha & = & 2 \\ \gamma & = & 5 & \Lambda & = & 800\ . \end{array}$$

The performances of this adaptive 3SMC are presented by Figure 9.11. In a finite time, the position and velocity converge to the reference trajectory in spite of the perturbation force. The tracking error and the layer detection are presented in Figure 9.12. It shows that when the wave form of the reference trajectory changes, the system trajectories are transitorily evolving in $\mathcal{L}_1$ which makes the gain increase. After a finite time, the system trajectories reach again $\mathcal{L}_2$: then, the gain starts to decrease. Then, high frequency switching between the two layers appears and the real third order sliding mode is established with an accuracy slightly larger than the width of $\mathcal{L}_2$.
A comparison is made between the proposed controller and the Quasi-Continuous HOSM controller Levant [2005b]. The control gain α is tuned at the similar level as the average value of K_m for adaptive 3SM *i.e.* $\alpha = 3500$. Note that, for the HOSM controller, the acceleration must also be estimated by a differentiator (in this case, TWLD has been used). The performance of the HOSMC is presented by Figure 9.13. A detailed comparison between these two methods is given in Table 9.6. Thanks to the remove of second order derivative used in the control law, the 3SMC shows its advantages in the tracking accuracy. Moreover, the adaptation gain law helps to reduce the convergence time.

9.6 Conclusion

- This chapter deals with the position control problem of an electropneumatic system which is an uncertain and perturbed nonlinear system.

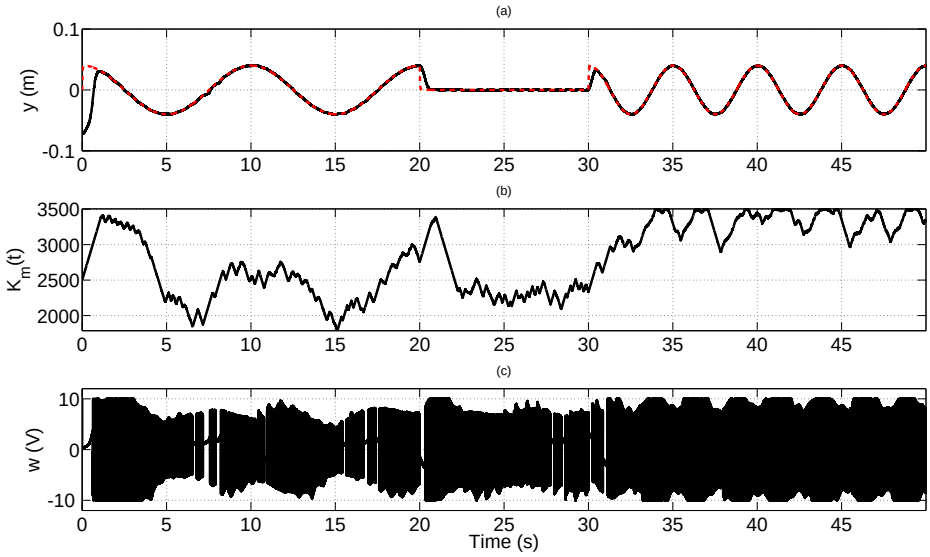

Figure 9.11 – **Experimental results of adaptive 3SMC. (a).** Reference position (red dotted) and measured position $y\ (m)$ (black solid) versus time (sec); **(b).** Control gain K_m versus time (sec); **(c).** Control input $w\ (V)$ versus time (sec).

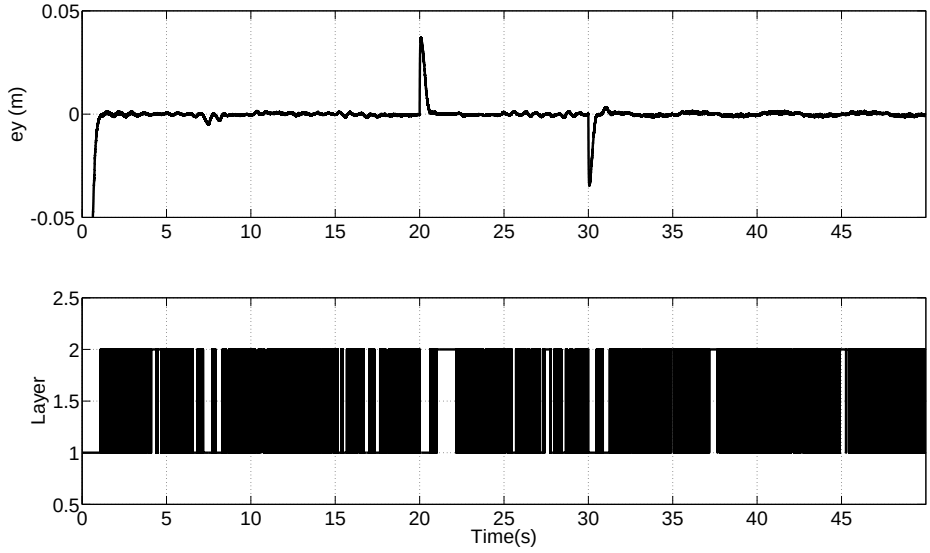

Figure 9.12 – **Experimental results of adaptive 3SMC. (Top).** Position tracking error $y - y_{ref}$ (m) versus time (sec); **(Bottom).** Layer detection L versus time (sec).

	Adaptive 3SMC	HOSM
$Mean(\|e_y\|)$	2.2×10^{-3}	5.9×10^{-3}
$Std(e_y)$	0.012	0.017
$Mean(\|w\|)$	3.33	1.42
mean(resp time)	0.61	1.70

Table 9.6 – Comparison between adaptive 3SMC and HOSMC

- Three second order sliding mode control laws, the twisting control (TWC), the second

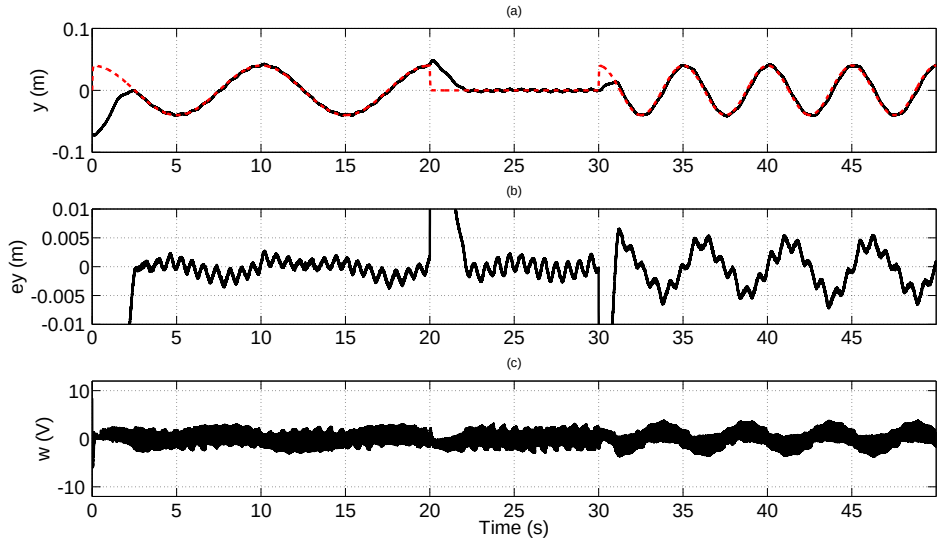

Figure 9.13 – **Experimental results of HOSMC. (a).** Reference position (red dotted) and measured position $y\ (m)$ (black solid) versus time (sec); **(b).** Position tracking error versus time (sec); **(c).** Control input $w\ (V)$ versus time (sec).

order sliding mode output feedback control (2SMOFC) and the twisting-like control (TWLC) are firstly applied to the system : the TWLC shows its advantages on the better tracking accuracy and a faster convergence time.

- Adaptive versions of 2SMOFC and TWLC are also applied to the electropneumatic system. The gain adaptation law helps to improve the tracking accuracy and to reduce the convergence time. The previously presented adaptive third order sliding mode control (adaptive 3SMC) is also tested on the experimental system.
- Thanks to the suppression of high order differentiation of the sliding variable in the controller, the 3SMC performs better tracking accuracy and a faster convergence time, compared to a Quasi-Continuous HOSM controller Levant [2005b].

10

Application to 3DOF Quanser helicopter

Contents

This chapter deals with the attitude control problem of an Unmanned Aerial Vehicle system named 3DOF Quanser helicopter Quanser [2006]. The scheme of the controller has been initially developed in Odelga et al. [2012] and used in Chriette and Plestan [2012]; Chriette et al. [2015]; Plestan and Chriette [2012]: it allows to decouple the system thanks to the introduction of both virtual inputs for travel and elevation angles, and to design a desired reference for the pitch angle. Moreover, such system requires a continuous control input due to the high sensitivity of its actuators versus the vibrations. Then, based on the twisting-like control (TWLC) presented in Chapter 4, an integral twisting-like control (integral TWLC) is developed Yan et al. [2016b]. This control law can be applied to systems with a relative degree equal to one, and provides a continuous input. In the experimental tests, the performance of this new method is compared to the super-twisting algorithm.

10.1 Description of 3DOF helicopter

The 3DOF Quanser helicopter studied in this chapter (see Figure 10.1, parameters are given in Table 10.1) is composed by the helicopter body, which is a small arm with one propeller at each end, and an arm (named in the sequel "helicopter arm"), which links the body to a **fixed basis**. Although the system cannot exhibit *translational motion*, given that it is fixed to a support, it can *rotate freely around three axis*. The helicopter position is characterized by the pitch, travel and elevation angles. The pitch motion corresponds to the rotation of the helicopter body around the helicopter arm, the travel motion corresponds to the rotation of the helicopter arm around the vertical axis, and the elevation motion corresponds to the rotation of

the helicopter arm around the horizontal axis.

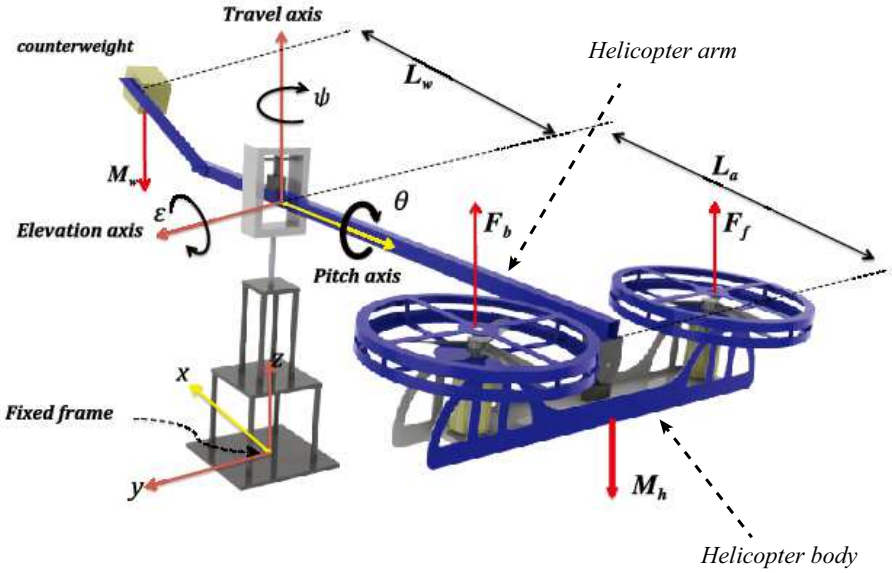

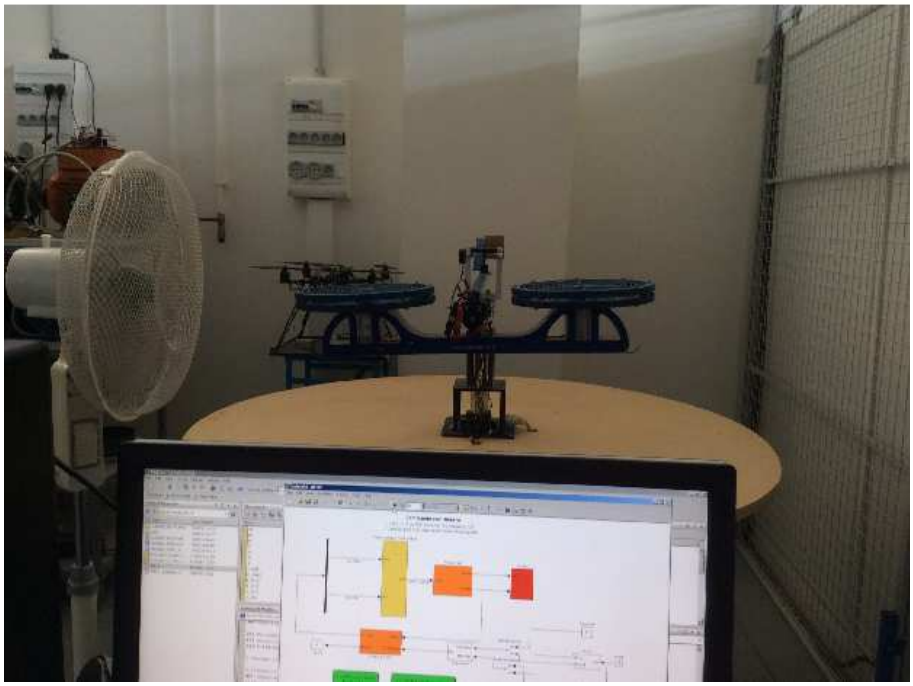

Figure 10.1 – **Top.** Scheme of Quanser 3DOF tandem helicopter; **Bottom.** Photo of the experimental set-up (with the fan on the left hand side, producing perturbations as wind gusts, and the control PC on foreground, with Matlab/Simulink software).

The helicopter has two DC motors, which drive two propellers. The helicopter attitude is controlled by means of the thrust forces F_b and F_f generated by the two propellers *i.e.*

$$\begin{bmatrix} F_f \\ F_b \end{bmatrix} = \begin{bmatrix} K_F V_f \\ K_F V_b \end{bmatrix} \tag{10.1}$$

with K_F the propeller force-thrust constant, V_f and V_b represents the voltage signal sent to the motors. The control laws for V_f and V_b are realized by Matlab/Simulink with a positive

Symbol	Description	Value	Unit
V_f & V_b	DC motor voltage of the front and back motors	[-24 ; +24]	V
K_F	Propeller force-thrust constant	0.1188	N/V
g	Gravity constant	9.81	$m.s^2$
M_h	Mass of the helicopter	1.426	kg
M_w	Mass of the counterweight	1.87	kg
L_a	Distance between travel axis to helicopter body	0.660	m
L_w	Distance between travel axis to the counterweight	0.470	m
L_h	Distance between pitch axis to each motor	0.178	m
J_ε	Moment of inertia about elevation	1.0348	$kg.m^2$
J_θ	Moment of inertia about pitch	0.0451	$kg.m^2$
J_ψ	Moment of inertia about travel	1.0348	$kg.m^2$

Table 10.1 – 3DOF Helicopter system specifications Quanser [2006]

sampling time T_e.
Notice that this system is an underactuated system, *i.e.* this system has 2 control forces whereas there are 3 degrees of freedom represented by the 3 attitude angles (the *travel* angle ψ, the *elevation* angle ϵ and the *pitch* angle θ).

10.2 Dynamics of the system

Neglecting the joint friction, air resistance and centrifugal forces, the nonlinear model used for the design of the attitude controller for the 3DOF helicopter reads as Odelga et al. [2012]

$$\begin{aligned} J_\epsilon \ddot{\epsilon} &= g(M_w L_w - M_h L_a)\cos\epsilon + L_a \cos\theta \; u_1 + F_\epsilon \\ J_\theta \ddot{\theta} &= L_h \; u_2 + F_\theta \\ J_\psi \ddot{\psi} &= L_a \cos\epsilon \sin\theta \; u_1 + F_\psi \end{aligned} \tag{10.2}$$

with the control input expressed in terms of the control forces as

$$\begin{bmatrix} u_1 \\ u_2 \end{bmatrix} = \begin{bmatrix} F_f + F_b \\ F_f - F_b \end{bmatrix}. \tag{10.3}$$

Front and back control motor voltages are derived from (10.1) and (10.3) and read as

$$V_f = \frac{1}{2K_F}(u_1 + u_2), \quad V_b = \frac{1}{2K_F}(u_1 - u_2)\,. \tag{10.4}$$

The functions F_ϵ, F_θ and F_ψ represent all the uncertainties and perturbations terms which are assumed to be bounded. Furthermore,

- pitch angle θ is defined on the interval $-45° \leq \theta \leq +45°$, whereas
- elevation angle ϵ is defined on $-27.5° \leq \epsilon \leq +30°$.

From ψ-dynamics, it appears that it is not possible to control travel angle when $\theta = 0$. Then, it is necessary to produce a pitch motion in order to change travel angle. It is a key-point in the design of the attitude controller.

10.3 Design of attitude controller

A key point of the control scheme consists in defining "virtual" control inputs allowing to linearize and decouple the system, by an input-output point-of-view: by this way, the system will be viewed as three perturbed double integrators, each double integrator concerning an attitude angle. Define

$$\begin{aligned} \nu_1 &= u_1 \cos\epsilon \sin\theta \\ \nu_2 &= u_1 \cos\theta \end{aligned} \tag{10.5}$$

and

$$\nu_1^* = \nu_1, \quad \nu_2^* = \frac{1}{L_a}\left[L_a\nu_2 + G\cos\epsilon\right], \tag{10.6}$$

with $G = g(M_w L_w - M_h L_a)$. From (10.2), one gets

$$\begin{aligned} J_\psi \ddot{\psi} &= L_a\nu_1^* + F_\psi \\ J_\epsilon \ddot{\epsilon} &= L_a\nu_2^* + F_\epsilon \\ J_\theta \ddot{\theta} &= L_h u_2 + F_\theta \end{aligned} \tag{10.7}$$

From (10.5)-(10.7), ψ is not controllable if $\theta = 0$. So, a desired trajectory for θ should be induced from the trajectories of ϵ and ψ. Then, the attitude controller scheme reads as follows (see Figure 10.2)

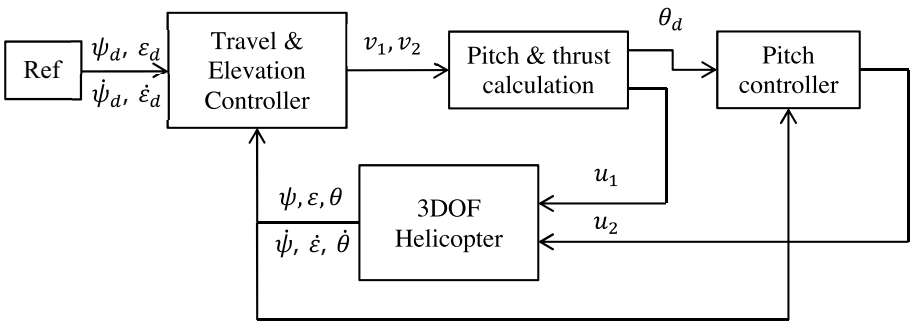

Figure 10.2 – Attitude controller scheme Chriette et al. [2015].

- The first part of the controller allows to compute the control inputs ν_1 and ν_2 from the tracking errors between ψ and ϵ and their desired trajectories $\psi_d(t)$ and $\epsilon_d(t)$ (through ν_1^* and ν_2^*)

$$\nu_1 = \nu_1^*, \quad \nu_2 = \frac{1}{L_a}\left[L_a\nu_2^* - G\cos\epsilon\right]. \tag{10.8}$$

  where ν_1^* and ν_2^* will be detailed latter.

- The second part of the controller aims to compute the control input u_1. From (10.5), one gets

$$u_1^2 \sin^2\theta = \frac{\nu_1^2}{\cos^2\epsilon} \quad \text{and} \quad u_1^2\cos^2\theta = \nu_2^2. \tag{10.9}$$

  Then, one has

$$u_1 = S \cdot \sqrt{\frac{\nu_1^2}{\cos^2\epsilon} + \nu_2^2} \tag{10.10}$$

  with S defined as

$$S = \begin{cases} \text{sign}(\nu_2) & \text{if } \nu_2 \neq 0 \\ 0 & \text{if } \nu_2 = 0 \end{cases} \tag{10.11}$$

- The angle θ is forced to track a desired trajectory θ_d. From (10.5), it is obvious that θ has to verify

$$\tan\theta = \frac{\nu_1}{\cos\epsilon\nu_2} \tag{10.12}$$

Then, the desired trajectory θ_d reads as

$$\theta_d(t) = \tan^{-1}\left(\frac{\nu_1}{\cos\epsilon\nu_2}\right). \tag{10.13}$$

From this latter desired trajectory, the pitch controller allows to provide u_2.

10.4 Integral twisting-like control

In Chapter 4, the twisting-like controller (TWLC) has been presented. It has been initially designed for systems with relative degree equal to two. The main features of this control law can be summarized as follows:

- a real second order sliding mode with respect to σ is ensured in a finite time;
- only the measurement of σ is required but not its derivatives;
- the performances (in the terms of convergence time and accuracy) of this control law are close to those obtained with twisting control;
- a switching gain strategy is used for this control law and the switching conditions depend on the detection of the sign commutations of σ and an online updated variable τ_i.

In this section, the TWLC is extended to systems with relative degree equal to one, using integral strategy, so that, one obtains a relative smooth control input allowing to reduce the chattering. Consider a single-input uncertain nonlinear system

$$\dot{x} = f(x) + g(x)\nu \tag{10.14}$$

with $x \in \mathbb{R}^n$ the state vector, $\nu \in \mathbb{R}$ the control input. Function $f(x)$ is a differentiable, partially known, vector field. $g(x)$ is a known non-zero function. The sliding variable $\sigma = \sigma(x,t) \in \mathbb{R}$ is designed so that the control objective is fulfilled if $\sigma(x,t) = 0$. The system (10.14) has a relative degree equal to one with respect to σ, and the internal dynamics is stable. Therefore, the sliding variable dynamics reads as

$$\begin{aligned} \dot{\sigma} &= \underbrace{\frac{\partial\sigma}{\partial t} + \frac{\partial\sigma}{\partial x}f(x)}_{\varphi(x,t)} + \underbrace{\frac{\partial\sigma}{\partial x}g(x)\nu}_{w} \\ &= \varphi(x,t) + w \end{aligned} \tag{10.15}$$

One supposes that

Assumption 10.4.1. *The term $\dfrac{\partial\sigma}{\partial x}g(x)$ is known and define $w = \dfrac{\partial\sigma}{\partial x}g(x)\nu$ as the new control input.*

Assumption 10.4.2. *The function $\varphi(\cdot)$ is uncertain and bounded, and reads as*

$$\varphi(\cdot) = \varphi_0(\cdot) + \Delta\varphi(\cdot), \tag{10.16}$$

with φ_0, the known nominal terms, and $\Delta\varphi$ the uncertain parts. The term $\Delta\varphi$ fulfills

$$\left|\frac{d\Delta\varphi}{dt}\right| < \Delta\varphi_M$$

with $\Delta\varphi_M$ positive constant.

Assumption 10.4.3. *The controller is updated in discrete-time with the sampling period T_e, which is a strictly positive constant.*

The problem consists in establishing a real second order sliding mode with respect to σ in spite of the uncertainties/perturbations.
The integral TWLC algorithm reads as ($k \in \mathbb{N}$)

$$\begin{array}{rcl} w & = & -\varphi_0(\cdot) - \alpha\sigma + v(t) \\ \dot{v}(t) & = & u(kT_e) \text{ for } t \in [kT_e, (k+1)T_e[\ , k \in \mathbb{N} \\ u(kT_e) & = & -K(kT_e) \cdot \text{sign}(\sigma(kT_e)) \end{array} \tag{10.17}$$

with $\alpha > 0$. The control input w is composed by three terms. The term $-\varphi_0(\cdot)$ is the equivalent control which compensates the known part of φ. The term $v(t)$ is designed based on the TWLC algorithm, which ensures the establishment of the real 2SM with respect to σ. The linear term $-\alpha\sigma$ cooperates with the TWLC to ensure the stability of the internal dynamics of σ.
The gain K is defined as

$$K(kT_e) \;=\; \begin{cases} K_m & \text{if} \quad kT_e \notin \mathcal{T}_{\mathcal{H}} \\ \gamma K_m & \text{if} \quad kT_e \in \mathcal{T}_{\mathcal{H}} \end{cases} \tag{10.18}$$

where $\mathcal{T}_{\mathcal{H}}$ represents the gain commutation condition which is given by

$$\mathcal{T}_{\mathcal{H}} \;=\; \{kT_e \mid T_s^i \leq kT_e \leq T_s^i + \tau_i, i \in \mathbb{N}\}\ . \tag{10.19}$$

T_s^i is the time at which the i^{th} σ-sign switching is detected (which makes the gain switching from the small gain K_m to the large gain γK_m), whereas τ_i is the duration of the large gain for $t \in [T_s^i,\ T_s^{i+1}[$.
The computation of the duration τ_i is detailed in the sequel.
Firstly, denote

$$\begin{array}{ll} K_m^{max} = K_m + \Delta\varphi_M, & K_m^{min} = K_m - \Delta\varphi_M \\ K_M^{max} = \gamma K_m + \Delta\varphi_M, & K_M^{min} = \gamma K_m - \Delta\varphi_M. \end{array}$$

If the gain is tuned such that $K_m > \Delta\varphi_M$ and $\gamma > 2$, one as

$$K_m^{min} > 0 \quad , \quad K_M^{min} > K_m^{max}\ . \tag{10.20}$$

Then, τ_i is defined as

$$\tau_i = \max(\tau_i', T_e) \tag{10.21}$$

with

$$\tau_i' \;=\; T_e \cdot \text{floor}\left[2\alpha \frac{\tau_{i-1}K_M^{min} + \bar{\tau}_{i-1}K_m^{min}}{K_M^{max}T_e} - 1\right] \tag{10.22}$$

in which α and $\bar{\tau}_i$ are defined as

$$\alpha \;=\; \frac{\sqrt{K_m^{min}}}{\sqrt{K_M^{max}} + \sqrt{K_m^{min}}} \tag{10.23}$$

and

$$\bar{\tau}_i \;=\; \max(0,\ T_s^{i+1} - T_s^i - \tau_i)\ . \tag{10.24}$$

Remark that $\bar{\tau}_i$ corresponds to the duration of the i^{th} small gain control $K = K_m$. For $i = 0$ set $T_s^0 = 0$ and $\tau_0 = 0$. Then, the integral TWLC is summarized by the following theorem.

Theorem 10.1 (Yan et al. [2016b]). *Consider system (10.14) with the sliding variable $\sigma(x,t)$ and its associated dynamics (10.15). Suppose that Assumptions H1-H4 are fulfilled. Then, a real second order sliding mode with respect to σ is ensured after a finite time, thanks to the integral TWLC (10.17)-(10.18)-(10.19) with $K_m > \Delta\varphi_M$ and $\gamma > 2$ and τ_i defined by (10.21)-(10.24).*

Proof. The proof of Theorem 10.1 is based on the TWLC method Yan et al. [2016d]. Consider the sliding variable $\sigma(x,t)$ and its associated dynamics (10.15) under the control law (10.17)-(10.18)-(10.19). One has

$$\begin{aligned} \dot{\sigma} &= \Delta\varphi - \alpha\sigma + v \\ \ddot{\sigma} &= \frac{d\Delta\varphi}{dt} - \alpha\dot{\sigma} + u(kT_e) \end{aligned} \tag{10.25}$$

In the second order time derivative of σ, three terms appear: $u(kT_e)$ based on TWLC, $-\alpha\dot{\sigma}$ and the uncertainty $\frac{d\Delta\varphi}{dt}$. If $-\alpha\dot{\sigma}$ plays the leading role in $\ddot{\sigma}$, the convergence of $\dot{\sigma}$ is guaranteed. On the other hand, if $u(kT_e)$ is playing the leading role according to Yan et al. [2016d], the real SOSM with respect to σ is ensured. So, in the sequel, three cases are considered to discuss the roles played by $u(kT_e)$ and $-\alpha\dot{\sigma}$.

Case 1: Consider the case that

$$-\alpha\dot{\sigma}\cdot u \;\geq\; 0\,. \tag{10.26}$$

It means that the two control terms $-\alpha\dot{\sigma}$ and u have the same sign. These two terms cooperate to make $\dot{\sigma}$ to converge. Given that $K_m > \Delta\varphi_M$, one has $|u| > |\frac{d\Delta\varphi}{dt}|$ which yields that

$$\text{sign}(\frac{d\Delta\varphi}{dt} - \alpha\dot{\sigma} + u(kT_e)) \;=\; -\text{sign}(\dot{\sigma})\,. \tag{10.27}$$

It leads to $\ddot{\sigma}\dot{\sigma} \leq 0$, then, $\dot{\sigma}$ will asymptotically converge to zero. Then, with the term $\alpha\dot{\sigma}$ small enough, the term $u(kT_e)$ can drive σ to zero, and ensure the establishment of second order sliding mode.

Case 2: Consider now

$$-\alpha\dot{\sigma}\cdot u \;<\; 0\,. \tag{10.28}$$

It means that these two terms do not cooperate with each other.
Case 2.a: Suppose now

$$\text{sign}(\frac{d\Delta\varphi}{dt} - \alpha\dot{\sigma} + u(kT_e)) \;=\; -\text{sign}(\dot{\sigma}) \tag{10.29}$$

which means that the term $-\alpha\dot{\sigma}$ is playing the leading role. As proved in the first case, $\dot{\sigma}$ converges to zero. With the convergence of $\dot{\sigma}$, the term $-\alpha\dot{\sigma}$ approaches to zero and the following case will happen next.

Case 2.b: Suppose

$$\text{sign}(\frac{d\Delta\varphi}{dt} - \alpha\dot{\sigma} + u(kT_e)) \;=\; \text{sign}(u) \tag{10.30}$$

It means that the term u is playing the leading role in $\ddot{\sigma}$. In this case, $K_m > |\frac{d\Delta\varphi}{dt} - \alpha\dot{\sigma}|$ holds. According to the result in Theorem 4.1, σ and $\dot{\sigma}$ will converge to zero, and a real second order sliding mode with respect to σ is ensured after a finite time.

10.5 Experimental validation

In the experimental tests, an external perturbation is applied thanks to a fan (see Figure 10.1-Bottom), this fan being located in order to provide wind in side direction, *i.e.* it is mainly acting on the travel and pitch angles. For the validation of the designed controllers, stabilization and trajectories tracking are considered. For the trajectories tracking, desired trajectories for elevation and travel, respectively $\epsilon_d(t)$ and $\psi_d(t)$, are used, the desired trajectory $\theta_d(t)$ of the pitch angle being computed online by the inner loop (see Figure 10.2). The trajectories used in the sequel are time-varying desired angles defined by two sinus waves. The elevation wave period is two times greater than the travel wave period; by this way, the desired trajectory in the (ψ, ϵ)-workspace is cyclic and forms a turned 8-like pattern as presented by Figure 10.3 Chriette et al. [2015]. Note that these trajectories are designed by taking into account constraints on

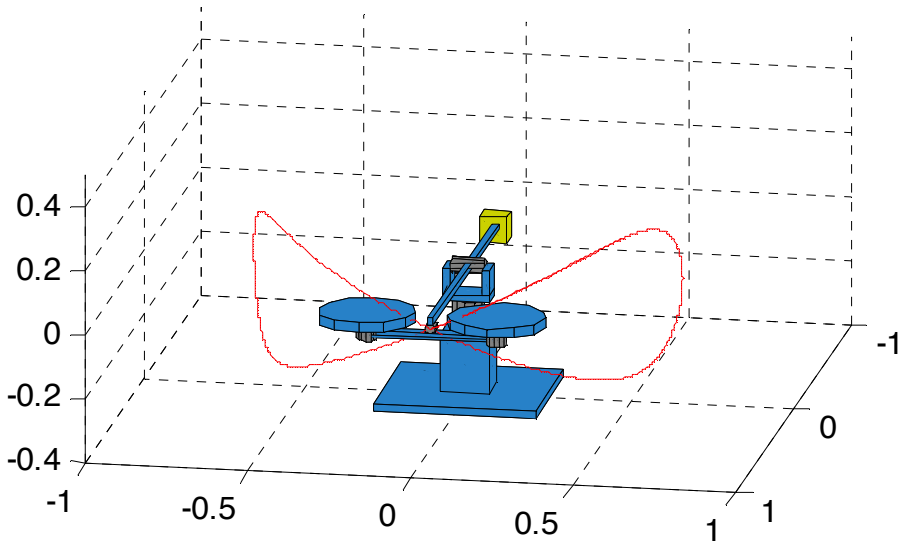

Figure 10.3 – **3D Desired Trajectory.** Sinusoidal trajectories.

maximal values of velocity, acceleration, and control inputs. Then, three sliding variables are defined respectively from the reference signal $\epsilon_d(t)$, $\psi_d(t)$ and $\theta_d(t)$. It yields

$$\begin{bmatrix} \sigma_\psi \\ \sigma_\epsilon \\ \sigma_\theta \end{bmatrix} = \begin{bmatrix} \left(\dot{\psi}(t) - \dot{\psi}_d(t)\right) + \lambda_\psi \left(\psi(t) - \psi_d(t)\right) \\ \left(\dot{\epsilon}(t) - \dot{\epsilon}_d(t)\right) + \lambda_\epsilon \left(\epsilon(t) - \epsilon_d(t)\right) \\ \left(\dot{\theta}(t) - \dot{\theta}_d(t)\right) + \lambda_\theta \left(\theta(t) - \theta_d(t)\right) \end{bmatrix} \tag{10.31}$$

From (10.7), with $\sigma = [\sigma_\psi \ \sigma_\epsilon \ \sigma_\theta]^T$, one gets the expression for $\dot{\sigma}$ as follows

$$\dot{\sigma} = \begin{bmatrix} \frac{L_a}{J_\psi}\nu_1^* - \ddot{\psi}_d(t) + \lambda_\psi(\dot{\psi} - \dot{\psi}_d(t)) + \frac{F_\psi}{J_\psi} \\ \frac{L_a}{J_\epsilon}\nu_2^* - \ddot{\epsilon}_d(t) + \lambda_\epsilon(\dot{\epsilon} - \dot{\epsilon}_d(t)) + \frac{F_\epsilon}{J_\epsilon} \\ \frac{L_h}{J_\theta}u_2 - \ddot{\theta}_d(t) + \lambda_\theta(\dot{\theta} - \dot{\theta}_d(t)) + \frac{F_\theta}{J_\theta} \end{bmatrix} \tag{10.32}$$

Assumptions 10.4.1-10.4.3 are fulfilled. The control laws $[\nu_1^* \ \nu_2^* \ u_2]^T$ are inspired from the integral TWLC presented in Theorem 10.1 and are defined as

$$\begin{bmatrix} \nu_1^* \\ \nu_2^* \\ u_2 \end{bmatrix} = \begin{bmatrix} \frac{J_\psi}{L_a}\left(w_1^* - \lambda_\psi(\dot{\psi} - \dot{\psi}_d(t)) + \ddot{\psi}_d(t)\right) \\ \frac{J_\epsilon}{L_a}\left(w_2^* - \lambda_\epsilon(\dot{\epsilon} - \dot{\epsilon}_d(t)) + \ddot{\epsilon}_d(t)\right) \\ \frac{J_\theta}{L_h}\left(w_2 - \lambda_\theta(\dot{\theta} - \dot{\theta}_d(t)) + \ddot{\theta}_d(t)\right) \end{bmatrix} \tag{10.33}$$

with

$$\begin{array}{rcl} w_1^*(t) & = & -\alpha_\psi\sigma_\psi + v_\psi(t) \\ \dot{v}_\psi(t) & = & u_\psi(kT_e) \text{ for } t \in [kT_e, (k+1)T_e[\ , k \in I\!N \\ u_\psi(kT_e) & = & -K_\psi \text{sign}(\sigma_\psi(kT_e)) \\ \\ w_2^*(t) & = & -\alpha_\epsilon\sigma_\epsilon + v_\epsilon(t) \\ \dot{v}_\epsilon(t) & = & u_\epsilon(kT_e) \text{ for } t \in [kT_e, (k+1)T_e[\ , k \in I\!N \\ u_\epsilon(kT_e) & = & -K_\epsilon \text{sign}(\sigma_\epsilon(kT_e)) \\ \\ w_2(t) & = & -\alpha_\theta\sigma_\theta + v_\theta(t) \\ \dot{v}_\theta(t) & = & u_\theta(kT_e) \text{ for } t \in [kT_e, (k+1)T_e[\ , k \in I\!N \\ u_\theta(kT_e) & = & -K_\theta \text{sign}(\sigma_\theta(kT_e)) \\ \\ K_X(kT_e) & = & \left\{ \begin{array}{ll} K_m & \text{if } \ t \notin \mathcal{T}_\mathcal{H} \\ \gamma K_m & \text{if } \ t \in \mathcal{T}_\mathcal{H} \end{array} \right. \quad X = \{\psi, \epsilon, \theta\} \end{array} \tag{10.34}$$

The parameters of integral TWLC are defined as described in Table 10.2. The choice of these parameters has been made in order to get accurate and robust results.

Parameters	λ	α	K_m	γ	$\Delta\varphi_M$
Travel ψ	2	2	0.05	5	1.25×10^{-3}
Elevation ϵ	3	2	0.05	5	1.25×10^{-3}
Pitch θ	1	1	0.0125	5	1.25×10^{-3}

Table 10.2 – Parameters of the attitude controller based on integral TWLC.

The helicopter and its actuators are very sensitive to the vibrations: then, a smooth control input is required. In the context of sliding mode control the super-twisting algorithm (STWC) Levant [1993] offers a continuous input. In this section, a comparison between integral TWLC and STWC is presented. In the current case, the super-twisting control law reads as (10.33) with

$$\begin{array}{rcl} w_1^* & = & -p_\psi|\sigma_\psi|^{1/2}\text{sign}(\sigma_\psi) - \displaystyle\int_0^t \frac{q_\psi}{2}\text{sign}(\sigma_\psi(\tau))\text{d}\tau \\ \\ w_2^* & = & -p_\epsilon|\sigma_\epsilon|^{1/2}\text{sign}(\sigma_\epsilon) - \displaystyle\int_0^t \frac{q_\epsilon}{2}\text{sign}(\sigma_\epsilon(\tau))\text{d}\tau \\ \\ w_2 & = & -p_\theta|\sigma_\theta|^{1/2}\text{sign}(\sigma_\theta) - \displaystyle\int_0^t \frac{q_\theta}{2}\text{sign}(\sigma_\theta(\tau))\text{d}\tau \end{array} \tag{10.35}$$

The tuned parameters of STWC is detailed in Table 10.3. The experimental tests have been made with perturbation produced by the fan at around $t = 100\ sec$. Figures 10.4 and 10.5 display the obtained trajectories of attitude angles, and the system performances under integral

TWLC and STWC. In Table 10.4, the performances of these two controllers are compared. The mean and standard deviation of tracking errors of elevation, pitch and travel angles are calculated respectively for $t \in [80\,\text{sec}; 200\,\text{sec}]$.
It shows that the control inputs V_f and V_b for these two methods have a similar form. For the tracking accuracy of elevation, the results obtained with these two control laws reach the same level. However, the convergence time obtained with integral TWLC is shorter. Furthermore, for the tracking performance of travel and pitch, the integral TWLC offers a smoother desired reference θ_d and a better tracking accuracy.

Parameters	p	q
Travel ψ	0.25	0.05
Elevation ϵ	0.35	0.07
Pitch θ	0.3	0.06

Table 10.3 – Parameters of the attitude controller based on STWC.

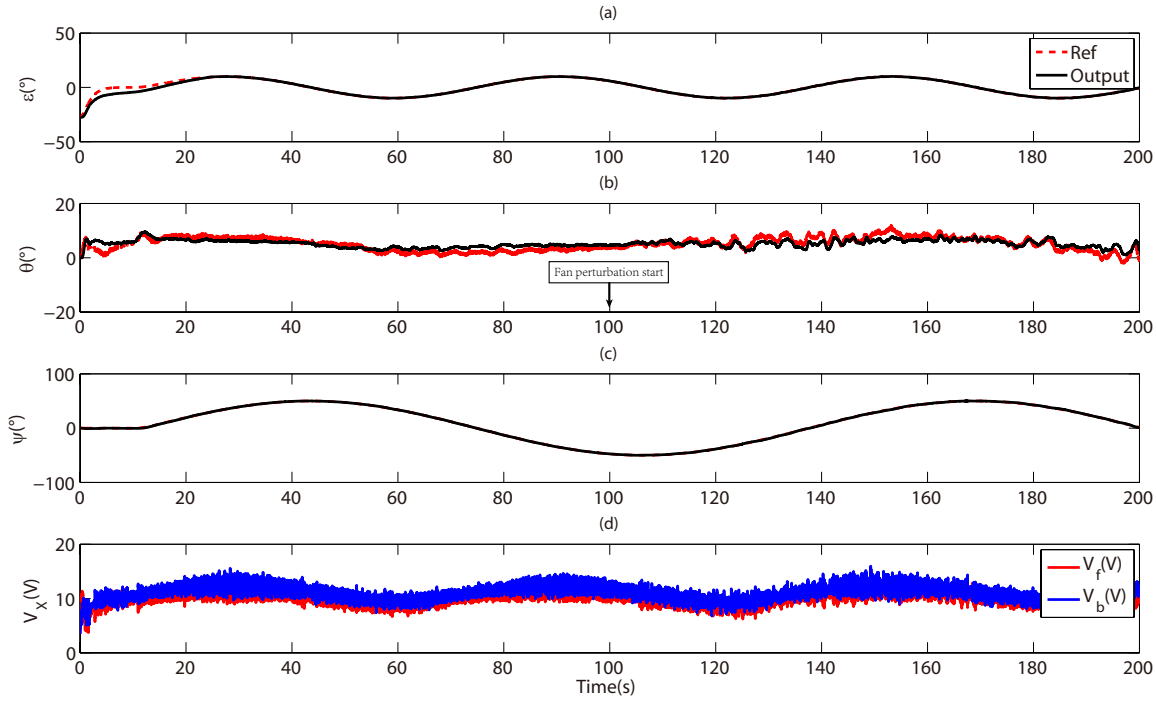

Figure 10.4 – **Integral TWLC – Experimental results for trajectory tracking.** (a) elevation angle ϵ (black) and ϵ_d (red) versus time (sec); (b) pitch angle θ (black) and θ_d (red) versus time (sec); (c) travel angle ψ (black) and ψ_d (red) versus time (sec); (d) control input V_f (red) and V_b (blue) versus time (sec).

10.6 Conclusion

- This chapter deals with the attitude control problem of a 3DOF helicopter.
- The control scheme is designed such that the closed-loop system is decoupled into three perturbed double integrators.

	Integral TWLC	STWC
Mean($\|e_\epsilon\|$) (deg)	0.0850	0.1242
Mean($\|e_\theta\|$) (deg)	1.3850	1.2196
Mean($\|e_\psi\|$) (deg)	0.2210	0.4610
Std(e_ϵ)	0.1076	0.1548
Std(e_θ)	1.6665	1.6984
Std(e_ψ)	0.2943	0.7301
Mean($\|V_f\|$) (V)	10.1553	10.1331
Mean($\|V_b\|$) (V)	10.1553	10.1331
Std(V_f)	1.2678	1.1168
Std(V_b)	1.2678	1.1168
ϵ convergence time	<25sec	>32sec

Table 10.4 – Evaluation of the performances of integral TWLC and STWC.

- The integral twisting-like control (integral TWLC) is developed and applicable to the system with relative degree equal to one, and provides a continuous input.
- The experimental comparison is made between the integral TWLC and the super-twisting algorithm.
- The integral TWLC shows its advantages with a faster convergence time and better tracking accuracy.

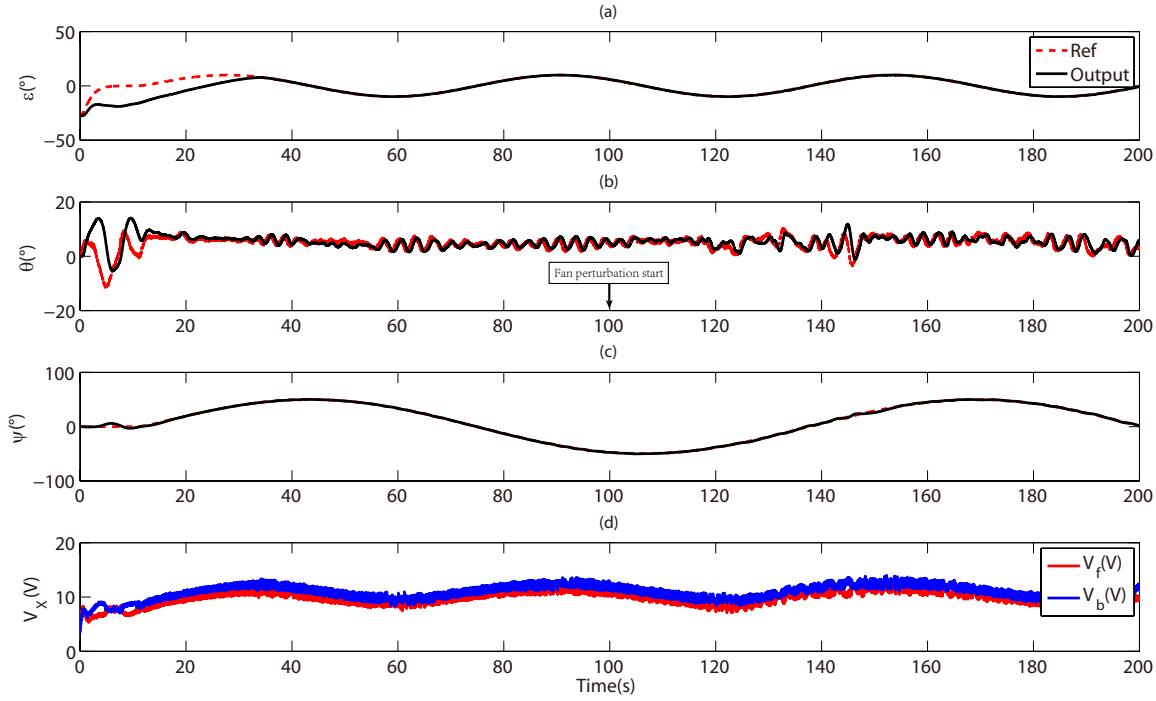

Figure 10.5 – **STWC – Experimental results for trajectory tracking.**(a) elevation angle ϵ (black) and ϵ_d (red) versus time (sec); (b) pitch angle θ (black) and θ_d (red) versus time (sec); (c) travel angle ψ (black) and ψ_d (red) versus time (sec); (d) control input V_f (red) and V_b (blue) versus time (sec).

Concluding remarks and future works

In this thesis, some robust control strategies have been developed based on the sliding mode theory for nonlinear systems with uncertainties and perturbations. This work has been focused on two topics:

- the development of high order sliding mode control laws with a reduced use of time derivatives of the sliding variable;
- the sliding mode control with gain adaptation.

In Chapter 3 the gain commutation formalism has been presented. For the control approaches in this formalism, the control input can switch between two levels: a level with small magnitude and another level with large magnitude. Then, the twisting control (TWC) Levantovsky [1985] and the second order sliding mode output feedback control (2SMOFC) Plestan et al. [2010a] can be rewritten in this unified frame. For TWC, the large gain input is applied when z_1 and z_2 have the same sign. For 2SMOFC the large gain is applied during one sampling period, after every detection of z_1 sign commutation. The convergence analysis for these two control strategies has been made based on a geometric analysis of system trajectories in the phase plane.
Moreover, in Chapter 4, a new second order sliding mode control law named twisting-like control (TWLC) has been presented. The key-point for TWLC is the time varying duration τ_i of the large gain input. Compared to the second order sliding mode output feedback control (2SMOFC) presented in Section 3.4, for TWLC, the large gain input is applied during a time varying duration τ_i. Its computation depends on the control gains K_m, K_M and the time gap between two successive z_1-sign commutations. Thanks to the application of u_H during multiple sampling periods, the performance of system (2.3) under TWLC is close to the one with twisting control. Furthermore, the use of time derivative of the sliding variable is removed. The comparisons made in Chapter 5 have shown that this new control law inherits the output feedback feature from 2SMOFC and also the advantage of fast convergence time from TWC. One inconvenient for TWLC is that its algorithm for τ_i requires the estimated bounds for function a and b.

In Chapter 7, the adaptive version algorithms of 2SMOFC and TWLC have been presented. This gain adaptation algorithm is based on the time gap between two successive sign switching of the sliding variable. Then, under this adaptive mechanism, the gain decreases when the system trajectory reaches a vicinity of zero, and increases in the opposite case. According to the simulation results, the gain adaptation law allows to further improve the tracking accuracy and the convergence time, compared to the standard 2SMOFC and TWCL respectively.
In Chapter 8, an adaptive third order sliding mode has been proposed Yan et al. [2016c]. For the third order sliding mode control, both the first and second order time derivatives of the sliding variable should be known. For this new algorithm, the use of second order time derivative is removed. This feature helps to reduce the additional disturbance introduced by the high order differentiator. Moreover, the gain adaptation is also used to simplify the gain tuning process.

Chapter 9 and 10 presented the applications of these new control laws to experimental systems. In Chapter 9 the position control problem of the electropneumatic system has been considered. This is a typical nonlinear system with uncertainty and perturbations. Three second order sliding mode control laws, the twisting control (TWC), the second order sliding mode output feedback control (2SMOFC) and the twisting-like control (TWLC) have been firstly applied to the system : the TWLC shows its advantages on the better tracking accuracy and a faster convergence time. Adaptive versions of 2SMOFC and TWLC have been also applied to the electropneumatic system. The gain adaptation law helps to improve the tracking accuracy and to reduce the convergence time. The previously presented adaptive third order sliding mode control (adaptive 3SMC) has been also tested on the experimental system. Compared to a Quasi-Continuous HOSM controller Levant [2005b], thanks to the remove of high order differentiation of the sliding variable in the controller, the 3SMC performs better tracking accuracy and a faster convergence time.
In Chapter 10, the attitude control of a Unmanned Aerial Vehicles system with three degrees of freedom Quanser [2006] has been considered. Due to the high sensitivity of the actuators to the vibration, continuous control input is required for this system. Then, in this chapter the integral version of twisting-like control (integral TWLC) has been developed Yan et al. [2016b]. This control law can be applied to the system with relative degree equal to one, and gives a continuous input. In the experimental tests this method shows its advantages with a faster convergence time and better tracking accuracy.

Some works remain to be developed in the future. This includes in particular the following topics.

- Based on the twisting-like algorithm, the use as a second order differentiator (TWLD) has been presented in this work. It may be interesting to extend this result to higher order differentiation. One possible solution is to contact multiple TWLD in series. It would be a solution for observation of uncertain nonlinear systems. However, it would be necessary to intensively study the performances of such differentiation solutions with respect to existing ones.
- In this lecture, the proposed third order sliding mode control law requires the sliding variable and its first time derivative. It will be interesting to develop a third order sliding mode algorithm that uses only the sliding variable. Consider system (8.2), the sign of z_2 can be deduced from the increasing or decreasing of z_1. Knowing z_2-sign, z_2 and z_3 can be forced to zero, by using TWLC. Then, the remaining task is to vanish z_1, by designing a control input depending on z_1 and z_2-sign.
- The integral twisting-like control and the super-twisting control can be applied to systems with a relative degree equal to one, ensure a second order sliding mode and offer a continuous input. Such attempt can be also made for systems with relative degree equal to two. Based on the 3SMC presented in this thesis, in the future work, a third order sliding mode control law which can be applied to systems with relative degree equal to two with a smooth input could be developed.
- It is also worth to combine the TWLC with the impulsive sliding mode control Shtessel et al. [2013]. The impulsion helps to reduce the convergence time, when the system trajectories are far from origin. Once it reaches a vicinity of zero, the TWLC is used to keep the trajectories around the origin. For this latter phase, the use of time derivative of the sliding variable can be removed.

List of Figures

List of Tables

Bibliography

G. Bartolini, A. Ferrara, and E. Usai. Sub-optimal sliding mode control of uncertain second order dynamical systems. In *IFAC World Congress*. San Francisco, US, 1996. 14

G. Bartolini, A. Ferrara, and E. Usai. Output tracking control of uncertain nonlinear second-order systems. *Automatica*, 33(12):2203–2212, 1997. 21

G. Bartolini, A A. Ferrara, and E. Usani. Chattering avoidance by second-order sliding mode control. *IEEE transactions on Automatic Control*, 43(2):241–246, 1998. 13, 14

G. Bartolini, A. Ferrara, A. Levant, and E. Usai. On second order sliding mode controllers. *Variable structure systems, sliding mode and nonlinear control*, pages 329–350, 1999. 14

G. Bartolini, A. Pisano, and E. Usai. Digital second-order sliding mode control for uncertain nonlinear systems. *Automatica*, 37(9):1371–1377, 2001. 14

G. Bartolini, A. Levant, and et al. A real-sliding criterion for control adaptation. In *2002 Workshop on Variable Structure System (VSS)*. Sarajevo, Yugoslavia, 2002. 69

M. Belgharbi, D. Thomasset, S. Scavarda, and S. Sesmat. Analytical model of the flow stage of a pneumatic servo-distributor for simulation and nonlinear control. In *Scandinavian International Conference on Fluid Power*. Tampere, Finland, 1999. 97, 99

M. Bouri and D. Thomasset. Sliding mode of an electropneumatic actuator using an integral switching surface. *IEEE Transactions on Control System Technology*, 9(2):368–375, 2001. 1, 19, 98

X. Brun, S. Sesmat, D. Thomasset, and S. Scavarda. A comparative study between two control laws of an electopneumatic actuator. In *European Control Conference (ECC)*. Karlsruhe, Germany, 1999. 3, 97

JA. Burton and AS.I. Zinober. Continuous approximation of variable structure control. *International journal of systems science*, 17(6):875–885, 1986. 12

S. Chillari, S. Guccione, and G. Muscato. An experimental comparison between several pneumatic position control methods. In *IEEE Conference on Decision and Control(CDC)*. Orlando, FL, USA, 2001. 3, 19, 98

A. Chriette and F. Plestan. Nonlinear modeling and control of a 3dof helicopter. In *ASME Biennal Conference on Engineering Systems Design and Analysis ESDA*. Nantes, France, 2012. 113

A. Chriette, H. Castañeda F. Plestan, M. Pal, M. Guillo, M. Odelga, S. Rajappa, and R. Chandra. Adaptive robust attitude control for uavs - design and experimental validation. *Int. J. Adapt. Control Signal Process*, 2015. 113, 116, 120, 129

M. Defoort, F. Nollet, T. Floquet, and et al. A third order sliding mode controller for a stepper motor. *IEEE Transactions on Industrial Electronics*, 56(9):3337–3346, 2009. 66

A. Estrada and F. Plestan. Second order sliding mode output feedback control: Impulsive gain and extension with adaptation. In *IEEE Conference on Decision and Control (CDC)*. Maui, Hawwii, USA, 2012. 27, 40, 65, 68, 89

A. Estrada and F. Plestan. Second order sliding mode output feedback control with switching gains—application to the control of a pneumatic actuator. *Journal of the Franklin Institute*, 351(4):2335–2355, 2014. 27, 41, 65

A. Estrada, F. Plestan, and B. Allouche. An adaptive version of a second order sliding mode output feedback controller. In *European Control Conference (ECC),*. Zurich, Switzerland, 2013. 17, 27, 65

F.Dinuzzo and A.Ferrara. Higher order sliding mode controllers with optimal reaching. *IEEE Transactions on Automatic Control*, 54(9):2126–2136, 2009. 66

Y. Feng, X. Yu, and Z. Man. Non-singular terminal sliding mode control of rigid manipulators. *Automatica*, 38(12):2159–2167, 2002. 81

A. Girin and F. Plestan. A new experimental setup for a high performance double electropneumatic actuators system. In *American Control Conference (ACC)*. Saint-Louis, Missouri, 2009. 19, 97, 98

A. Girin, F. Plestan, X. Brun, and A. Glumineau. Robust control of an electropneumatic actuator : application to an aeronautical benchmark. *IEEE Trans. Control Syst. Technology*, 17(3): 633–645, 2009. 1, 19

J. Guldner and V. Utkin. The chattering problem in sliding mode systems. In *14th Int. Symp. Math. Theory Netw. Syst.(MTNS), Perpignan, France*, 2000. 11

A. Isidori. *Nonlinear control systems*. Springer Science & Business Media, 2013. 8

S. Laghrouche. *Commande par modes glissants d'ordre supérieur: théorie et application*. PhD thesis, Ecole Centrale de Nantes, 2004. 11

S. Laghrouche, M. Smaoui, and F. Plestan. Third-order sliding mode controller for electropneumatic actuators. In *IEEE Conference on Decision and Control (CDC)*, 2004. 1, 19

S. Laghrouche, F. Plestan, and A. Glumineau. Higher order sliding mode control based on integral sliding mode. *Automatica*, 43(3):531–537, 2007. 13, 14, 16

A. Levant. Sliding order and sliding accuracy in sliding mode control. *International journal of control*, 58(6):1247–1263, 1993. 20, 29, 37, 38, 49, 80, 121

A. Levant. Robust exact differentiation via sliding mode technique. *Automatica*, 34(3):379–384, 1998. 2, 4, 15, 20, 21, 27, 57

A. Levant. Higher-order sliding modes, differentiation and output-feedback control. *International journal of Control*, 76(9-10):924–941, 2003. 13, 14, 18, 20, 21, 49, 80

A. Levant. Homogeneity approach to high-order sliding mode design. *Automatica*, 41(5):823–830, 2005a. 13, 14

A. Levant. Quasi continuous high order sliding mode controllers. *IEEE Transactions on Automatic Control*, 50(11):1812–1816, 2005b. 3, 16, 20, 22, 108, 109, 111, 126

A. Levant. Principles of 2-sliding mode design. *Automatica*, 43(4):576–586, 2007. 56, 127

LV. Levantovsky. Second order sliding algorithms: their realization. *Dynamics of Heterogeneous Systems*, pages 32–43, 1985. 2, 15, 20, 21, 27, 31, 37, 38, 125

H. Morioka, A. Nishiuchi, K. Kurahara, K. Tanaka, and M. Oka. Practical robust control design of pneumatic servo systems. In *Industrial Electronics Society, 2000. IECON 2000. 26th Annual Conference of the IEEE*. Nagoya, Japan, 2000. 97

M. Odelga, F. Plestan, and A. Chriette. Control of 3 dof helicopter: a novel autopilot scheme based on adaptive sliding mode control. In *American Control Conference (ACC)*. Montreal, Canada, 2012. 113, 115

A. Paul, J. Mishra, and M. Radke. Reduced order sliding mode control for pneumatic actuator. *IEEE Transactions on Control Systems Technology*, 2(3):271–276, 1994. 98

F. Plestan and A. Chriette. A robust autopilot based on adaptive super-twisting algorithm for a 3dof helicopter. In *IEEE Conference on Decision and Control (CDC)*. Maui, USA, 2012. 113

F. Plestan and A. Girin. A new experimental setup for a high performance double electropneumatic actuators system. In *American Control Conference*. Saint Louis, United States, 2009. 1, 19

F. Plestan, A. Glumineau, and S. Laghrouche. A new algorithm for high-order sliding mode control. *International Journal of Robust and Nonlinear Control*, 18(4-5):441–453, 2008a. 14, 16

F. Plestan, E. Moulay, A. Glumineau, and T. Cheviron. Output feedback control: a robust solution based on second order sliding mode. In *IFAC World Congress*. Seoul, South-Korea, 2008b. 71

F. Plestan, E. Moulay, A. Glumineau, and T. Cheviron. Robust output feedback sampling control based on second-order sliding mode. *Automatica*, 46(6):1096–1100, 2010a. 2, 14, 21, 27, 31, 37, 40, 69, 125

F. Plestan, Y. Shtessel, V. Bregeault, and A. Poznyak. New methodologies for adaptive sliding mode control. *International journal of control*, 83(9):1907–1919, 2010b. 2, 17

Quanser. *3-dof helicopter reference manual*. Technical report, Quanser Consulting Inc, Markham, 2006. 3, 22, 113, 115, 126, 131

Y. Shtessel, M. Taleb, and F. Plestan. A novel adaptive-gain supertwisting sliding mode controller: methodology and application. *Automatica*, 48(5):759–769, 2012. 16

Y. Shtessel, A. Glumineau, F. Plestan, and M. Weiss. Hybrid-impulsive second order sliding mode control: Lyapunov approach. In *IFAC*. Grenoble, France, 2013. 126

Y. Shtessel, C. Edwards, L. Fridman, and A. Levant. *Sliding mode control and observation*. Springer, New York, USA, 2014. 14, 15, 20, 27, 37

M. Smaoui, X. Brun, and D. Thomasset. Systematic control of an electropneumatic system: integrator backstepping and sliding mode control. *IEEE Trans. Control Syst. Technology*, 14 (5):905–913, 2001. 1, 19, 98

M. Smaoui, X. Brun, and D. Thomasset. A combined first and second order sliding mode approach for position and pressure control of an electropneumatic system. In *American Control Conference*. Portland, Oregon, USA, 2005. 1, 19

M. Smaoui, X. Brun, and D. Thomasset. A study on tracking position control of an electropneumatic system using backstepping design. *Control Engineering Practice*, 14(8):923–933, 2006. 98

M. Taleb and F. Plestan. Adaptive second order sliding mode control: Application to position and force control of electro-pneumatic actuators. In *ASME 2012 11th Biennial Conference on Engineering Systems Design and Analysis*. Nantes, France, 2012. 17, 104

M. Taleb, A. Levant, and F. Plestan. Pneumatic actuator control: solution based on adaptive twisting and experimentation. *Control Engineering Practice*, 21(5):727–736, 2013. 2, 17, 65, 99, 100, 102, 104

M. Taleb, X. Yan, and F. Plestan. Third order sliding mode controller based on adaptive integral sliding mode concept: Experimental application to an electropneumatic actuator. In *IEEE Conference on Decision and Control (CDC),*. Los Angeles, California, USA, 2014. 5, 23, 65

P. Trivedi and B. Bandyopadhyay. An algorithm for third order sliding mode control by keeping a 2-sliding constraint. In *12th IEEE International Workshop on Variable Structure Systems (VSS)*. Mumbai, India, 2012. 66

V. Utkin. Variable structure systems with sliding modes. *IEEE Transactions on Automatic Control*, 22(2):212–222, 1977. 8

V. Utkin. *Sliding modes in control and optimization*. Springer, Berlin, Germany, 1992. 8, 10

V. Utkin and H. Lee. Chattering problem in sliding mode control systems. In *International Workshop on Variable Structure Systems, 2006. VSS 2006.* Alghero, Italy, 2006. 11

V. Utkin and J. Shi. Integral sliding mode in systems operating under uncertainty conditions. In *IEEE Conference on Decision and Control (CDC)*. Kobe, Japan, 1996. 11

X. Yan, F. Plestan, and M. Primot. Perturbation observer for a pneumatic system: High gain versus higher order sliding mode solutions. In *European Control Conference (ECC)*. Strasbourg, France,, 2014a. 4, 23

X. Yan, M. Primot, and F. Plestan. Comparison of differentiation schemes for the velocity and acceleration estimations of a pneumatic system. In *IFAC World Congress*. Cape Town, South-Africa, 2014b. 2, 4, 18, 21, 23, 27, 104

X. Yan, F. Plestan, and M. Primot. Higher order sliding mode control with a reduced use of sliding variable time derivatives. In *American Control Conference (ACC),*. Chicago, IL, USA, 2015. 5, 23

X. Yan, A. Estrada, and F. Plestan. Adaptive pulse output feedback controller based on second-order sliding mode: Methodology and application. *IEEE Transactions on Control Systems Technology*, PP(99):1–8, 2016a. 4, 23, 69, 75

X. Yan, F. Plestan, and M. Primot. Integral twisting-like control with application to uavs attitude control. In *IEEE Multi-Conference on Systems and Control, International Conference on Control Applications (CCA)*. Buenos Aires, Argentina, 2016b. 4, 5, 22, 24, 113, 119, 126

X. Yan, F. Plestan, and M. Primot. A new third order sliding mode controller – application to an electropneumatic actuator. *IEEE Transactions on Control Systems Technology*, PP(99):1–8, 2016c. 3, 4, 22, 23, 66, 80, 82, 83, 84, 87, 88, 89, 125

X. Yan, M. Primot, and F. Plestan. Output feedback relay control in the second order sliding mode context with application to electropneumatic system. *International journal of robust and nonlinear control (third lecture submit)*, 2016d. 3, 4, 21, 23, 28, 33, 43, 44, 45, 47, 65, 73, 74, 119

X. Yan, M. Primot, and F. Plestan. An unified formalism based on gain switching for second order sliding mode control. In *International Workshop on Variable Structure Systems (VSS),*. Nanjing, China, 2016e. 2, 5, 21, 23, 37, 38

X. Yan, M. Primot, and F. Plestan. Electropneumatic actuator position control using second order sliding mode. *e& i Special Issue on Automation and Control - Sliding Mode Applications in Hydraulics and Pneumatics*, PP(99):1–8, 2016f. 4, 23

X. Yu and RB. Potts. Analysis of discrete variable structure systems with pseudo-sliding modes. *International journal of systems science*, 23(4):503–516, 1992. 12

UNIVERSITE BRETAGNE LOIRE

Centrale Nantes

Thèse de Doctorat

Xinming YAN

Développement de commandes robustes basées sur la théorie des modes glissants pour les systèmes non linéaires incertains

Development of robust control based on sliding mode for nonlinear uncertain systems

Résumé
Le travail de thèse présenté dans ce mémoire s'inscrit dans le cadre du développement de lois de commande pour des systèmes non linéaires incertains, basées sur la théorie des modes glissants. Les méthodes classiques de la commande par modes glissants sont des lois de commande par retour d'état, où la variable de glissement et ses dérivées sont nécessaires. Le premier objectif de cette thèse est de proposer des lois de commande par modes glissants d'ordre supérieur avec une réduction de l'ordre de dérivation de la variable de glissement. Le deuxième objectif est de combiner les nouvelles lois de commande avec un mécanisme de gain adaptatif. L'utilisation d'un gain adaptatif permet de simplifier le réglage du gain, de réduire le temps de convergence et d'améliorer la précision. Enfin, l'applicabilité de ces approches est démontrée à travers leur application au banc d'essais électropneumatique de l'IRCCyN, et à un système volant à trois degrés de liberté.

Mots clés
Modes glissants d'ordre deux, modes glissants d'ordre supérieur, modes glissants adaptatifs, système électropneumatique, système volant.

Abstract
This work deals with the development of control laws for nonlinear uncertain systems based on sliding mode theory. The standard sliding mode control approaches are state feedback ones, in which the sliding variable and its time derivatives are required. This first objective of this thesis is to propose high order sliding mode control laws with a reduced use of sliding variable time derivatives. The contributions are made for the second and third order sliding mode control. The second objective is to combine the proposed control laws with a gain adaptation mechanism. The use of adaptive gain law allows to simplify the tuning process, to reduce the convergence time and to improve the accuracy. Finally, the applicability of the proposed approaches is shown on IRCCyN pneumatic benchmark. Applications are also made on 3DOF flying system.

Key Words
Second order sliding mode, higher order sliding mode, adaptive sliding mode, electropneumatic system, flying system.